OPTIMIZATION OF SPECTRUM SENSING SCHEMES IN COGNITIVE SENSOR NETWORKS

by

Amir Sepasi Zahmati

BSc, K.N. Toosi University of Technology, Tehran, Iran, 2004
MSc, Iran University of Science and Tech., Tehran, Iran, 2007

A dissertation
presented to Ryerson University

in partial fulfillment of the
requirements for the degree of
Doctor of Philosophy
in the Program of
Electrical and Computer Engineering

Toronto, Ontario, Canada, 2013
©Amir Sepasi Zahmati 2013

I hereby declare that I am the sole author of this dissertation. This is a true copy of the dissertation, including any required final revisions, as accepted by my examiners.

I authorize Ryerson University to lend this dissertation to other institutions or individuals for the purpose of scholarly research.

I further authorize Ryerson University to reproduce this dissertation by photocopying or by other means, in total or in part, at the request of other institutions or individuals for the purpose of scholarly research.

I understand that my dissertation may be made electronically available to the public.

Optimization of Spectrum Sensing Schemes in Cognitive Sensor Networks

Doctor of Philosophy 2013

Amir Sepasi Zahmati

Electrical and Computer Engineering

Ryerson University

Abstract

The currently dominant spectrum allocation policy is reported to be inefficient. Cognitive radio, therefore, has been proposed in the literature to improve the spectrum usage efficiency. This dissertation proposes the optimization of spectrum sensing schemes in cognitive sensor networks. The modeling of the spectrum occupancy is a prerequisite for cognitive radio analysis. We describe the radio spectrum occupancy as a continuous-time Markov chain, and mathematically define the model by deriving the transition rate matrix and the probability state vector.

The dissertation addresses an important aspect of spectrum sensing that has been often overlooked in the literature. While the cognitive radio is supposed to be aware of its surroundings, existing work does not consider the characteristics of unlicensed users for finding the optimum sensing period. In this work, we propose an application-specific method that finds the optimal sensing period according to the characteristics of both secondary and primary networks. According to the unlicensed user's state in the Markov chain, two optimization problems are formulated to derive the optimum sensing

periods. The secondary network's throughput and power consumption are also studied and the corresponding parameters are derived. By numerical and simulation analyses, it is elaborated that the proposed method increases the secondary network's throughput by up to 11% and significantly decreases the power consumption of the secondary network by as low as 33% of the non-hybrid approach.

In addition, we study cooperative spectrum sensing in cognitive sensor networks and address two important issues. First, an optimization problem is solved to obtain the minimum required number of cognitive users. Second, we define a metric for sensing accuracy and propose a novel energy-aware secondary user selection method that identifies the most eligible cognitive users through a probability-based approach. The network's lifetime is compared at several sensing accuracy thresholds and the trade-off between sensing accuracy and network lifetime is studied. Finally, the effects of several fusion rules on the proposed method are studied through simulation and numerical analyses. It is discussed that the Majority rule has the best performance among the examined rules.

Acknowledgements

This research project would not have been possible without the support of many people. I would like to express my deepest gratitude to my Ph.D. supervisor, Prof. Xavier Fernando, for his support, creative advising, and guidance throughout this work. I especially acknowledge Dr. Fernando's encouragement to think out of the box, which led me to the opportunity to be a Research Intern at Honeywell Aerospace during 2010-2011. I would like to extend my deepest gratitude and appreciation to Dr. Hassan Kojori for his invaluable guidance, background knowledge, and continued support since the beginning of my internship at Honeywell Aerospace.

I would also like to recognize Dr. Ali Grami, my Ph.D. co-supervisor, for his guidance, patience and editing skills in the completion of this dissertation. Prof. Grami read my numerous revisions, and helped make some sense of the confusion. Dr. Grami's insight, in particular, directed me towards the selection of my Ph.D. research area.

To the other members of my committee, Dr. Jamal Deen, Dr. Kaamran Raahemifar and Dr. Matthew Kyan, thank you for the feedback, direction, and assistance when I needed it. Special thanks to my friends and colleagues in the Ryerson Communications Lab (RCL) research group for their insightful discussions and professional collaborations.

I would also like to acknowledge my brother, Hamid Sepasy Zahmaty, and his wife, Banafsheh Heydarzadeh, for their continued support and endless love. There is no doubt in my mind that without their help I could not have completed this long process.

Dedication

This Doctoral dissertation is lovingly dedicated to my late father, Abbas, and my mother, Maliheh, for their unconditional love, sacrifice, hard work and strength. My mother, in particular, always had confidence in me and offered me encouragement and support in all my endeavours; I owe her every single accomplishment in my life.

Table of Contents

List of Tables

List of Figures

xii

List of Acronyms

AWGN   Additive White Gaussian Noise

CR   Cognitive Radio

CSN   Cognitive Sensor Network

CTMC   Continuous-Time Markov Chain

DSA   Dynamic Spectrum Access

FC   Fusion Centre

FCC   Federal Communications Commission

HD   High-Definition

HMM   Hidden Markov Model

IID   Independent and Identically Distributed

ISM   Industrial, Scientific and Medical band

MAC   Medium Access Control

NBP   National Broadband Plan

PDF   Probability Density Function

PPR   Primary Protection Region

PU   Primary User

RF   Radio Frequency

SNR   Signal-to-Noise Ratio

SSP   Stationary State Probability

SU   Secondary User

TVWS   TV White Spaces

WRAN   Wireless Regional Area Network

WSN   Wireless Sensor Network

List of Symbols

$\Delta_i(n)$ Total number of differences between the ith secondary user's local sensing and the FC's global decision, during the setup phase

Δ_{th} Sensing accuracy threshold

$D_i(n)$ The result of local sensing performed by the ith secondary user, during the nth sensing task

e_0 Energy consumption to perform a single sensing/reporting task

e_u Initial energy of secondary users

E Total energy consumption of the secondary network

ϵ Decision threshold to decide on the presence or absence of the PU

η_i Weighting factor assigned to the ith secondary user

$F(n)$ The result of the FC's decision at the nth round

Γ_s Average throughput of the secondary network s

γ_d Global probability of detection threshold

γ_f Global probability of false alarm threshold

$k_i(t)$ Channel gain of the sensing channel between the ith SU and the PU

L Number of rounds within the operational phase

λ_P PU's arrival rate

λ_i The ith secondary user's arrival rate

M Number of received samples

μ_P PU's departure rate

μ_i The ith secondary user's departure rate

$n_i(t)$ Additive white Gaussian noise at the ith secondary user

N Number of secondary users

N^* Minimum number of required secondary users

P Total power consumption of the secondary network

P_f	Probability of false alarm
P_d	Probability of detection
Π_i	The steady-state probability of being at state i
Q_d	Global probability of detection
Q_f	Global probability of false alarm
$r_i(t)$	Received signal at the ith secondary user
r_i	Maximal data rate of the ith secondary user
R_I	Interference ratio
R_I^{th}	Interference ratio threshold
R_I^{NH}	Interference ratio in the non-hybrid method
R_U	Undetected opportunity ratio
R_U^{th}	Undetected opportunity ratio threshold
R_U^{NH}	Undetected opportunity ratio in the non-hybrid method
$s(t)$	Primary user transmitted signal
σ_n^2	Variance of the noise
σ_s^2	Variance of the transmitted signal
T_{sim}	Simulation time
T_I^*	Optimal idle time
T_T^*	Optimal transmission time
T_O	Observation time
ς_d	Probability of detection threshold
ς_f	Probability of false alarm threshold
W	Number of rounds within the setup phase
Y	Test statistic in the energy detection method

Chapter 1

Introduction

Currently, the radio spectrum is mainly used based on a fixed assignment policy, where either the spectrum is allocated to licensed service providers, such as TV bands, or it is open to the public for use with an agreed-upon etiquette, such as the ISM band. While the fixed allocation policy dominates the current wireless systems, it is inefficient [3]. For instance, a spectrum usage measurement by the US Federal Communications Commission (FCC) indicates that a large portion of the assigned radio spectrum is severely under-utilized, while the demand for the radio spectrum is rapidly increasing [4].

The usable portion of the radio spectrum is limited; therefore, dynamic spectrum access (DSA) has gained momentum in both academia and industry to overcome the issue of spectrum scarcity. In particular, cognitive radio (CR), an increasingly developing technology, has been viewed as a promising approach to tackle this concern [5].

A CR is an intelligent wireless communication system that is aware of its surroundings, and adapts its internal parameters to achieve a reliable communication and efficient utilization of the spectrum [6, 7]. Through CR technology, the vacant portions of the radio spectrum that is originally assigned to licensed/primary users (PUs) can be opportunistically utilized by unlicensed/secondary users (SUs). A band of frequencies that is originally assigned to PUs but is temporarily vacant and thus can be used by SUs, is called a spectrum hole or a white space.

1.1 CR Research Challenges

Through CR technology, the radio spectrum can be utilized by both licensed and unlicensed users. Developing analytical models that consider the occupancy of the radio spectrum by the two types of users, therefore, is listed as one of the major research challenges in CR. It is important to understand the theory behind CR algorithms and to evaluate the performance of different algorithms.

As a CR network should be aware of its surroundings, spectrum sensing has been considered as an important necessity for the realization of cognitive technology. Through spectrum sensing, SUs monitor the primary network's activity to opportunistically use the spectrum and to vacate the spectrum in cases where a PU appears. Several challenges are associated with the task of spectrum sensing. In a group of sensing methods, non-

cooperative spectrum sensing, the sensing task is performed by each SU individually. In other words, there is no collaboration between different SUs. In such approaches, it is important to obtain the optimal sensing frequency in order to achieve a predetermined objective, such as maximization of the secondary network's throughput.

Through another group of sensing methods, cooperative spectrum sensing, SUs do collaborate to perform the sensing task. In Fig. 1.1, the non-cooperative (local) spectrum sensing is compared with the cooperative sensing scheme. As shown, in the local sensing scheme, each sensor must have the ability to sense the whole channel and determine an optimal scheme to maximize its benefits, such as its throughput. However, in the cooperative sensing scheme, each SU senses the spectrum, and reports its local sensing result to a single entity called a fusion centre (FC). The FC gathers all local sensing results, and makes a final decision on the presence or absence of the PU. The final decision is then forwarded to all SUs.

In cooperative spectrum sensing, design challenges include but are not limited to finding the minimum number of required cooperative users, and choosing the most qualified SUs in terms of energy level and sensing accuracy.

3
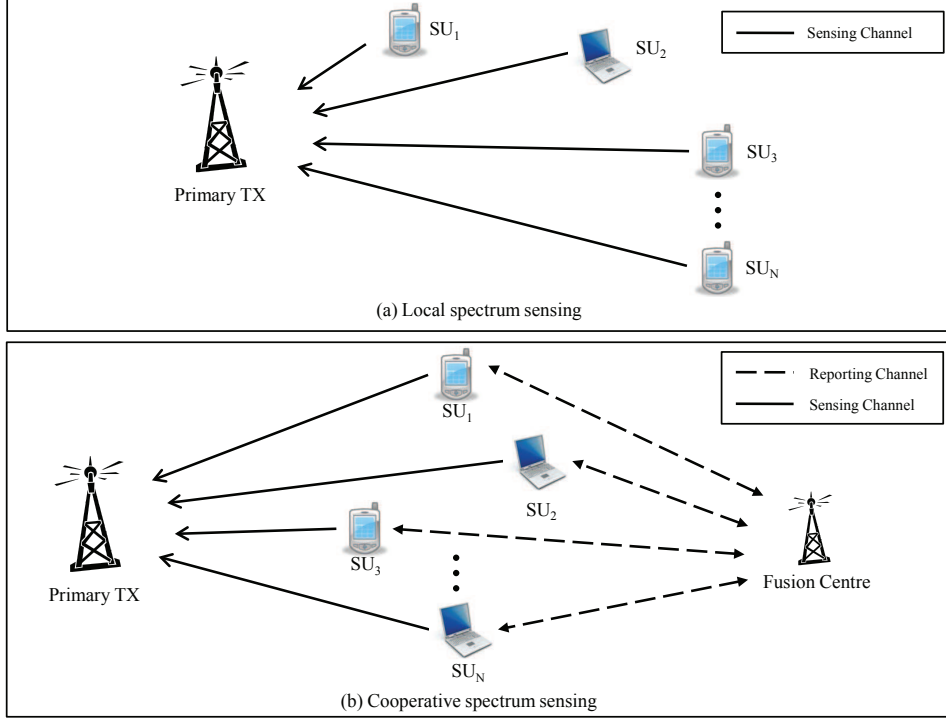
Figure 1.1: Local spectrum sensing vs. cooperative spectrum sensing.

1.2 Major Contributions of the Dissertation

In this dissertation, we use a continuous-time Markov chain (CTMC) to describe the spectrum occupancy by both primary and secondary networks. By analytical work, we obtain the transition rate matrix for the proposed model. In addition, we perform steady-state analysis to analytically derive the probability state vector. The CTMC is then employed to serve as a base model for further analysis and proposals in the rest of this work.

In addition, we address the problem of local spectrum sensing optimization in CR from a novel perspective. In contrast with a majority of existing work, where the sensing

optimization is performed according to the properties of the primary network only, we propose an application-specific[1] sensing method that finds the SUs' sensing period according to the properties of both primary and secondary networks. Moreover, the interference and the undetected opportunity ratios are derived, and two optimization problems are formulated to find the optimum sensing period, based on the CTMC model presented in this work. In addition, the non-interfered system throughput and the total power consumption of the secondary network are derived. We also derive the corresponding parameters in a non-application-specific[2] method for comparison purposes.

Furthermore, we apply cooperative sensing in CR to further enhance the performance of spectrum sensing. First, we analytically obtain the minimum number of cooperative users needed to perform the sensing task, while meeting the sensing requirements. Second, the most eligible SUs are identified based on a probability-based approach that utilizes a sensing accuracy metric and a weighting function. Figure 1.2 shows the inter-relationship between different chapters of this dissertation.

1.3   Organization of the Dissertation

The dissertation is established in six chapters, as follows:

---

[1]The terms "application-specific" and "hybrid" will be used interchangeably in this dissertation.

[2]The terms "non-application-specific" and "non-hybrid" will be used interchangeably in this dissertation.
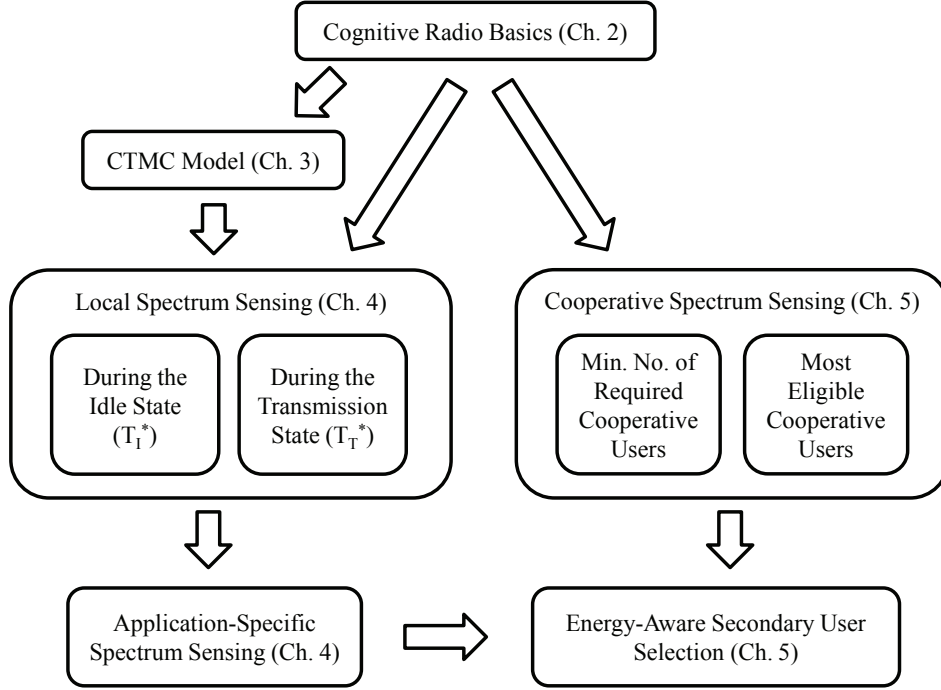
Figure 1.2: Inter-relationship diagram between the dissertation chapters.

Chapter 1: Introduction

In this chapter, a brief introduction to the dissertation is presented. Major research challenges are discussed along with our major contributions to overcome the challenges.

Chapter 2: Cognitive Radio Technology

A short background of CR technology is presented in this chapter. We address spectrum sensing as an important necessity in the realization of cognitive systems and study recent advancements in the field.

Chapter 3: Spectrum Occupancy Model

This chapter studies a CTMC system to accurately model the spectrum occupancy by

the primary and secondary networks in CR. The system will serve as a base model for our proposals through the dissertation.

Chapter 4: Application-Specific Spectrum Sensing

An application-specific sensing method is proposed in this chapter to provide a customized solution for various secondary applications. The proposed method is a hybrid approach that considers the properties of both primary and secondary networks to obtain optimal sensing period.

Chapter 5: Energy-Aware Secondary User Selection in Cooperative Spectrum Sensing

In this chapter, we apply cooperative spectrum sensing to further improve the sensing performance. An energy-aware secondary user selection method is proposed that accurately obtains the minimum number of required secondary users to minimize the secondary network's energy consumption. In addition, the proposed method sets a merit for sensing accuracy based on recent sensing results, and selects the most eligible users through a probability-based approach. The selected secondary users then sense the licensed channel and report their sensing results to a fusion centre.

Chapter 6: Conclusions and Future Work

This chapter presents the concluding remarks of this work, and some suggestions for future research are made.

Chapter 2

Cognitive Radio Technology

2.1 Basic Concepts

Cognitive radio is recognized by two main characteristics: cognitive capability and recon-figurability. A CR system can identify and exploit the unused portions of the spectrum without interference with the licensed users, through real-time interaction with the radio environment (cognitive capability). In addition, a cognitive system can be programmed to transmit and receive on a variety of frequencies and use different access technologies that are supported by its hardware design (reconfigurability) [8].

In order to provide cognitive capabilities, cognitive systems require novel radio fre-quency (RF) transceiver architectures. The CR functionality mainly relies on the RF hardware technologies, such as wideband antenna, power amplifier, and adaptive filter.

Therefore, the RF hardware should be capable of being tuned to any part of a large range of spectrum. In addition, a CR transceiver should be able to receive signals from various transmitters operating at different power levels, bandwidths, and locations [3].

The dynamic spectrum access (DSA) concept is not a novel idea, and it might be as old as radio communication itself. For instance, maritime communication systems were using shared radio resources in 1910s. The use of shared channels in land mobile communication were allowed by the FCC around 1960. In the 1970s, the Aloha protocol enabled sharing of radio channels without using a centralized entity. The integrated communications navigation and identification architecture (ICNIA) by Air Force Rome Labs was the first project to realize DSA in 1987. The ultra wideband communication was issued by the FCC 98-153 docket in 2002. Finally, CR has been employed to develop an air interface to opportunistically access the TV bands in regional area networks in 2011 [9]. Table 2.1 depicts a brief history for the CR-like systems mentioned above.

Table 2.1: A brief history of CR-like communication systems.

Date	Project	Communication Scheme
1910	Maritime Communication	Hardware Radio
1960	Shared Channel in Land Mobile Communications	Hardware Radio
1970	ALOHA	Hardware Radio
1987	ICNIA	Software Defined Radio
2002	Ultra Wideband Communication	DSA
2011	IEEE 802.22	Cognitive Radio

2.2 Cognitive Sensor Networks

Rapid advances in processing capability, memory capacity, and radio technology have enabled the development of distributed networks with small and inexpensive communication nodes. These nodes are capable of sensing and communicating and can be deployed at a cost much lower than those of traditional wired sensor systems. Such systems are called wireless sensor networks (WSNs) [10, 11]. The limited communication bandwidth assigned to WSNs is one of the main challenges of these networks.

To overcome the limited communication bandwidth assigned to WSNs, a new concept of cognitive sensor networks (CSNs) has been recently introduced in the literature [11–15]. A CSN is defined as a wireless network of low-power radios which gain secondary spectrum access following the CR paradigm [16]. Similar to the existing WSNs, a CSN consists of many tiny and inexpensive sensor nodes that operate on limited battery energy. Hence, sensor nodes are supposed to be energy efficient. In a WSN, each node either sends data, receives data, or it is in the idle state. However, in a CSN, there exists another state called *spectrum sensing*, where sensor nodes sense the spectrum to detect spectrum opportunities. Figure 2.1 depicts different states for these networks.

Adding cognition to WSNs provides several advantages. A CSN could provide access not only to new spectrum (rather than the worldwide available 2.4 GHz band), but also to the spectrum with possibly better propagation characteristics [13]. For instance,
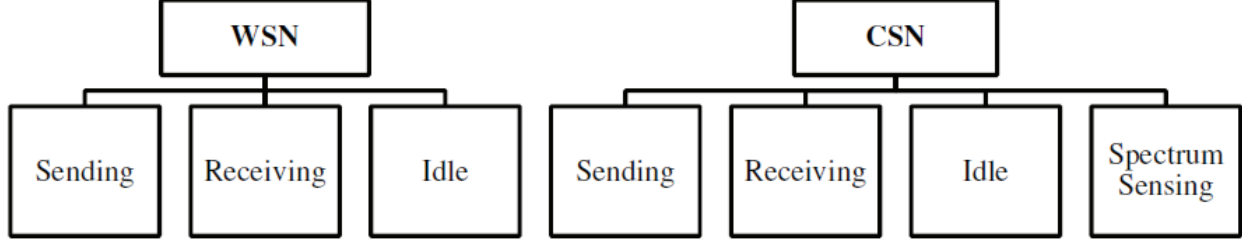
Figure 2.1: Different states in a WSN vs. a CSN.

the transmission range can be increased by using lower frequencies since the path loss decreases as the operating frequency decreases [17]. The higher communication range provides CSNs with a smaller number of hops per route. Thus, the average end-to-end delays would also be smaller.

Due to the fact that sensor nodes are equipped with limited energy sources, researchers have been working on innovative methods to improve the network's energy consumption in CSNs. The sensing task is a repetitive process and it consumes extra energy from battery powered sensors. Therefore, it is important to employ energy-aware methods in these networks.

2.3 Spectrum Sensing

A CR network is designed to be aware of the changes in its surroundings. Spectrum sensing, therefore, is an important requirement for the realization of cognitive technology. Through spectrum sensing, cognitive users reliably detect the spectrum holes and protect

PUs from the adverse interference from SUs. For instance, in IEEE 802.22 standard, spectrum sensing is included as a mandatory task, where SUs sense the spectrum for three different PUs: analog television, digital television, and licensed low-power auxiliary devices such as wireless microphones.

A variety of methods can be employed for this purpose. The existing sensing methods are classified into two main categories, as shown in Figure 2.2. In the first group of methods, the PU is in charge to provide SUs with the latest spectrum usage information. There are three schemes in this category as follows [18]: In the *database registry* method, the channel information is registered at a centralized database. In another method called *beacon signals*, the channel information is broadcasted on a predefined channel. In a third method, PUs periodically transmit a pilot signal on a subcarrier if that subcarrier is occupied by licensed users. By detecting the presence of such a pilot signal, SUs determine if that particular subcarrier is available or not. While leading to simplified secondary transceivers, these methods require some modifications to the current PUs and are incompatible with the existing primary network.

In the second group of methods, spectrum sensing solely relies on the secondary system to periodically sense the channel and detect the spectrum holes. In addition, SUs should monitor the activation of PUs to immediately vacate the occupied spectrum in case a PU appears. Due to its relatively low infrastructure cost and compatibility with
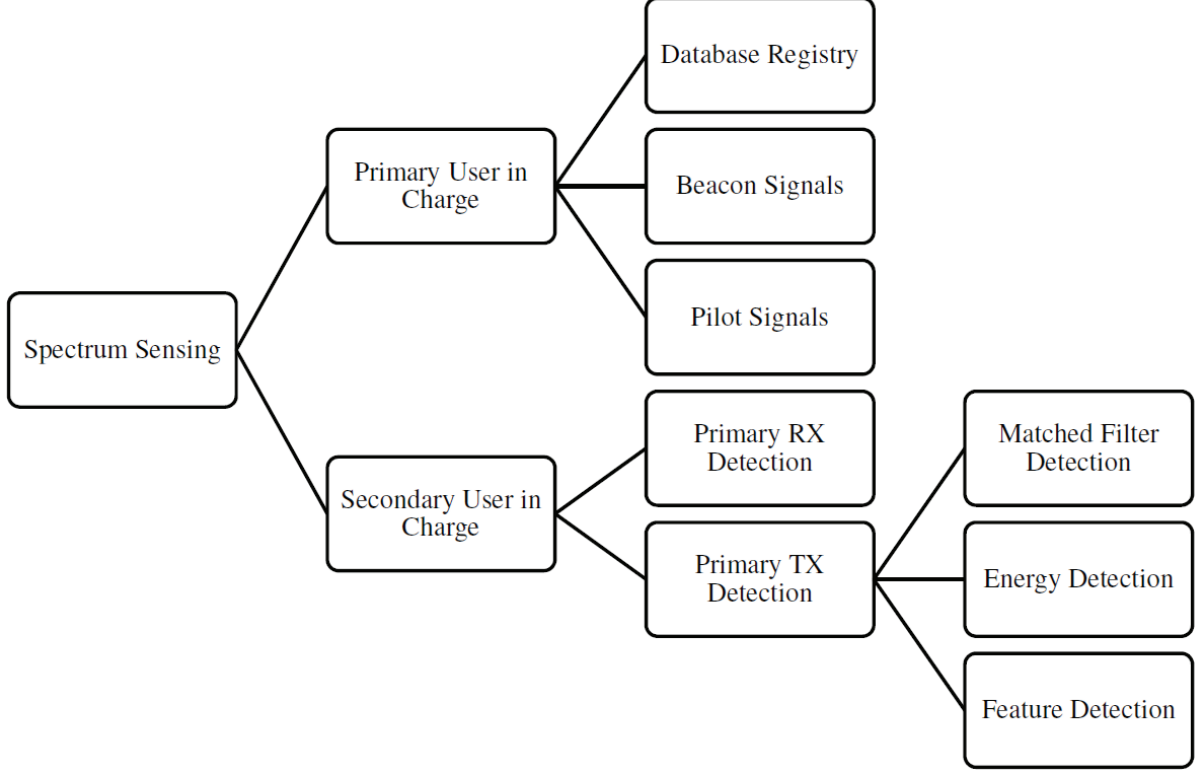
Figure 2.2: Classification of spectrum sensing methods.

the existing primary systems, the second group of methods has received more attention than other candidates. For instance, it is included in the IEEE 802.22 standard [19].

As shown in Fig. 2.2, there exist two schemes when SUs are in control: in the *primary receiver detection* method, secondary users detect spectrum holes by monitoring the primary users that are receiving data within their communication range. In reality, however, it is difficult for an SU to have a direct measurement of a channel between a primary receiver and a transmitter [17]. Thus, the most recent work focuses on the *primary transmitter detection* based on cognitive users' observation. The transmitter

detection approach is based on the detection of weak signals from the PU through local observations of SUs. Three schemes are generally used for the transmitter detection method as follows [17, 20].

When the information of the PU's signal is known to the secondary network, the optimal detector in additive white Gaussian noise (AWGN) is the *matched filter detector* because it maximizes the received signal-to-noise ratio (SNR) [20]. However, a matched filter detector requires a priori knowledge of the primary signal such as the modulation type and the pulse shape. To this effect, if this information is not accurate, the method performs poorly.

If the receiver cannot gather sufficient information about the primary signal, a simpler alternative method called *energy detection* is helpful. An energy detector simply measures the energy received on a primary band during an observation time and declares a spectrum hole if the measured energy is less than a threshold. While compared to matched filtering, energy detection requires a longer sensing time to achieve a desired performance level, its low cost and implementation simplicity have made it a favorable candidate for spectrum sensing in CR.

A basic hypothesis model for the energy detection method can be defined as follows [21]:

$$r_i(t) = \begin{cases} n_i(t) & : H_0 \\ \\ k_i(t)s(t) + n_i(t) & : H_1 \end{cases}$$

where $r_i(t)$ is the received signal at the ith secondary user, $s(t)$ is the transmitted signal by the PU, $n_i(t)$ is the AWGN at the ith SU, and $k_i(t)$ is the channel gain of the sensing channel between the PU and the ith SU. The H_0 is a null hypothesis, which states that there is no primary signal in a certain spectrum band. On the other hand, H_1 is an alternative hypothesis, which indicates that there exists a primary signal.

Modulated signals are in general coupled with sine wave carriers. This characteristic has been used in the *feature detection* method, where the frequency characteristics are detected by analyzing a spectral correlation function. The main advantage of the feature detection method is that it can differentiate the noise energy from modulated signal energy, which is a result of the fact that the noise is a wide-sense stationary signal with no correlation to the primary signal. Therefore, a feature detector can perform better than energy detector in discriminating against noise due to its robustness to the uncertainty in noise power [22]. However, it is computationally complex and requires significantly long observation time [3, 23].

There are a number of difficulties in the noted methods. First, an SU may interfere

with a PU in case the primary transmitter is not in the secondary user's communication range. As shown in Fig. 2.3 (a), the primary transmitter is not in the communication range of SU_1. Therefore, it starts to operate in the primary channel and interfere with PU_1. This is called the *receiver uncertainty* problem. Another difficulty arises in case an SU cannot detect a primary transmitter because of shadowing, and starts to communicate with a busy primary receiver. As shown in Fig. 2.3 (b), SU_1 cannot detect the primary transmitter due to shadowing from an obstacle, and thus interfere with PU_1. To overcome these problems, cooperative spectrum sensing schemes have been proposed in the literature [24, 25]. A cooperative detection refers to the spectrum sensing methods where information from multiple SUs are incorporated to detect the presence of the primary network.

2.4 Recent Advancements

During the past few years, several major developments have been performed in the spectrum allocation policy to accelerate the opportunistic use of the radio spectrum. This includes the publication of the National Broadband Plan (NBP), a policy document released by the FCC that describes the spectrum management scheme to facilitate the broadband usage for the upcoming years. The NBP recommends providing further proceedings on opportunistic use of the spectrum in addition to the already completed TV

(a) Receiver uncertainty problem

(b) Shadowing uncertainty problem
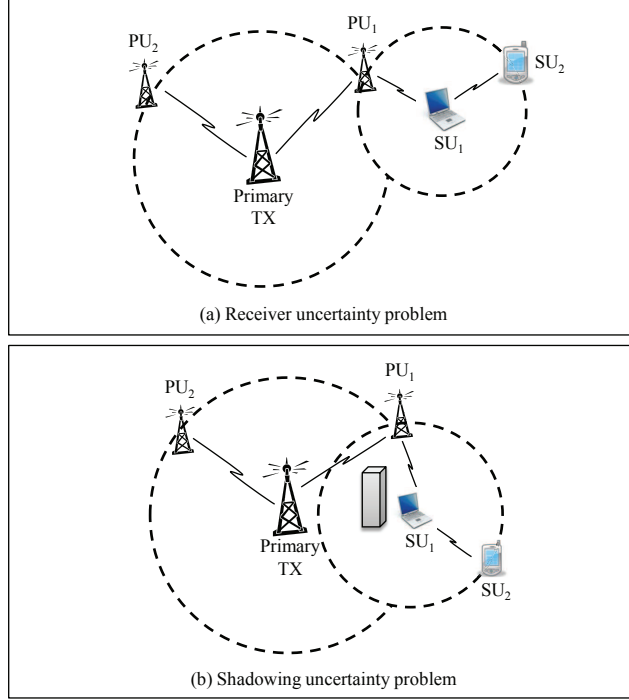
Figure 2.3: Receiver uncertainty and shadowing uncertainty problems in the transmitter detection method.

white spaces (TVWS) proceedings. Moreover, the plan recommends vacating 500 MHz for broadband use within the next ten years, and 300 MHz for mobile use in the next five years.

In addition, the IEEE 802.11 has standardized the final rules for unlicensed devices in TV bands [26]. A self-organizing network of beacon devices[1] is under development (IEEE 802.22.1), which is expected to provide additional protection for low-power PUs. Moreover, the development of an IEEE 802.11 amendment to utilize the TVWS operation for WLANs is led by IEEE 802.11af. Also, the IEEE 802.19.1 Working Group is aiming

[1]A beacon device generates beacons so that the network users can detect its presence [27].

to develop a standard for wireless coexistence in the TVWS that will help mitigating interference issues among CR-based Field Area Network/Automated Meter Infrastructure in smart grids. In addition, there is an ongoing effort for secondary use of the 2360-2400 MHz band for medical body area networks [28]. An IEEE 802.15 Study Group has been also created to investigate the use of TVWS.

In the field of sensor networks, which is mainly discussed in this dissertation, several research works have been directed towards applying cognitive technology in wireless sensor networks (WSNs) [13, 29–31]. The authors in [13] propose a CR-based WSN and compare its performance with a standard ZigBee/IEEE 802.15.4 WSN; both designs were built on the standard OPNET model that operate in the 2.4 GHz band. By simulation work, the authors concluded that the maximum communication range in the CR-based WSN is almost twice the standard ZigBee/IEEE 802.15.4 WSN for the same transmission power. The longer communication range reduces the number of hops required in a multi-hop routing technique. In addition, it reduces the chance of having the receiver uncertainty problem. Therefore, it improves the efficiency of the multi-hop routing. Moreover, the authors claimed that the overall system throughput is improved in the CR-based WSN.

The main design principles, advantages, and applications of CSNs are discussed in [29]. In addition, the possibility of applying existing cognitive techniques to WSNs is

investigated and several challenges in doing so are reported. Moreover, a distributed WSN-based control system for intelligent and reliable operation of large power grids is proposed in [30]. The network consists of several intelligent nodes that communicate with nearby nodes as well as a *control station*. The proposed method employs dynamic decision making and intelligent data fusion; therefore, even under changing environments, dynamic reconfiguration is possible without grid downtime. Also, a cognitive WSN that understands conflicting design objectives, finds optimum tradeoffs with given constraints, and adapts to the dynamics of the network is proposed in [31].

The energy efficiency has been also addressed as a key design metric in CSNs. For instance, a resource allocation problem from an energy efficiency standpoint is proposed in [32]. A fully distributed channel selection and power allocation scheme has been proposed to cover all subcarriers, subject to the required data rate and power constraints.

Recently, there have been worldwide efforts to provide international standards to utilize the spectrum through CR technology. The FCC in the United States, the Office of Communications (Ofcom) in the United Kingdom, and the Electronic Communications Committee (ECC) of the Conference of European Post and Telecommunications (CEPT) in Europe are the major regulatory agencies responsible for research and development of the opportunistic use of the spectrum. Several standards including IEEE 802.22 [26], IEEE 802.11af, ECMA 392 [33], IEEE SCC41, and ETSI RRS [34] are either under

development or have already been finalized. In the following, we discuss a few standards in detail.

IEEE 802.22

The IEEE 802.22-based wireless regional area network (WRAN) aims to utilize the geographically unused spectrum by applying CR technology to coexist with the legacy TV services on 54-862 MHz band, and to provide broadband access to hard-to-reach low-population-density areas such as rural environments [26]. The IEEE 802.22 standard, therefore, has been recognized as the CR standard [35]. Due to the fact that TV bands employ low frequency, their propagation characteristics are suitable for long-range transmission (up to 10-100 Km), and the IEEE 802.22 standard could be used for large-scale smart grid networks. Hence, the standard has the potential for wide applicability worldwide. While the IEEE 802.22 standard supports cognitive communication for WRANs, it is not intended to support low data rate, low energy consumption requirements of sensor networks. Currently, there is no standard for cognitive communication within CSNs.

In the IEEE 802.22 standard, spectrum sensing is listed as one of the main requirements of the cognitive process [36]. The sensing task consists of two stages: fast and fine sensing [37]. In the fast sensing stage, a coarse sensing algorithm is applied, such as the energy detection method. In the fine sensing stage, however, a more complicated

20

method is employed such as waveform-based sensing, cyclostationary feature detection, or matched filtering method. The standard requires certain conditions to be met, such as the probability of detection has to be greater than 0.9, and the probability of false alarm must be be smaller than 0.1 [38].

ECMA 392

ECMA 392 is the first CR standard that supports TVWS usage by personal/portable devices [39]. The standard was initiated by the Cognitive Networking Alliance (CogNeA), and a draft was later transferred to TC48-TG1. The standard documents the PHY and MAC layers with several characteristics including flexible network formation and real-time multimedia traffic support [39]. It is expected that new applications will be enabled by ECMA 392 such as in-home high-definition (HD) video streaming for personal/portable devices, campus-wide wireless coverage, and interactive TV broadcasting services.

2.5   Summary

This chapter discussed a brief introduction to the cognitive radio technology along with several definitions associated with the cognitive radio concept. The spectrum sensing was addressed as an important task in the realization of cognitive systems with an emphasize

on the energy detection technique. The chapter also reviewed recent advancements and

standards in the field of cognitive radio.

Chapter 3

Spectrum Occupancy Model

3.1   Background

In CR, appropriate modeling of the spectrum occupancy by both primary and secondary

networks is a prerequisite for CR analysis. The existence of a Markov chain by collecting

real-time measurements in 928-948 MHz is validated in [40]; the same methodology can

be applied to any spectrum band. A CTMC model is setup for dynamic spectrum access

in [41], where the radio systems attempt to operate in the same band. In [42], the wireless

channel in a CR network is modeled by using a Hidden Markov Model (HMM) trained

by the Genetic Algorithm. An HMM based channel status predictor is proposed in [43]

which provides the CR network with the functionality to find alternative channels to

perform the spectrum handover. Moreover, [44] assumes the spectrum usage statistics to

be Poisson distributed, and proposes a technique to improve the performance of cognitive networks by performing predictions on the channel usage behavior of PUs.

A channel usage model for the PU usage pattern is proposed in [45, 46]. The primary channel is modeled as an ON-OFF source alternating between ON (busy) and OFF (idle) periods. Once an OFF period is detected, SUs can utilize any portion of the remaining OFF period for their own transmission. The time until the next transition (sojourn time) of the ON and OFF periods for channel i are modeled by random variables T_{ON}^i and T_{OFF}^i with the probability density function (PDF) $f_{T_{ON}^i}(y), y > 0$ and $f_{T_{OFF}^i}(x), x > 0$ respectively. The ON and OFF periods are assumed to be independent and identically distributed (i.i.d.) random variables.

A CTMC approximation to model the primary channel usage pattern is suggested in [47, 48]. Figure 3.1 depicts a transition diagram consisting of packet transmissions and idle periods, where λ is the arrival rate of the PU and μ is the departure rate of the PU. The holding time in the transmit state corresponds to the length of the packets, which is largely influenced by the type of traffic. The packet lengths are assumed to be deterministic in the traffic scenario to be analyzed [49].

In [50], a CR network is studied with fixed primary network structure and mobile SUs in the same geographical area. As shown in Fig. 3.2, the primary network is further divided in several cells, where each cell consists of a single access point and several
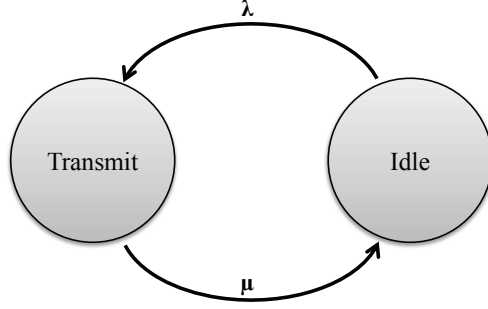
Figure 3.1: A CTMC approximation to model the primary channel usage pattern.

primary receivers. A mobile SU can only operate in the spectrum when its distance from the PU is greater than a system threshold or the PU is inactive, so as to avoid interference with licensed users. A three-state CTMC system is then developed that models the mobility-aware channel availability experienced by the mobile SUs. As shown in Fig. 3.3, the system can be at busy, idle or primary protection region (PPR) state. A primary channel is available when the SU is located outside the PPR, or the SU is located inside the PPR but the PU is idle. Next, the model is reduced into a two-state CTMC by merging the idle and PPR states into the OFF state, as shown in Fig. 3.3.

The process of spectrum occupancy as a CTMC system is modeled in [2]. The spectrum is assumed to consist of M_B primary bands where each band is divided into N_{SB} sub-bands. The $M_B \times N_{SB}$ sub-bands are shared by the primary and secondary networks. In this case, states are described by an integer pair (i, j), where i is the total number of sub-bands used by SUs and j is the total number of primary bands used by PUs. The arrivals of SUs and PUs are assumed to be Poisson processes with arrival rates λ_a and
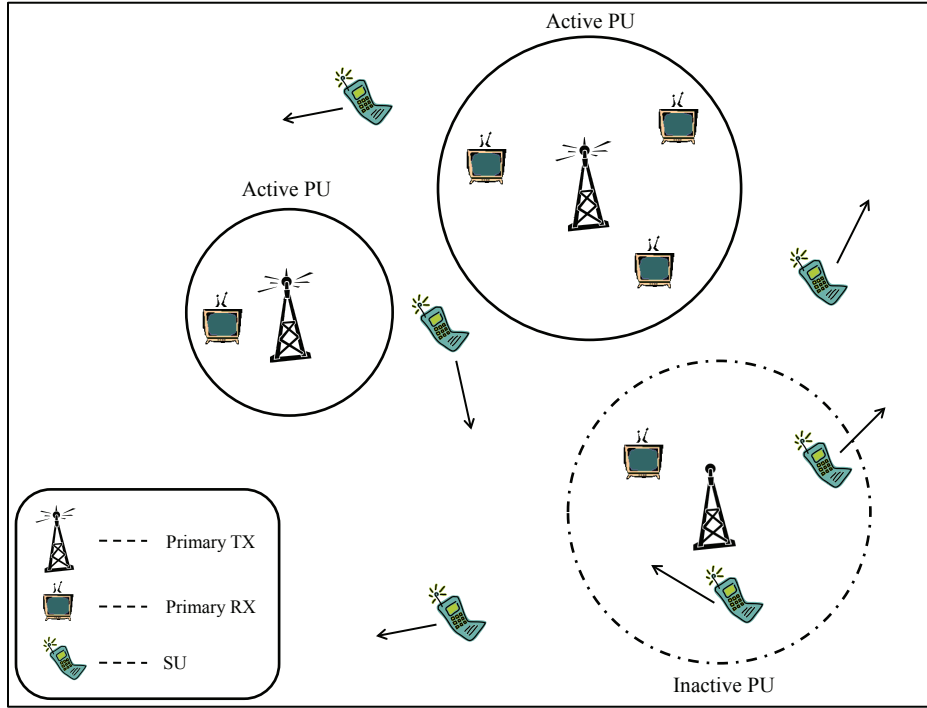
Figure 3.2: A CR network with mobile SUs.
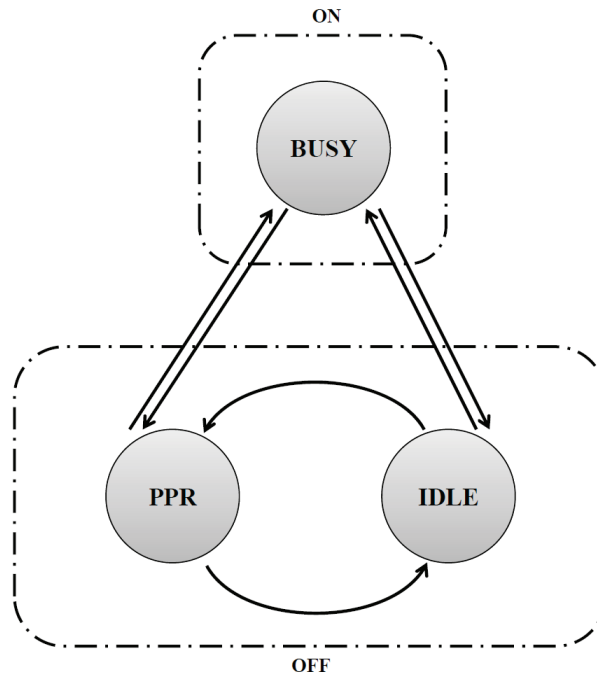
Figure 3.3: A three-state CTMC system to model the mobility-aware channel availability experienced by SUs.

λ_b respectively. The corresponding service times are also assumed to be exponentially distributed with rates μ_a and μ_b respectively.

As the PUs have the priority to use the spectrum, the SUs are forced to vacate the band if a PU operates in the spectrum. Depending on the number of sub-bands occupied by SUs in the new primary band, a forced termination in state (i, j) will move the state to one of $(i, j+1), (i-1, j+1), (i-2, j+1), ..., (i-(N_{SB}-1), j+1), (i-N_{SB}, j+1)$ states, as shown in Fig. 3.4.

The majority of existing work assumes a simple cognitive system and analyze it using Markov modeling. A cognitive network with one primary and two secondary users is considered, and a primary-prioritized CTMC model is proposed in [51]. In [52], a CTMC model is proposed to predict the behavior of open (un-utilized) spectrum access in unlicensed bands. The model considers two types of secondary systems, but the analysis does not include the PU. Moreover, [2] presents the CTMC model for a simple case of one primary system and one secondary system.

In this chapter, we assume a CR network consisting of N secondary users (with various traffic conditions) and one primary user[1]. We describe the radio spectrum occupancy as a CTMC model, and analytically derive the transition rate matrix based on the model.

---

[1]This model is easily expanded in case of multiple primary users. As long as this model is considered, when a primary user starts transmission, the secondary users must quit transmission. Furthermore, the primary users share the channel with a predefined medium access control protocol.
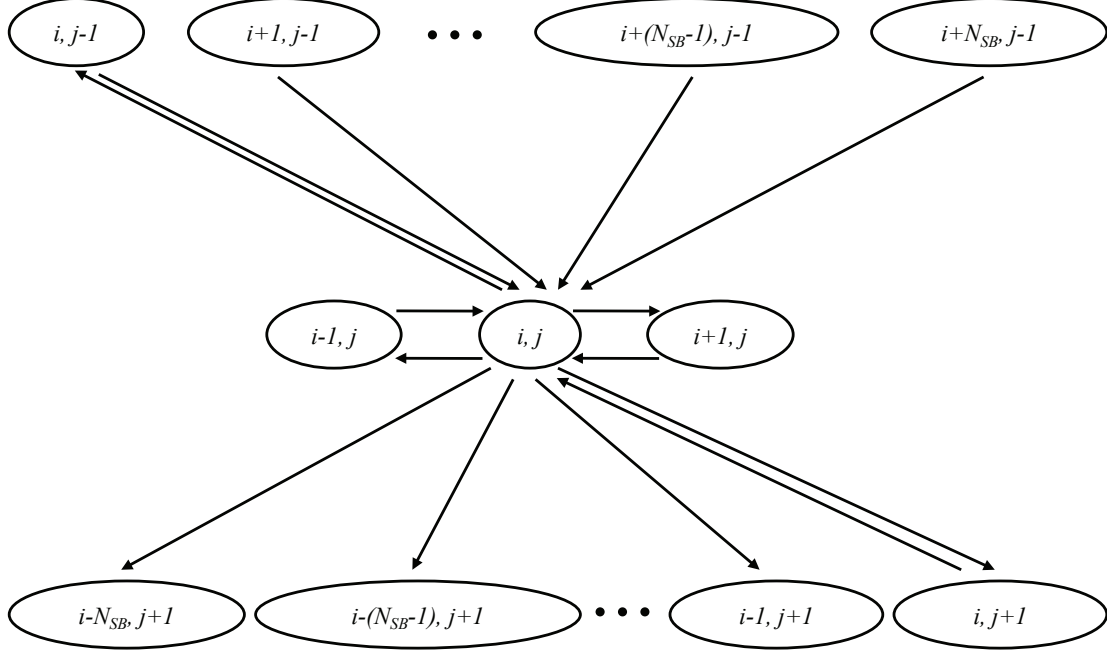
Figure 3.4: A Markov chain model for CR; i is the total number of sub-bands used by SUs, and j is the total number of primary bands used by the PU [2].

Moreover, an steady-state analysis is performed to derive the stationary state probability

(SSP) vector.

3.2 System Model

A CR network with one primary user and N secondary users $U = \{u_i \ : 1 \leq i \leq N\}$

is studied[2]. The secondary users are assumed to form a single-hop CR Network within

the transmission range of which there are no other secondary networks interfering or

---

[2]From the secondary network's perspective, the licensed channel cannot be used if a PU is present. In other words, it is not a secondary network's concern which PU is operating in the spectrum. We assume a representative for the PUs; therefore, the secondary network cannot use the spectrum if a primary representative is present.

cooperating with that secondary network. Secondary users sense the primary channel to discover spectrum opportunities. Each secondary user is assumed to be equipped with a single identical antenna. We assume that the arrival and departure of the primary and secondary users' traffic are independent, continuous-time Poisson processes. Therefore, we can model the spectrum access process by a continuous-time Markov chain (CTMC) system. The primary users' traffic is modeled with two random processes. The service request is modeled as a Poisson process with arrival rate λ_P (s^{-1}), and the service duration (access duration) is negative-exponentially distributed with mean time $1/\mu_P$ (s), so the departure of the primary user's traffic is another Poisson process with departure rate μ_P (s^{-1}) [51]. Similarly, the arrival and departure rates of secondary user i ($1 \leq i \leq N$) are modeled as independent Poisson processes with λ_i (s^{-1}) and μ_i (s^{-1}) respectively.

We assume that the spectrum cannot be occupied by more than one user at any time, i.e., there is no overlap between any two users. Therefore, the spectrum access process is given by the model shown in Fig. 3.5. The state space vector $\mathbf{x}$ for the model is

$$\mathbf{x} = \{O, S_1, S_2, \ldots, S_N, P\}. \tag{3.1}$$

In (3.1), state O (idle) means no user operates in the spectrum, state P means the primary user operates in the spectrum, and state S_i means the ith secondary user operates

in the spectrum ($1 \leq i \leq N$). We assume the initial state of the system to be state O. As shown in Fig. 3.5, the system enters state P with arrival rate λ_P whenever the primary user appears, and it returns to state O with departure rate μ_P when the primary user's service is complete. While the system is in state O, and the ith secondary user enters into the spectrum, the system enters state S_i with arrival rate λ_i. In case the primary user arrives before the secondary user i's service is complete, the system transits to state P with arrival rate λ_P. Otherwise, the ith secondary user returns to state O with departure rate μ_i when its service is complete. In the CTMC, when the secondary users contend to access the idle spectrum using carrier sense multiple access, collisions occur only when their service requests arrive exactly at the same time; this case rarely happens for independent Poisson process [51]. Therefore, we disregard the collision state of the secondary users.

3.3   Derivation of the Steady-State Probabilities

The state space vector ($\mathbf{x}$) and the transition rate matrix $\mathbf{Q}$ are needed for a complete CTMC model definition [53]. The state space vector is defined in (3.1). The transition
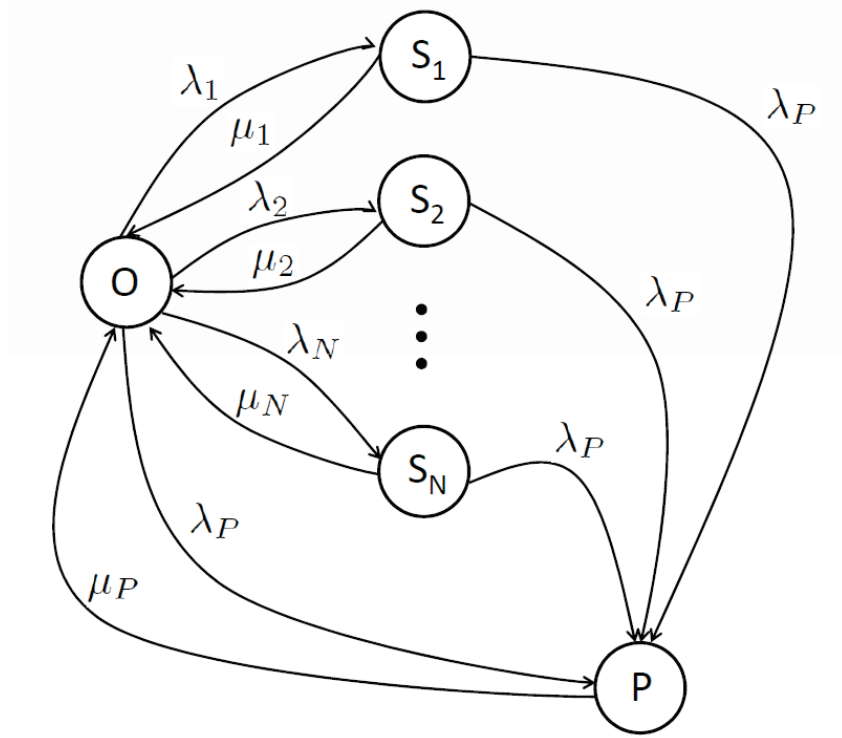
Figure 3.5: The state transition rate diagram for the proposed CTMC model.

rate matrix is obtained for the CTMC model shown in for Fig. 3.5, as follows:

$$
\mathbf{Q} =
\begin{bmatrix}
-(\lambda_1 + \lambda_2 + \ldots + \lambda_N + \lambda_P) & \lambda_1 & \lambda_2 & \ldots & \lambda_N & \lambda_P \\
\mu_1 & -(\mu_1 + \lambda_P) & 0 & \ldots & 0 & \lambda_P \\
\mu_2 & 0 & -(\mu_2 + \lambda_P) & \ldots & 0 & \lambda_P \\
\vdots & \vdots & \vdots & \ddots & \vdots & \vdots \\
\mu_N & 0 & 0 & \ldots & -(\mu_N + \lambda_P) & \lambda_P \\
\mu_P & 0 & 0 & \ldots & 0 & -\mu_P
\end{bmatrix}
\tag{3.2}
$$

In the derivation of (3.2), the following points have been taken into consideration:

31

- It is assumed that the system is stationary where all the transition probabilities, $P_{ij}(s,t) = P[x(t) = j|x(s) = i], (s \leq t, \text{and } i, j \in \mathbf{x})$, are independent of the absolute time instants s and t, and depend on only the time difference $(t - s)$ [54]. Therefore, the transition rate matrix $\mathbf{Q}(t)$ is independent of t, that is, $\mathbf{Q}(t) = \mathbf{Q}$.

- An off-diagonal element of the transition rate matrix, $(q_{ij}, (i \neq j))$, represents the Poisson process rate of transition from state i to state j.

- A diagonal element q_{ii}, $(1 \leq i \leq N + 2)$ is determined by

$$q_{ii} = - \sum_{all j, \ i \neq j} q_{ij}, \tag{3.3}$$

where $1 \leq j \leq N + 2$.

An important objective of Markov chain analysis is to determine the state probability vector $\mathbf{\Pi}(t) = [\Pi_0(t), \Pi_1(t), \Pi_2(t), \dots, \Pi_N(t), \Pi_P(t)]$, where the ith element of $\mathbf{\Pi}(t)$ is given by [55]

$$\Pi_i(t) = P[x(t) = i], \forall i \in \mathbf{x}. \tag{3.4}$$

The $\Pi_i(t)$ denotes the probability to find the system at state i at specific time instants. Now, we perform the steady-state analysis by assuming that system has been running long enough, and all parameters have achieved their steady state values [56]. Therefore

the steady-state probability of state i is

$$\Pi_i = \lim_{t\to\infty} \Pi_i(t), \tag{3.5}$$

The steady-state probability (SSP) vector ($\mathbf{\Pi}$) is determined by solving (3.6) and (3.7) given below:

$$\mathbf{\Pi Q = 0} \tag{3.6}$$

$$\sum_{\forall j \in \mathbf{x}} \Pi_j = 1 \tag{3.7}$$

The matrix equation in (3.6) can be expanded into a system of linear equations presented in (3.8-3.10), as follows:

$$-\Pi_0(\lambda_1 + \lambda_2 + \ldots + \lambda_N + \lambda_P) + \Pi_1\mu_1 + \Pi_2\mu_2 + \ldots + \Pi_N\mu_N + \Pi_P\mu_P = 0, \tag{3.8}$$

$$\Pi_0\lambda_i - \Pi_i(\mu_i + \lambda_P) = 0 \qquad (1 \le i \le N), \tag{3.9}$$

$$(\Pi_0 + \Pi_1 + \ldots + \Pi_N)\lambda_P - \Pi_P\mu_P = 0. \tag{3.10}$$

Substituting Π_P from (3.8) into (3.7), we get

$$\Pi_0 + \Pi_1 + \ldots + \Pi_N + \Pi_P = 1 \Rightarrow$$

$$\Pi_0 + \Pi_1 + \ldots + \Pi_N + \frac{\lambda_P}{\mu_P}(\Pi_0 + \Pi_1 + \ldots + \Pi_N) = 1 \Rightarrow$$

$$\Pi_0 + \Pi_1 + \ldots + \Pi_N = \frac{\mu_P}{\mu_P + \lambda_P}. \qquad (3.11)$$

Now, we substitute (3.9) into (3.11) to obtain Π_0:

$$\Pi_0 + \frac{\Pi_0 \lambda_1}{\mu_1 + \lambda_P} + \ldots + \frac{\Pi_0 \lambda_N}{\mu_N + \lambda_P} = \frac{\mu_P}{\mu_P + \lambda_P} \Rightarrow$$

$$\Pi_0(1 + \frac{\lambda_1}{\mu_1 + \lambda_P} + \ldots + \frac{\lambda_N}{\mu_N + \lambda_P}) = \frac{\mu_P}{\mu_P + \lambda_P} \Rightarrow$$

$$\Pi_0 = \frac{\mu_P}{(\mu_P + \lambda_P)(1 + \sum_{i=1}^{N} \frac{\lambda_i}{\mu_i + \lambda_P})}. \qquad (3.12)$$

Therefore, $\Pi_1, \Pi_2, \ldots, \Pi_N$ given by (3.9) are as follows:

$$\Pi_i = \frac{\lambda_i}{\mu_i + \lambda_P}\Pi_0 \qquad (1 \leq i \leq N), \qquad (3.13)$$

where Π_0 is given by (3.12).

Finally, we substitute (3.11) into (3.7) to derive Π_P as follows:

$$\Pi_P = 1 - \Pi_0 - \Pi_1 - \ldots - \Pi_N = 1 - \frac{\mu_P}{\mu_P + \lambda_P} = \frac{\lambda_P}{\mu_P + \lambda_P}. \qquad (3.14)$$

Therefore, the SSP vector is determined by (3.12)-(3.14). As shown in (3.14), the probability of being in state P is solely a function of the primary user parameters (λ_p and μ_p) as expected. However, the probability of being in state S_i (Π_i) is a function of both the primary and secondary user parameters as well as the number of secondary users (N).

3.4   Numerical Analysis

In this section, we perform numerical analysis to evaluate our model. First, we study a CR network with no active secondary user ($N = 0$), and compare the proposed model with an existing model in the literature. Second, we consider a CR network with three secondary users ($N = 3$) and examine the effects of the secondary users' arrival and departure rates on the SSP vector. Finally, we examine a case with a very large number of secondary users.

3.4.1   No Active Secondary User ($N = 0$)

Here, the proposed model is evaluated for a special case where ($N = 0$). Fig. 3.6-(a) depicts the state transition diagram in this case, where the state space vector is

$\mathbf{x} = \{O, P\}$. The SSP vector $\mathbf{\Pi} = [\Pi_0, \Pi_P]$ is given by (3.12) and (3.14) as follows:

$$\Pi_0 = \frac{\mu_P}{\mu_P + \lambda_P} \tag{3.15}$$

$$\Pi_P = \frac{\lambda_P}{\mu_P + \lambda_P} \tag{3.16}$$

In [1], the primary channel is modeled as an ON-OFF source alternating between ON (busy) and OFF (idle) periods, as shown in Fig. 3.6-(b). Two parameters (u) and $(1-u)$ have been defined in [1] as the fraction of time in which the primary channel is in ON and OFF respectively, as follows:

$$u = \frac{\lambda_{OFF}}{\lambda_{ON} + \lambda_{OFF}} \tag{3.17}$$

$$1 - u = \frac{\lambda_{ON}}{\lambda_{ON} + \lambda_{OFF}} \tag{3.18}$$

where λ_{OFF} and λ_{ON} are the inverse of the mean values of T_{OFF} and T_{ON} respectively, i.e., $E[T_{OFF}] = \frac{1}{\lambda_{OFF}}$ and $E[T_{ON}] = \frac{1}{\lambda_{ON}}$.

As can be seen in (3.15-3.18), Π_P and Π_0 in our model represent u and $(1 - u)$ in [1] respectively. Moreover, λ_{OFF} and λ_{ON} in [1] correspond to μ_P and λ_P respectively. Therefore, our proposed model at this special case $(N = 0)$ agrees with the model in [1]. Table 3.1 summarizes the above notations and results.

36
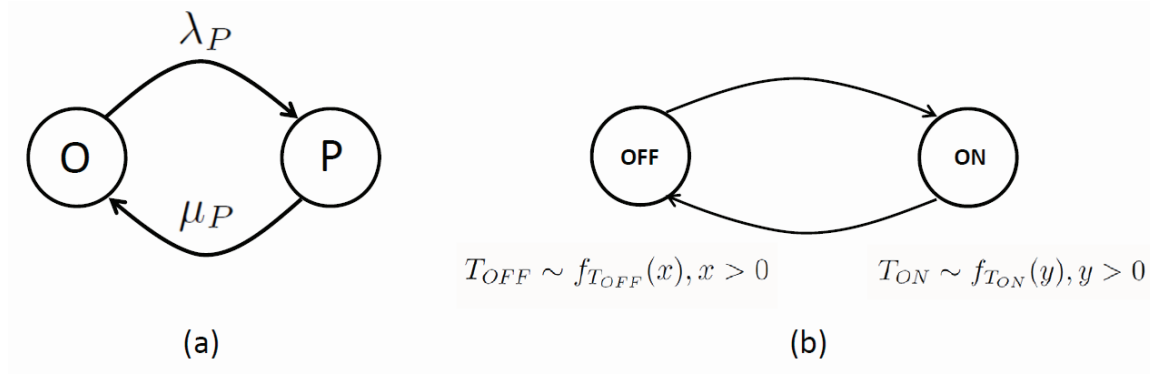
Figure 3.6: The state transition diagram in: (a) our model at $N = 0$, (b) the existing model in [1].

3.4.2 Three Secondary Users $(N = 3)$

Here, a CR network with three secondary users $(N = 3)$ is considered, where the state space vector is $\mathbf{x} = \{O, S_1, S_2, S_3, P\}$, and the state transition diagram is shown in Fig. 3.7. The secondary users' stationary state probabilities (Π_1, Π_2, Π_3) are given by (3.13), and Π_P is calculated by (3.14). For this case, we arbitrarily set the primary user's arrival and departure rates to be $\lambda_P = 2$ (s^{-1}) and $\mu_P = 4$ (s^{-1}) respectively, and investigate the effect of secondary users' parameters on the SSP vector for three cases as follows:

Table 3.1: The proposed model at $N = 0$ agrees with the existing model in [1].

The proposed model	Existing model [1]
μ_P	λ_{OFF}
λ_P	λ_{ON}
$\Pi_P = \frac{\lambda_P}{\lambda_P + \mu_P}$	$u = \frac{\lambda_{OFF}}{\lambda_{ON} + \lambda_{OFF}}$
$\Pi_0 = \frac{\mu_P}{\lambda_P + \mu_P}$	$1 - u = \frac{\lambda_{ON}}{\lambda_{ON} + \lambda_{OFF}}$

37
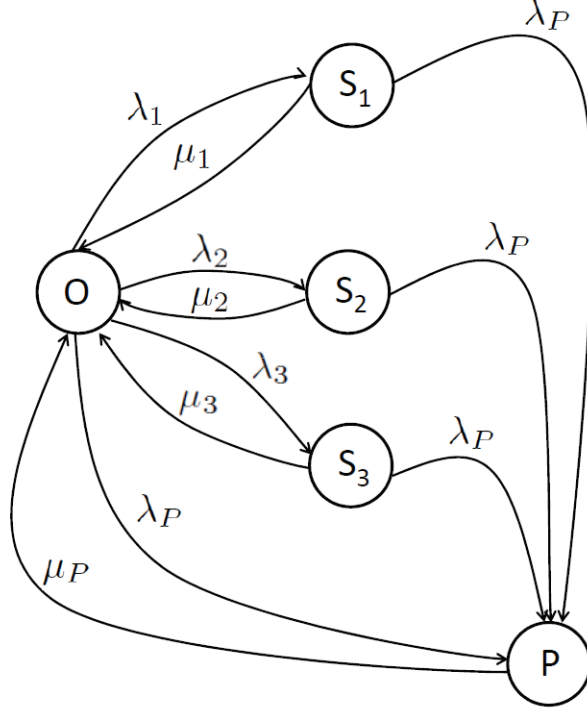
Figure 3.7: The state transition rate diagram for $N = 3$.

Case-I: Different Departure Rates and Identical Arrival Rates

We assume different departure rates $\mu_1 < \mu_2 < \mu_3$, and assume identical arrival rates $\lambda_1 = \lambda_2 = \lambda_3 = \lambda$. Thus, (3.13) simplifies to

$$\Pi_i = \frac{\lambda}{\mu_i + \lambda_P}\Pi_0 \qquad (1 \le i \le 3). \tag{3.19}$$

From the above equation, $\mu_1 < \mu_2 < \mu_3$ yields $\Pi_1 > \Pi_2 > \Pi_3$, which confirms that for a fixed value of λ, there is a higher probability to find the system at a state with lower departure rate (μ). Fig. 3.8 (a) shows the stationary state probabilities for a secondary

38

network with the following parameters, where the secondary user i is denoted by SU_i, and λ_i and μ_i are both in (s^{-1}).

$$SU_1 : \begin{cases} \lambda_1 = 3 \\ \\ \mu_1 = 2 \end{cases} , SU_2 : \begin{cases} \lambda_2 = 3 \\ \\ \mu_2 = 4 \end{cases} , SU_3 : \begin{cases} \lambda_3 = 3 \\ \\ \mu_3 = 6 \end{cases}$$

The SSP vector in this case is $\mathbf{\Pi} = [0.2540, 0.1905, 0.1270, 0.0952, 0.3333]$.

Case-II: Different Arrival Rates and Identical Departure Rates

We assume different arrival rates $\lambda_1 < \lambda_2 < \lambda_3$ but identical departure rates $\mu_1 = \mu_2 = \mu_3 = \mu$. Therefore, (3.13) simplifies to

$$\Pi_i = \frac{\lambda_i}{\mu + \lambda_P} \Pi_0 \qquad (1 \le i \le 3). \tag{3.20}$$

As shown in (3.20), $\lambda_1 < \lambda_2 < \lambda_3$ yields $\Pi_1 < \Pi_2 < \Pi_3$. This confirms that for a fixed value of μ, there is a higher probability to find the system at a state with larger arrival rate (λ). The secondary users' parameters are set as follows:

$$SU_1 : \begin{cases} \lambda_1 = 2 \\ \\ \mu_1 = 3 \end{cases} , SU_2 : \begin{cases} \lambda_2 = 4 \\ \\ \mu_2 = 3 \end{cases} , SU_3 : \begin{cases} \lambda_3 = 6 \\ \\ \mu_3 = 3 \end{cases}$$
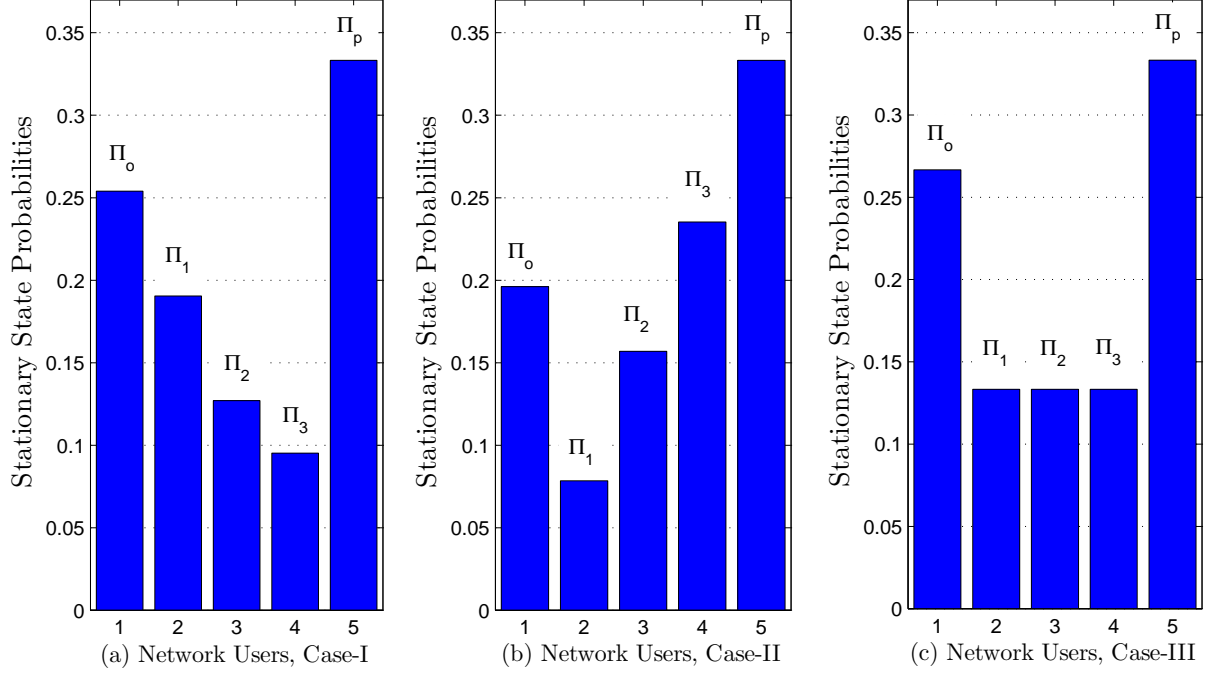
Figure 3.8: The stationary state probabilities for cases (a), (b), and (c).

The SSP vector is $\mathbf{\Pi} = [0.1961, 0.0784, 0.1569, 0.2353, 0.3333]$. Fig. 3.8 (b) shows the stationary state probabilities for this case.

Case-III: Identical Departure and Arrival Rates

In this part, we assume a secondary network where all secondary users have the same arrival rates ($\lambda_1 = \lambda_2 = \ldots = \lambda_N = \lambda$) and also have the same departure rates ($\mu_1 = \mu_2 = \ldots = \mu_N = \mu$). First, the SSP vector for a general case with N secondary users is derived. Then, we consider a secondary network with $N = 3$ users, and sketch the stationary state probabilities similar to the previous cases. Therefore, all the secondary

users have the same stationary state probabilities:

$$\Pi_i = \frac{\lambda \mu_P}{(\mu_P + \lambda_P)(\mu + \lambda_P + N\lambda)} \qquad (1 \leq i \leq N). \qquad (3.21)$$

Thus, for a CR network with $N = 3$ secondary users, and secondary users' parameters $\lambda = 4$ s^{-1} and $\mu = 6$ s^{-1}, the SSP vector is $\mathbf{\Pi} = [0.2667, 0.1333, 0.1333, 0.1333, 0.3333]$. Fig. 3.8 (c) shows the stationary state probabilities for this case.

Note that the primary user's stationary state probability (Π_P) presented in (3.14) is not a function of the number of secondary users (N) and the secondary users' parameters (λ and μ). Therefore, in all the above cases, Π_P has the same value $\Pi_P = 0.3333$.

3.4.3 Very Large Number of Secondary Users

Here, we consider a CR network with a very large number of secondary users ($N = 100$). Without loss of generality, we randomly select each secondary user's arrival and departure rates within $0.1 \leq \lambda_i \leq 5$ and $0.1 \leq \mu_i \leq 7.5$, and we set the primary user's parameters to be $\lambda_P = 2.5$ (s^{-1}) and $\mu_P = 5$ (s^{-1}). Secondary users' stationary state probabilities are determined by (3.12) and (3.13), and Π_P is given by (3.14).

In the CTMC model, the primary user is granted the highest priority to operate in the spectrum. Consequently, Π_P is independent of the number of secondary users (N),

41
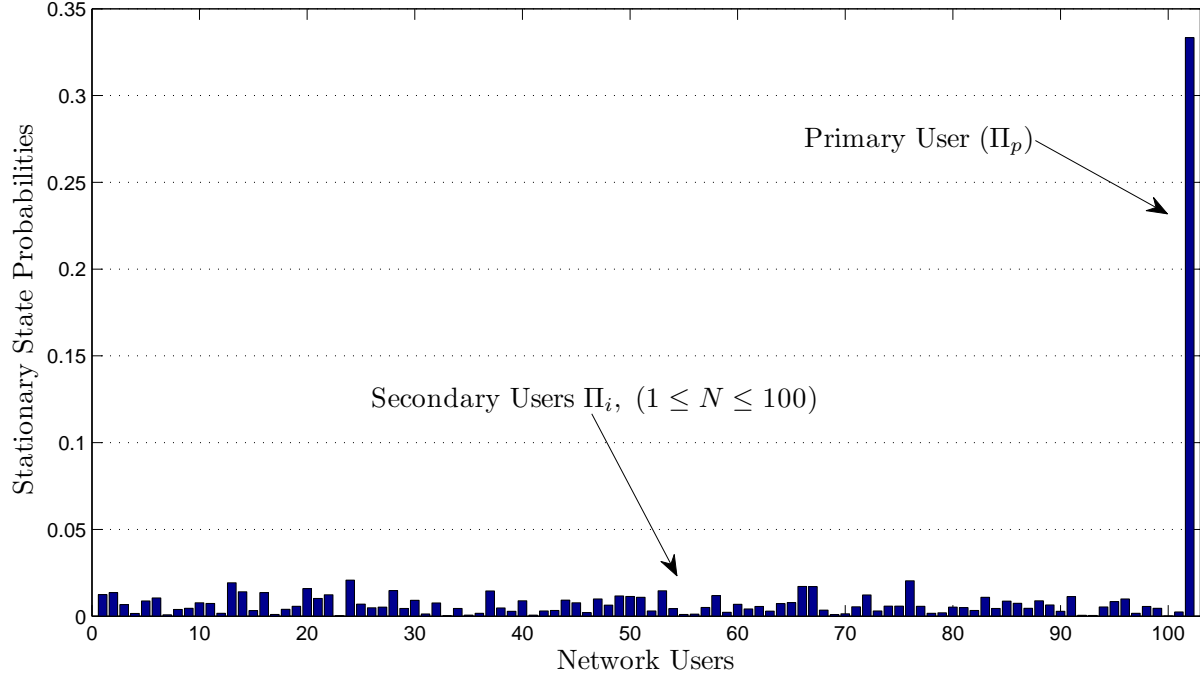
Figure 3.9: The stationary state probabilities in a secondary network with $N = 100$ SUs.

and does not change with a large N. As a result, the rest of the spectrum (which has not been used by the primary user) would be available for the secondary access. As shown in Fig. 3.9, due to the very large number of secondary users in this case ($N = 100$), the probability to find the system at each secondary state is quite small.

3.5   Summary

The modeling of the spectrum occupancy in a CR network was studied in this chapter. A continuous-time Markov chain (CTMC) was used to describe the spectrum occupation by both licensed and unlicensed users. By analytical work, we derived the transition rate

matrix and the probability state vector for the proposed model. In addition, numerical analysis was conducted to examine the proposed model, and to compare the proposed model with an existing model in the literature. We will use the CTMC model as a base model for further analysis in the following chapters.

Chapter 4

Application-Specific Spectrum

Sensing

4.1 Motivations

As the CR concept matures, CR networks are now envisioned to support a variety of applications, ranging from the smart grid, public safety and broadband cellular, and medical applications to wireless sensor networks (WSNs) [11, 57–59]. For instance, in the aerospace industry, major aircraft manufacturers and many supply research groups have shown strong interest in development and standardization of sensor networks for onboard use within aircraft, e.g., the "Wireless Avionics Intra-Communications (WAIC)" project by the Aerospace Vehicle System Institute. The WAIC refers to radio communication

between two or more points within a single aircraft (not air-to-ground or air-to-air) [60]. Table 4.1 shows several examples of WAIC applications. As depicted, different applications have various design requirements; for instance, a sensor network for temperature monitoring requires a low data rate link while some other application may require a high data rate link. From another point of view, an engine prognostic sensor network may have a high *probability of presence* due to its large data arrival rate, while a tire pressure sensor network may have a low probability of presence due to its small data arrival rate.

While a CR network is supposed to change its parameters according to the characteristics of both primary and secondary network environments, most existing algorithms consider only the primary network's characteristics to obtain the optimum sensing period. This implies that the optimum sensing period would be identical for diverse CR applications, while their characteristics could be vastly different. For instance, Fig. 4.1 compares a non-application-specific sensing approach with an application-specific sensing scheme in CR. The PU's properties are assumed to be the same for the two types of the secondary applications. As shown, in a non-application-specific approach, the sensing

Table 4.1: A few examples of sensor networks in the WAIC project.

Application Type	Low Data Rate	High Data Rate
Sensing	Fuel Tank, Temperature	Engine Prognostic, Structural Health Monitoring
Control and Communication	Cabin Functions	Avionics Communications Bus

period is identical for both applications. On the other hand, in the application-specific sensing method, the sensing period is selected to be greater for an application that has a lower probability of presence. This results in significant improvement in the usage of the CR network's valuable resources such as time and energy.

The desired sensing method, therefore, must distinguish different types of secondary applications, and provide a customized solution for each type. In this chapter, we propose an application-specific spectrum sensing method that considers both secondary and primary users characteristics, and accurately finds the optimum sensing period. The proposed method aims to reduce the cognitive network's energy consumption by avoiding unnecessary sensing tasks, while meeting the sensing requirements. To the best of our knowledge, this is the first work showing that significant power consumption can be obtained by considering the properties of both primary and secondary networks in cognitive radio.

4.2   Energy Detection Method

Recently, a number of methods have been proposed for spectrum sensing, including energy detection, matched filter detection, and cyclostationary feature detection. Among these methods, energy detection is the most popular spectrum sensing technique due to its
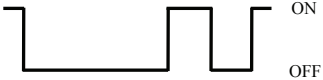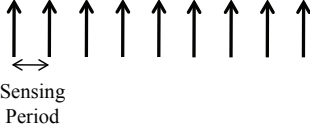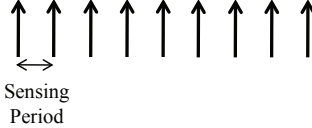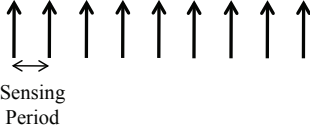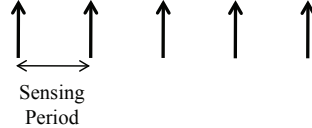
Figure 4.1: Non-application-specific spectrum sensing vs. application-specific spectrum sensing in CR. The PU's properties are assumed to be the same for the two types of applications.

simplicity of hardware implementation and low signal processing cost [16, 61–66]. In this work, we choose energy detection method as our spectrum sensing method for a CSN. An energy detector measures the energy received on a primary channel and decides on the existence of the PU by comparing it with a system threshold. A basic hypothesis model for the model can be defined as follows [21]:

$$
r_i(n) = \begin{cases} n_i(n) & : H_0 \\ k_i(n)s(n) + n_i(n) & : H_1 \end{cases} \tag{4.1}
$$

where $r_i(n)$ is the discrete received signal at the ith secondary user during the nth sensing

task, $s(n)$ is the transmitted signal by the PU, $n_i(n)$ is the additive white Gaussian noise at the ith SU, and $k_i(n)$ is the channel gain of the sensing channel between the ith SU and the PU. Both $n_i(n)$ and $s(n)$ are assumed to be real-value and i.i.d. random processes with zero mean and variance σ_n^2 and σ_s^2 respectively. Moreover, the transmitted signal is assumed to be independent of the noise $n_i(n)$. H_0 is a null hypothesis, which states that the PU is absent in a certain spectrum band. On the other hand, H_1 is the alternative hypothesis, which indicates that there exists the licensed user's signal.

In this method, the received signal is first pre-filtered by an ideal bandpass filter, and the output of the filter is then squared and integrated over a time interval called observation time T_O to produce the following test statistic:

$$Y_i = \frac{1}{M} \sum_{n=1}^{M} |r_i(n)|^2 \tag{4.2}$$

where, M is number of received samples within T_O. It can be shown that the test statistic Y has a Chi-square distribution [67]. However, assuming the number of samples (M) is large, the Chi-square distribution, based on the central limit theorem, can be closely approximated by a Gaussian distribution [68]. The test statistic is then as follows:

$$Y \sim \begin{cases} \mathcal{N}(M\sigma_n^2, 2M\sigma_n^4), & : H_0 \\ \mathcal{N}\left(M(\sigma_n^2 + \sigma_s^2), 2M(\sigma_n^2 + \sigma_s^2)^2\right) & : H_1 \end{cases} \tag{4.3}$$

48

where, $\mathcal{N}(\mu, \sigma^2)$ is the Gaussian distribution function with mean and variance μ and σ^2 respectively. In the above hypothesis testing, the probability of false alarm $P_f = \Pr[Y > \epsilon|H_0]$, and the probability of detection $P_d = \Pr[Y > \epsilon|H_1]$ can be expressed as follows:

$$P_f = Q\Big(\frac{\epsilon - M\sigma_n^2}{\sigma_n^2\sqrt{2M}}\Big), \tag{4.4}$$

$$P_d = Q\Big(\frac{\epsilon - M(\sigma_s^2 + \sigma_n^2)}{(\sigma_s^2 + \sigma_n^2)\sqrt{2M}}\Big) \tag{4.5}$$

where $Q(x) = \frac{1}{\sqrt{2\pi}}\int_x^\infty \exp(-\frac{u^2}{2})du$ is the Q-function, and ϵ is the decision threshold to decide on the presence or absence of the PU.

Note that in the energy detection method, the RF front-end cannot differentiate between the primary and secondary signals. In addition, it is assumed that SUs cannot perform the transmission and sensing tasks at the same time. Therefore, it is necessary to periodically perform the spectrum sensing task [12].

4.3 Application-Specific Spectrum Sensing

The proposed method is based on the continuous time Markov chain (CTMC) presented in Chapter 3. As shown in Fig. 4.2, the operation of both secondary and primary networks can be divided into three states. During the *idle* state, neither the secondary nor the primary network operates in the spectrum. The secondary network operates in

the spectrum within the *secondary network transmission* state, and the PU operates in the spectrum within the *primary user transmission* state. We assume without loss of generality a homogenous CSN with N secondary users, where each SU has the same arrival rates $\lambda_1 = \lambda_2 = \cdots \lambda_N = \lambda_s$ and also has the same departure rates $\mu_1 = \mu_2 = \cdots \mu_N = \mu_s$. Hence, the probability of being at the idle state Π_0, secondary network transmission state Π_s, and the primary user transmission state Π_P are given by (see Chapter 3):

$$\Pi_0 = \frac{\mu_P}{(\mu_P + \lambda_P)(1 + \frac{N\lambda_s}{\mu_s + \lambda_P})}, \tag{4.6}$$

$$\Pi_s = \frac{\lambda_s}{\mu_s + \lambda_P}\Pi_0, \tag{4.7}$$

$$\Pi_P = \frac{\lambda_P}{\mu_P + \lambda_P}. \tag{4.8}$$

During the secondary network transmission state, the secondary network must stop data transmission every T_T seconds and perform the sensing task. If the result of the sensing task suggests that the PU is present, the secondary network must immediately vacate the spectrum. However, if the sensing task suggests that the PU is still absent, the secondary network will continue to operate in the spectrum for another T_T seconds. The sensing period (T_{PT}) in the secondary network transmission state is then obtained by

$$T_{PT} = T_O + T_T \tag{4.9}$$
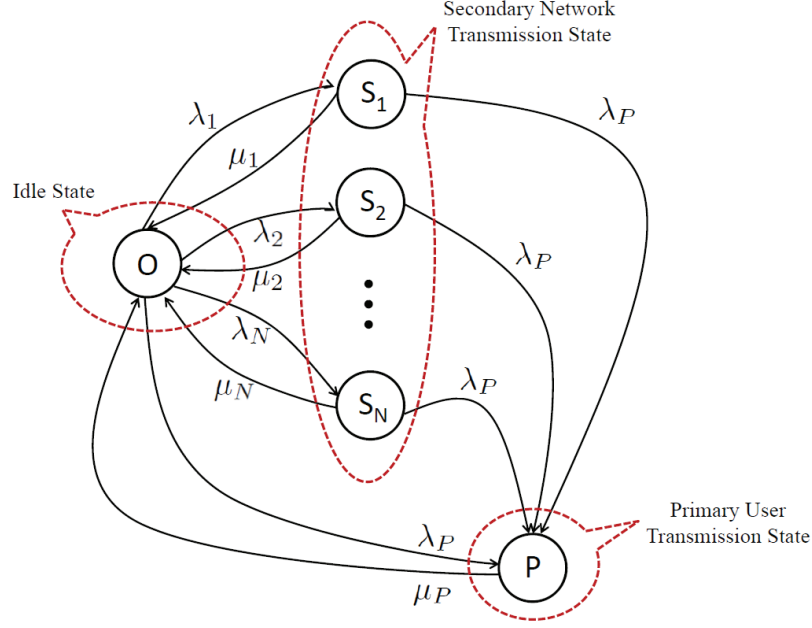
Figure 4.2: The operation of the CSN is divided into three states: idle, secondary network transmission, and primary user transmission.

where T_O is the observation time.

If the CSN is at the idle state, the sensing task is performed every T_{PI} seconds to detect the spectrum opportunities. Therefore, the T_{PI} is given by

$$T_{PI} = T_O + T_I. \tag{4.10}$$

4.3.1 Problem Definitions

- **Definition 1:** During the secondary network transmission state, the *interference ratio R_I* is defined as the expected fraction of the primary user transmission state interrupted by the transmission of the secondary network, which will be derived

51

in (4.19). The *interference ratio threshold* R_I^{th} is a predefined system parameter which denotes the maximum acceptable R_I.

- **Definition 2:** Within the idle state, the *undetected opportunity ratio* R_U is defined as the expected fraction of the spectrum opportunity undetected by the secondary network, which will be derived in (4.24). The *undetected opportunity threshold* R_U^{th} is a predefined system parameter that denotes the maximum acceptable R_U.

4.3.2 Derivation of R_I and R_U

In this section, we derive the interference ratio and undetected opportunity ratio for the proposed method. Fig. 4.3 depicts a tree-diagram to fully illustrate the situations where a partial or complete interference, undetected opportunity, or secondary network transmission may occur[1].

In Fig. 4.3, the probability that the PU operates in the spectrum is denoted by Π_P. Therefore, the probability that the PU does not operate in the spectrum is $(1 - \Pi_P)$. In addition, the probability that the secondary network is at the transmission state is given by $\sum_{i=1}^{N} \Pi_i$. Thus, the probability that the secondary network does not operate in the spectrum is given by $(1 - \sum_{i=1}^{N} \Pi_i)$. The hypothesis testing probabilities will be as follows:

---

[1]We assume that the secondary users share the licensed channel with a predefined medium access control protocol.

PU activity changes

$1 - e^{\frac{-T_T}{\mu_P}}$

$\pi_P.T_T$

0   T_T

Case-A: I_1 and T_1

SN has data, and starts transmission

$\sum_{i=1}^{N} \Pi_i$

PU activity does not change

$e^{\frac{-T_T}{\mu_P}}$

T_T

0   T_T

Case-B: I_2

Incorrect sensing

$Pr[0|1] = 1 - P_d$

SN has no traffic

$1 - \sum_{i=1}^{N} \Pi_i$ ✕

PU is present

Π_P

SN has data, but does not transmit

$\sum_{i=1}^{N} \Pi_i$

PU activity changes

$1 - e^{\frac{-T_I}{\mu_P}}$

$(1 - \pi_P).T_I$

0   T_I

Case-C: U_1

Correct sensing

$Pr[1|1] = P_d$

PU activity does not change

$e^{\frac{-T_I}{\mu_P}}$

T_I

0   T_I

Case-D: Neither I. nor U.

SN has no traffic

$1 - \sum_{i=1}^{N} \Pi_i$ ✕

SN has data, and starts transmission

$\sum_{i=1}^{N} \Pi_i$

PU activity changes

$1 - e^{\frac{-T_T}{\lambda_P}}$

$\pi_P.T_T$

0   T_T

Case-E: I_3 and T_2

Correct sensing

$Pr[0|0] = 1 - P_f$

PU activity does not change

$e^{\frac{-T_T}{\lambda_P}}$

0

0   T_T

Case-F: T_3

SU has no traffic

$1 - \sum_{i=1}^{N} \Pi_i$ ✕

PU is absent

$1 - \Pi_P$

SN has data, but does not transmit

$\sum_{i=1}^{N} \Pi_i$

PU activity changes

$1 - e^{\frac{-T_I}{\lambda_P}}$

$(1 - \pi_P).T_I$

0   T_I

Case-G: U_2

Incorrect sensing

$Pr[1|0] = P_f$

PU activity does not change

$e^{\frac{-T_I}{\lambda_P}}$

T_I

0   T_I

Case-H: U_3

SN has no traffic

$1 - \sum_{i=1}^{N} \Pi_i$ ✕

SN: Secondary network

Figure 4.3: Illustration of cases of interference, undetected spectrum opportunity, and interference-free transmission time in the hybrid spectrum sensing.

- P_d is the probability that the sensing result suggests that the PU is present, given that the PU is present.

- $\Pr[0|1] = 1 - P_d$ is the probability that the sensing result suggests that the PU is absent, given that the PU is present.

- P_f is the probability that the sensing result suggests that the PU is present, given that the PU is absent.

- $\Pr[0|0] = 1 - P_f$ is the probability that the sensing result suggests that the PU is absent, given that the PU is absent.

The probability that the PU's state varies within the transmission time T_T is also derived. If the PU is present, the probability that it continues to operate in the spectrum for T_T seconds is

$$\Pr[t > T_T | PU : \ present] = 1 - \Pr[t \le T_T | PU : \ present] \qquad (4.11)$$

$$= 1 - (1 - e^{-\frac{T_T}{\mu_P}}) = e^{-\frac{T_T}{\mu_P}}.$$

If the PU is present, the probability of at least one transition of the PU's state within T_T seconds is the complement event of (4.11). Therefore,

$$\Pr[t < T_T | PU : \ present] = 1 - e^{-\frac{T_T}{\mu_P}}. \qquad (4.12)$$

Similar to the above calculation, the probability that the PU's state varies within the idle time T_I can be derived by substituting T_I for T_T in (4.11) and (4.12).

If the PU is absent, the probability that the PU continues to be absent for T_T seconds is

$$\Pr[t > T_T | PU : \; absent] = e^{-\frac{T_T}{\lambda_P}}. \tag{4.13}$$

Therefore,, if the PU is absent, the probability of at least one transition of the PU's activity within T_T seconds is the complement event of (4.13), as follows:

$$\Pr[t < T_T | PU : \; absent] = 1 - e^{-\frac{T_T}{\lambda_P}}. \tag{4.14}$$

Equations (4.13) and (4.14) hold for cases where the CSN is at the idle state by substituting T_I for T_T.

As shown in Fig. 4.3, the secondary network will interrupt the primary user's activity at Case-A, Case-B and Case-E, as follows: The PU is operating in the spectrum, but the secondary network's sensing result suggests that the PU is absent (incorrect sensing result). In addition, the secondary network has data to send and starts data transmission for T_T seconds. This will cause interference with the primary network. Based on the PU's activity, two cases can occur as follows:

- Fig. 4.3 Case-A: If the PU's state changes at least once during the transmission

55

time (T_T), a partial interference happens (I_1). Therefore, the expected interference in this scenario can be expressed as

$$E[I_1] = \Pi_P \mathrm{Pr}[0|1](\sum_{i=1}^{N} \Pi_i)(1 - e^{-\frac{T_T}{\mu_P}})\Pi_P T_T. \tag{4.15}$$

- Fig. 4.3 Case-B: If the PU's state does not change during the transmission time, a complete interference occurs (I_2), and the secondary network will interfere with the PU during the whole transmission period $(T_T$ seconds). Therefore, the expected interference in this case is given by

$$E[I_2] = \Pi_P \mathrm{Pr}[0|1](\sum_{i=1}^{N} \Pi_i)(e^{-\frac{T_T}{\mu_P}})T_T. \tag{4.16}$$

A partial interference also happens under the following scenario: The PU is not operating in the spectrum, and the secondary network correctly detects the absence of the PU. In addition, the secondary network has data to send; therefore it starts data transmission for T_T seconds. However, the PU's state varies from the OFF state to the ON state during the transmission time, and causes a partial interference. Hence, the expected interference when the PU is initially absent during the transmission time T_T,

can be expressed as

$$E[I_3] = (1 - \Pi_P)\Pr[0|0](\sum_{i=1}^{N} \Pi_i)(1 - e^{-\frac{T_T}{\lambda_P}})\Pi_P T_T. \tag{4.17}$$

Finally, we obtain the interference ratio R_I as follows:

$$R_I = \frac{E[I_1] + E[I_2] + E[I_3]}{T_T \Pi_P} \tag{4.18}$$

where $E[I_1]$, $E[I_2]$, and $E[I_3]$ are derived in (4.15), (4.16), and (4.17) respectively. After some algebraic manipulation, R_I is obtained by

$$R_I = (\sum_{i=1}^{N} \Pi_i)\Big\{(1 - P_d)\Big(e^{-\frac{T_T}{\mu_P}}(1 - \Pi_P) + \Pi_P\Big) + (1 - \Pi_P)(1 - P_f)(1 - e^{-\frac{T_T}{\lambda_P}})\Big\}. \tag{4.19}$$

In addition, as depicted in Fig. 4.3, the spectrum opportunities will be undetected by the secondary network at the following circumstances:

- Fig. 4.3 Case-C: The PU is operating in the spectrum, and the secondary network correctly detects the presence of the PU. The secondary network has data to send, but it cannot start data transmission due to the result of the spectrum sensing. Therefore, the secondary network goes to the idle state for T_I seconds. However, the PU's state changes from the ON state to the OFF state within this period, so

the new opportunity will be undetected (U_1). The expected undetected spectrum opportunity in this case can be expressed as follows:

$$E[U_1] = \Pi_P \text{Pr}[1|1] (\sum_{i=1}^{N} \Pi_i)(1 - e^{-\frac{T_i}{\mu_P}})(1 - \Pi_P)T_I. \qquad (4.20)$$

There are also undetected spectrum opportunities at the following scenarios: The PU is not operating in the spectrum, but the secondary network suggests that the PU is present (incorrect sensing result). In addition, the secondary network has data to send, but it cannot perform data transmission due to the spectrum sensing result. Therefore, the secondary network goes to the idle state for T_I seconds. Based on the PU's activity, there will be two cases:

- Fig. 4.3 Case-G, PU's state changes during the idle time (T_I). Hence, a partial spectrum opportunity will occur (U_2). The expected undetected spectrum opportunity in this case can be expressed as follows:

$$E[U_2] = (1 - \Pi_P)\text{Pr}[1|0](\sum_{i=1}^{N} \Pi_i)(e^{-\frac{T_i}{\lambda_P}})T_I. \qquad (4.21)$$

- Fig. 4.3 Case-H: The PU's state does not change within the idle time (T_I), and the entire spectrum opportunity will be undetected (U_3). The expected undetected

spectrum opportunity in this case is given by

$$E[U_3] = (1 - \Pi_P)\Pr[0|0](\sum_{i=1}^{N}\Pi_i)(1 - e^{-\frac{T_T}{\lambda_P}})\Pi_P T_T. \tag{4.22}$$

We obtain the undetected opportunity ratio R_U as follows:

$$R_U = \frac{E[U_1] + E[U_2] + E[U_3]}{(1 - \Pi_P)T_I} \tag{4.23}$$

where $E[U_1]$, $E[U_2]$, and $E[U_3]$ are derived in (4.20), (4.21), and (4.22) respectively. After some algebraic manipulation, R_U is derived by

$$R_U = (\sum_{i=1}^{N}\Pi_i)\left\{P_f\left(\mu_P e^{-\frac{T_I}{\lambda_P}} + 1 - \Pi_P\right) + \Pi_P P_d(1 - e^{-\frac{T_I}{\mu_P}})\right\}. \tag{4.24}$$

4.3.3   Throughput Analysis

An important objective of dynamic spectrum allocation is to obtain a high throughput for the secondary network in a statistical sense. The more frequently the available spectrum is used by the secondary network, the more efficiently the CSN will perform. The maximal data rate of the ith secondary user is given by [69]

$$r_i = W \log_2(1 + \frac{P_i G_i}{n_0}) \tag{4.25}$$

59

where W is the communication bandwidth, P_i is the transmission power of user i, n_0 is the power of the additive white Gaussian noise (AWGN), and G_i is the channel gain for user i. Without loss of generality, we assume a homogenous CSN where all SUs achieve r_s, the maximal data rate of each SU.

We consider the interference-free secondary network's transmission for accurate throughput analysis. As shown in Fig. 4.3, the secondary network transmission can occur in one of the following circumstances:

- Fig. 4.3 Case-A: The PU is operating in the spectrum, but the secondary network's sensing result suggests that the PU is absent (incorrect sensing result). Also, the secondary network has data to send. Based on the sensing result, therefore, the secondary network starts data transmission for T_T seconds. This will cause interference with the PU's data transmission. However, if the PU's state changes during the transmission time, a partial interference-free secondary network's transmission happens (T_1). Therefore, the expected interference-free transmission in this case can be expressed as follows:

$$E[T_1] = \Pi_P \Pr[0|1] (\sum_{i=1}^{N} \Pi_i)(1 - e^{-\frac{T_T}{\mu_P}})(1 - \Pi_P T_T).$$

(4.26)

In addition, there are interference-free transmission cases as follows: the PU is not

operating in the spectrum, and the secondary network correctly detects the absence of

the PU. In addition, the secondary network has data to send; therefore, it starts data

transmission for T_T seconds. Based on the PU's activity, two cases can occur:

- Fig. 4.3 Case-E: if the PU's state varies from the OFF to the ON state during

  the transmission time, a partial interference will happen. Hence, the expected

  interference-free transmission in this case is given by

$$E[T_2] = (1 - \Pi_P)\Pr[0|0](\sum_{i=1}^{N}\Pi_i)(1 - e^{-\frac{T_T}{\lambda_P}})(1 - \Pi_P T_T). \qquad (4.27)$$

- Fig. 4.3 Case-F: a complete interference-free transmission can happen if the PU's

  state does not change during the transmission time T_T. The expected transmission

  in this case is obtained by

$$E[T_3] = (1 - \Pi_P)\Pr[0|0](\sum_{i=1}^{N}\Pi_i)(e^{-\frac{T_T}{\lambda_P}})T_T. \qquad (4.28)$$

After some algebraic manipulation, the average interference-free transmission time

$E[T_{NI}] = E[T_1] + E[T_2] + E[T_3]$ is derived as,

$$E[T_{NI}] = (\sum_{i=1}^{N}\Pi_i)\Big\{\Pi_P(1 - P_d)(1 - e^{-\frac{T_T}{\mu_P}})(1 - \Pi_P T_T) + (1 - \Pi_p)(1 - P_f) \qquad (4.29)$$

$$\times \Big((1 - e^{-\frac{T_T}{\lambda_P}})(1 - \Pi_P T_T) + (e^{-\frac{T_T}{\lambda_P}}).T_T\Big)\Big\}.$$

61

We define the average throughput of the secondary network as

$$\Gamma_s = r_s E[T_{NI}] \tag{4.30}$$

where r_s is given in (4.25).

4.3.4   Energy Consumption Analysis

The secondary network's energy consumption consists of three elements: The energy consumption to perform the sensing task E_s, the energy consumption for the data transmission E_t, and the energy consumption during the idle state E_{id}. In this work, we do not consider E_{id} as it is relatively small. Moreover, in contrast to the throughput analysis, where only the interference-free secondary network's transmission is considered, both interfered and non-interfered data transmission must be considered for the energy consumption calculation. In other words, both interfered and non-interfered data transmission will drain the secondary network's energy sources. As shown in Fig. 4.3, the probability that the secondary network's transmission state (both interfered and non-

interfered) $\Pr[T]$ can be derived as

$$\Pr[T] = \Pi_P(1 - P_d)(\sum_{i=1}^{N} \Pi_i) + (1 - \Pi_P)(1 - P_f)(\sum_{i=1}^{N} \Pi_i) \qquad (4.31)$$

$$= (\sum_{i=1}^{N} \Pi_i)\Big(\Pi_P(1 - P_d) + (1 - \Pi_P)(1 - P_f)\Big).$$

Therefore, the total energy consumption of the secondary network $E = E_s + E_t$ is given by,

$$E = \Big(\frac{T_{sim}}{E[T_P]}\Big)E_{s0} + \Big(T_{sim}.\Pr[T]\Big)P_{t0} \qquad (4.32)$$

where E_{s0} is the unit energy consumption for each sensing task (J), P_{t0} is the unit transmission power (J/S), and T_{sim} is the simulation time. In addition, the average of the sensing period $E[T_P]$ will be derived in (4.35). The total power consumption of the secondary network is obtained by $P = \frac{E}{t_{sim}}$.

4.3.5 Problem Formulation

According to the CTMC model shown in Fig. 4.2, the secondary network will be either at the *idle* state or at the *transmission* state. Hence, the CSN's objectives will be set for each of these states as follows:

4.3.5.1 Secondary Network Transmission State

If the secondary network is at the transmission state, the objective will be to maximize the duration of data transmission T_T. However, it is more likely to interfere with the PU when the transmission time increases. Therefore, T_T is allowed to increase only until the interference ratio reaches a predefined threshold value (R_I^{th}). Hence, in this state, the spectrum sensing problem is defined as follows:

Maximize: T_T^*

Subject to: $R_I \leq R_I^{th}$

where T_T^* is the optimal transmission time. Moreover, the optimum sensing period within the secondary network transmission state is then $T_{PT}^* = T_O + T_T^*$.

Note that R_I is an increasing function with respect to T_T; i.e., $\frac{dR_I}{dT_T} > 0$. Hence, at the maximum T_T, the interference ratio will be equal to the largest possible amount (R_I^{th}). Therefore, an exhaustive search over T_T from T_O to the first value that satisfies $R_I \leq R_I^{th}$ is employed to find T_T^*.

Proposition 1: R_I is a monotonically increasing function of T_T.

Proof: Differentiate R_I w.r.t. T_T; after some algebraic manipulation we have,

$$(\frac{1-P_f}{1-P_d})(\frac{\mu_P}{\lambda_P})e^{(\frac{1}{\mu_P}-\frac{1}{\lambda_P})T_T} > 0. \tag{4.33}$$

Therefore, R_I is a monotonically increasing function of T_T.

4.3.5.2 Secondary Network Idle State

If the CSN is at the idle state, the objective is to maximize the duration of the idle time T_I. It is expected that the energy consumption associated with the sensing task will be reduced by decreasing the sensing frequency. However, a large idle time increases the chance of missing spectrum opportunities. Therefore, T_I can only increase when the undetected opportunity ratio is below the predefined threshold (R_U^{th}). The spectrum sensing problem in this case is then defined as

Maximize: T_I^*

Subject to: $R_U \leq R_U^{th}$

where, T_I^* is the optimal idle time. In addition, the optimum sensing period when the secondary network is at the idle state will be $T_{PI}^* = T_O + T_I^*$.

Similar to the previous case, R_U is an increasing function with respect to T_I; i.e., $\frac{dR_U}{dT_I} > 0$. Hence, at the maximum T_I, the undetected opportunity ratio will have the largest possible value (R_U^{th}). Therefore, an exhaustive search over T_I from T_O to the first value that satisfies $R_U \leq R_U^{th}$ can be employed to find T_I^*.

Proposition 2: R_U is a monotonically increasing function of T_I.

Proof: Differentiate R_U w.r.t. T_I; after some algebraic manipulation we have

$$(\frac{P_d}{P_f})(\frac{\lambda_P}{\mu_P})e^{(\frac{1}{\lambda_P} - \frac{1}{\mu_P})T_I} > 0. \tag{4.34}$$

Therefore, R_U is a monotonically increasing function of T_I.

4.3.5.3   Optimum Sensing Period

As noted before, the secondary network is at the idle state with the probability of Π_0, and at the transmission state with the probability of $\sum_{i=1}^{N} \Pi_i$. Therefore, the average of the optimum sensing period is given by,

$$E[T_P^*] = \Pi_0 T_{PI}^* + (\sum_{i=1}^{N} \Pi_i)T_{PT}^*. \tag{4.35}$$

4.4   Non-Application-Specific Spectrum Sensing

In this section, a non-application-specific approach for spectrum sensing is presented for comparison purpose. In contrast with the hybrid method, where the properties of both PU and SUs are considered, a non-hybrid method solely considers the properties of the PU to find the optimal sensing period. Since the properties of SUs are unknown in this method, it is assumed that in an event of interference, SUs interfere with the PU over

the entire transmission time. Moreover, SUs miss the entire opportunity in an event of undetected spectrum opportunity. Fig. 4.4 depicts a tree-diagram to illustrate when interference and undetected spectrum opportunities happen in the non-hybrid scheme.

Similar to the hybrid method, the interference ratio R_I^{NH} and the undetected opportunity ratio R_U^{NH} in the non-hybrid method can be derived as follows:

$$R_I^{NH} = (1 - P_d)\left(e^{-\frac{T_T}{\mu_P}}(1 - \Pi_P) + \Pi_P\right) + (1 - \Pi_P)(1 - P_f)(1 - e^{-\frac{T_T}{\lambda_P}}), \qquad (4.36)$$

$$R_U^{NH} = P_f\left(\mu_P e^{-\frac{T_I}{\lambda_P}} + 1 - \Pi_P\right) + \Pi_P P_d(1 - e^{-\frac{T_I}{\mu_P}}). \qquad (4.37)$$

In addition, similar to the hybrid method, the average throughput of the secondary network can be written as

$$\Gamma_s^{NH} = r_s E[T_{NI}^{NH}] \qquad (4.38)$$

where r_s is given in (4.25), and $E[T_{NI}^{NH}]$ is derived by

$$E[T_{NI}^{NH}] = \Pi_P(1 - P_d)(1 - e^{-\frac{T_T}{\mu_P}})(1 - \Pi_P T_T) \qquad (4.39)$$

$$+(1 - \Pi_p)(1 - P_f)\left((1 - e^{-\frac{T_T}{\lambda_P}})(1 - \Pi_P T_T) + (e^{-\frac{T_T}{\lambda_P}}).T_T\right).$$

Moreover, similar to the hybrid method, the total energy consumption of the sec-
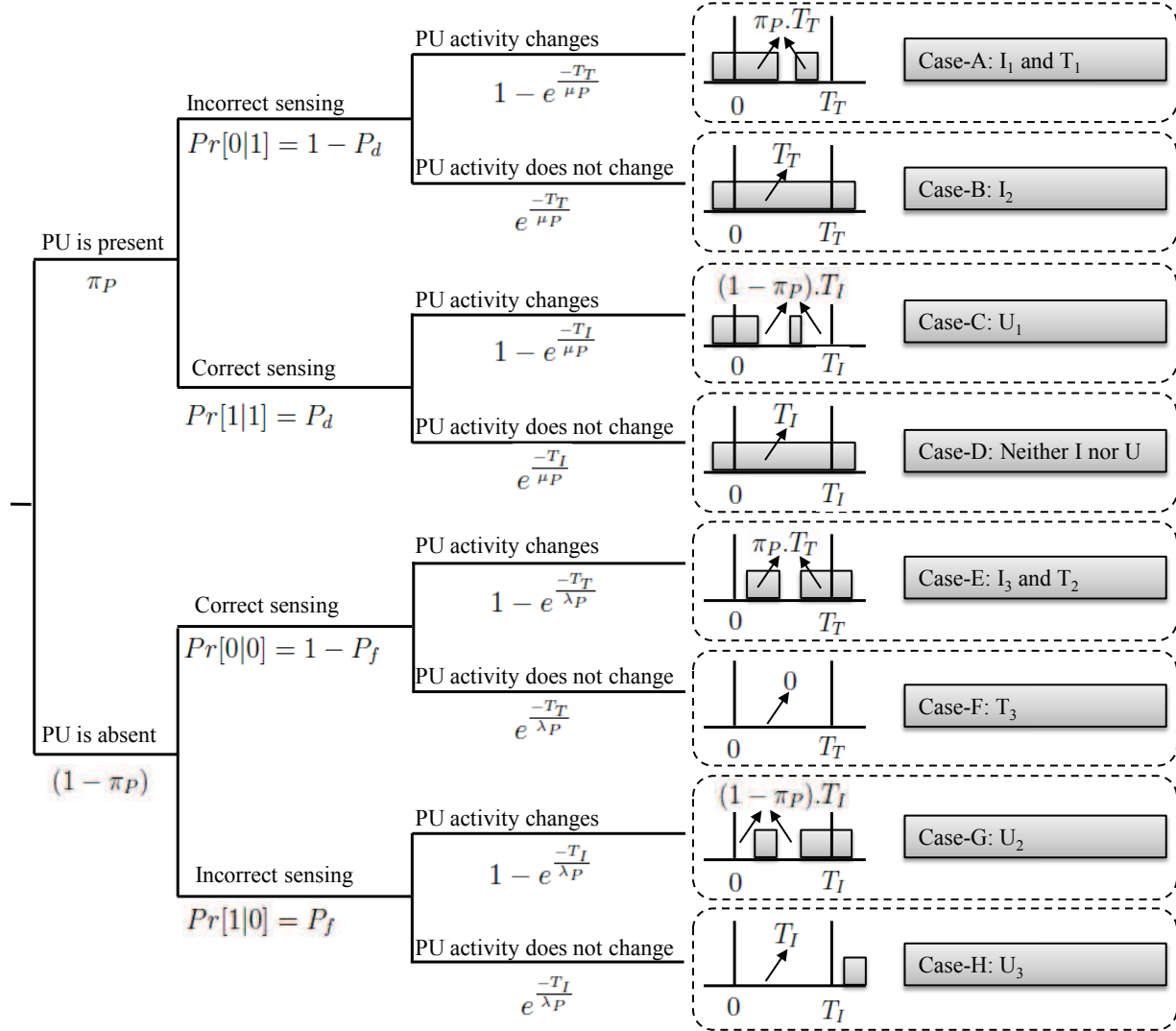
Figure 4.4: Illustration of the events of interference, undetected spectrum opportunity, and interference-free transmission time in the non-hybrid spectrum sensing.

ondary network in the non-hybrid method $E^{NH} = E_s^{NH} + E_t^{NH}$ can be obtained by

$$E^{NH} = \Big(\frac{T_{sim}}{E[T_P^{NH}]}\Big)E_{s0} + \big(T_{sim}.\Pr[T^{NH}]\big)P_{t0} \qquad (4.40)$$

where $E[T_P^{NH}] = (1 - \Pi_P)T_{PI} + \Pi_P T_{PT}$, and $\Pr[T^{NH}] = \Pi_P(1 - P_d) + (1 - \Pi_P)(1 - P_f)$.

The total power consumption of the secondary network in this case is obtained by $P^{NH} = \frac{E^{NH}}{T_{sim}}$.

4.5 Numerical and Simulation Results

We consider a homogenous CSN with two SUs ($N = 2$), and compare three CR networks

with different probabilities of presence ($\Pi_{s1} < \Pi_{s2} < \Pi_{s3}$). The arbitrary probabilities of

presence are selected as follows: $\Pi_{s1} = 0.24, \Pi_{s2} = 0.28$, and $\Pi_{s3} = 0.31$.

4.5.1 Interference Ratio Analysis

Fig. 4.5 depicts the interference ratio curves for the secondary network 1, secondary

network 2, and secondary network 3 along with the optimum transmission time T_T^* for

each network. As shown, T_T^* is decreased when the secondary network's probability of

presence is increased. This is due to fact that the interference ratio will sooner exceed

the R_I^{th} for a secondary network with a greater Π_s. In addition, the proposed method's

performance is compared with the non-hybrid method. As depicted, the interference ratio in the non-hybrid method R_I^{NH} is identical for all the secondary networks as the SU's properties are not considered in the non-hybrid method. Moreover, the proposed method manages to increase the SU's optimum transmission time T_T^*, as compared with the non-hybrid method to improve the secondary network's spectrum usage.

4.5.2 Undetected Opportunity Ratio Analysis

Similar to the previous simulation, three secondary networks are considered that have different probabilities of presence $\Pi_{s1} < \Pi_{s2} < \Pi_{s3}$. Fig. 4.6 depicts the undetected opportunity ratio curves for these networks along with the optimum idle time T_I^* for each network. As expected, the optimum idle time is decreased in a secondary network that has a greater Π_s to response to the demand for more spectrum usage in such a network. In addition, the proposed method's performance is compared with the non-hybrid approach. In the first place, the undetected opportunity ratio in the non-hybrid method R_U^{NH} is identical for all the above networks, as R_U^{NH} is not a function of the secondary network's parameters. In the second place, the proposed method manages to increase T_I^*, as compared with the non-hybrid method to reduce the frequency of the spectrum sensing, and thus to reduce the energy consumption associated with the sensing task.
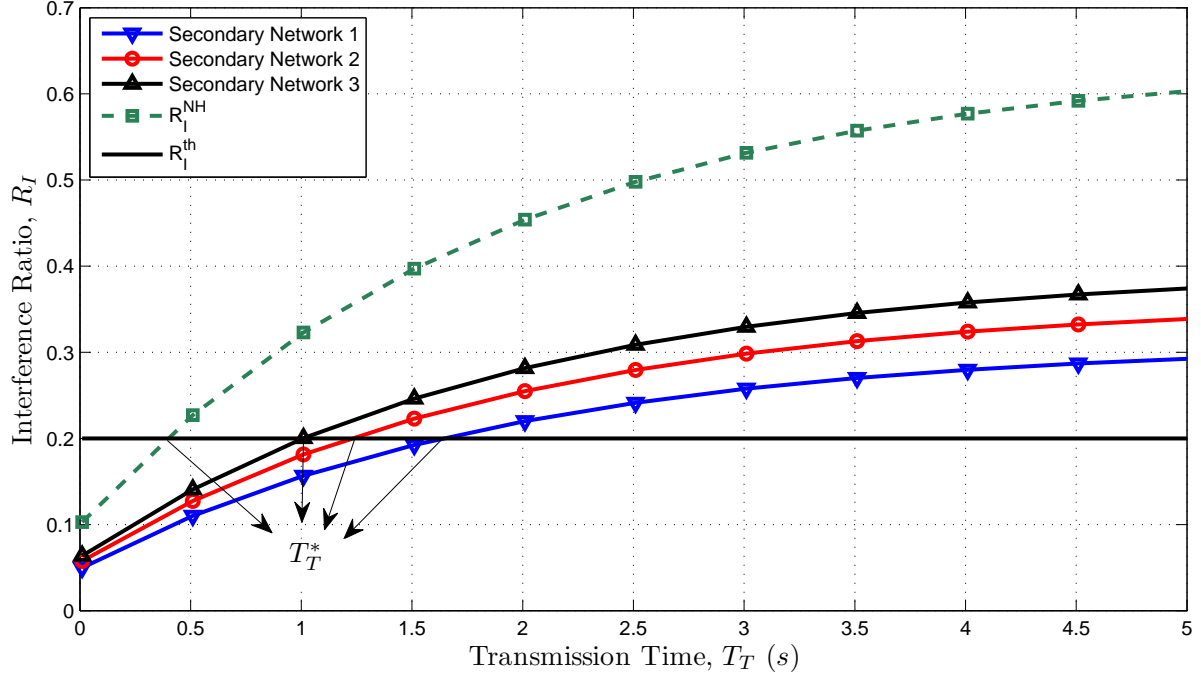
Figure 4.5: Interference ratio for the secondary network 1, 2, and 3 ($\Pi_{s1} < \Pi_{s2} < \Pi_{s3}$ and $R_I^{th} = 0.2$).
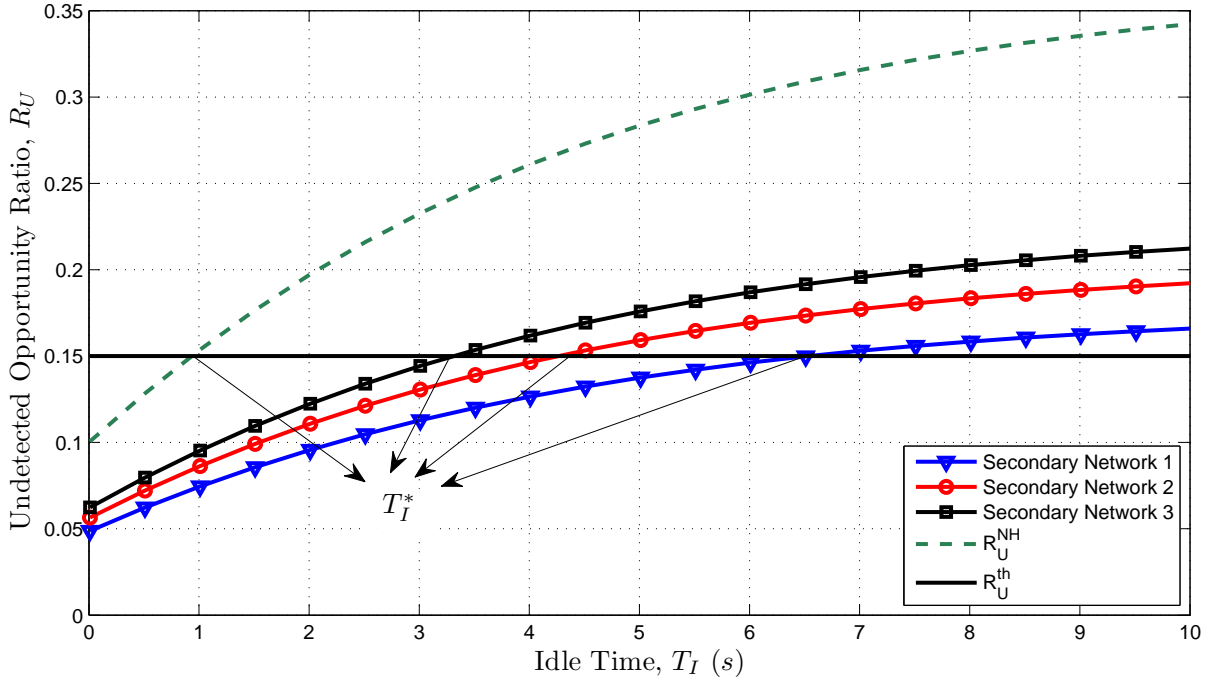
Figure 4.6: Undetected opportunity ratio for the secondary network 1, 2, and 3 ($\Pi_{s1} < \Pi_{s2} < \Pi_{s3}$ and $R_U^{th} = 0.15$).

4.5.3 Optimum Sensing Period Analysis

In this section, we study the optimum sensing period for two cases. First, the secondary network's departure rate μ_s is assumed to be fixed, and the secondary network's arrival rate λ_s varies (Case-I). Second, the secondary network's arrival rate λ_s is fixed, and the secondary network's departure rate μ_s varies (Case-II).

Case-I: Fixed μ_s, Variable λ_s

Fig. 4.7 depicts the average of the optimum sensing period $E[T_P^*]$ in Case-I. As shown, $E[T_P^*]$ is decreased when λ_s is increased. This is due to the fact that the secondary network's probability of presence is also increased when λ_s is increased. Therefore, in the proposed method, the optimum sensing period is decreased to provide greater sensing frequency (smaller $E[T_P^*]$) in response to the higher demand for spectrum usage in a secondary network with greater λ_s.

In addition, $E[T_P^*]$ is compared for different values of μ_s. As depicted in Fig. 4.7, $E[T_P^*]$ is increased when μ_s is increased. This is due to the fact that for a fixed value of λ_s, the secondary network's probability of presence Π_s is decreased when μ_s is increased. Therefore, $E[T_P^*]$ is increased to reduce the sensing frequency (larger $E[T_P^*]$) and thus to reduce the energy consumption associated with the sensing task.
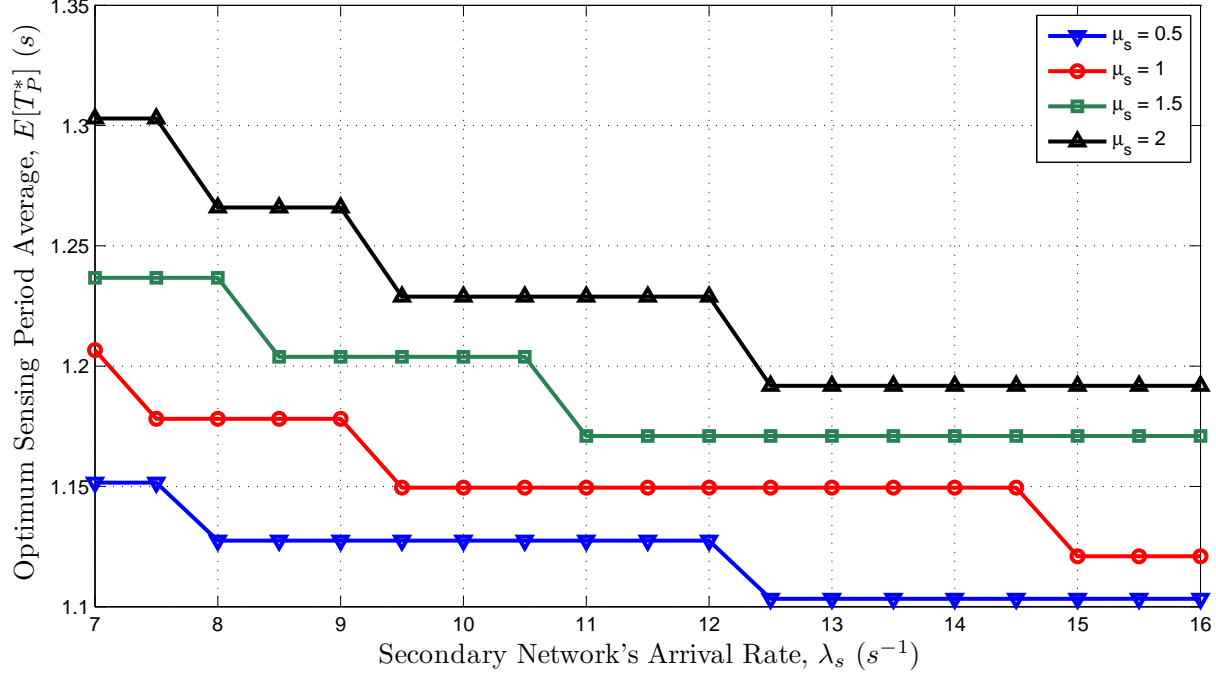
Figure 4.7: The average of the optimum sensing period in Case-I.

Case-II: Fixed λ_s, Variable μ_s

Fig. 4.8 depicts the average of the optimum sensing period $E[T_P^*]$ in Case-II. As shown, $E[T_P^*]$ is increased when μ_s is increased. This is due to the fact that Π_s is decreased when μ_s is increased (see (4.7) and (4.6)). Therefore, in the proposed method, the optimum sensing period is increased to provide smaller sensing frequency (larger $E[T_P^*]$). Hence, the energy consumption associated with the sensing task will be reduced in a secondary network with an smaller Π_s.

Furthermore, $E[T_P^*]$ is compared for different values of λ_s. As depicted in Fig. 4.8, $E[T_P^*]$ is increased when λ_s is decreased. This is due to the fact that for a fixed value of

μ_s, the secondary network's probability of presence Π_s is decreased when λ_s is decreased. Therefore, $E[T_P^*]$ is increased to reduce the sensing frequency (larger $E[T_P^*]$) and thus to reduce the energy consumption associated with the sensing task.

4.5.4 Throughput and Power Consumption Analysis

Fig. 4.9 depicts the average throughput Γ_s for two cognitive networks. As shown, Γ_s is increased when T_T is increased. Therefore, the optimum T_T^* yields to the maximum Γ_s for each secondary network. Each curve, therefore, is stopped at its corresponding T_T^* to avoid exceeding the R_I threshold. In addition, for a fixed value of T_T, Γ_s is greater for a secondary network that has a greater probability of presence Π_s, i.e, $\Gamma_2 > \Gamma_1$ when $\Pi_2 > \Pi_1$. The proposed method is also compared with the non-hybrid approach. As shown, the proposed method achieves up to a 11% greater throughput for the secondary network 2, as compared with the non-hybrid scheme.

Fig. 4.10 depicts the total power consumption (P) of the secondary networks 1 and 2. In the first place, P is decreased when T_I is increased, as expected. Hence, the optimum T_I^* yields to the minimum power consumption for each secondary network. Each curve, therefore, is stopped at its corresponding T_I^* to avoid exceeding the R_U threshold. In the second place, P is increased when the secondary network's probability of presence Π_s is increased, i.e, $P_2 > P_1$ when $\Pi_2 > \Pi_1$. Finally, the proposed method is compared with
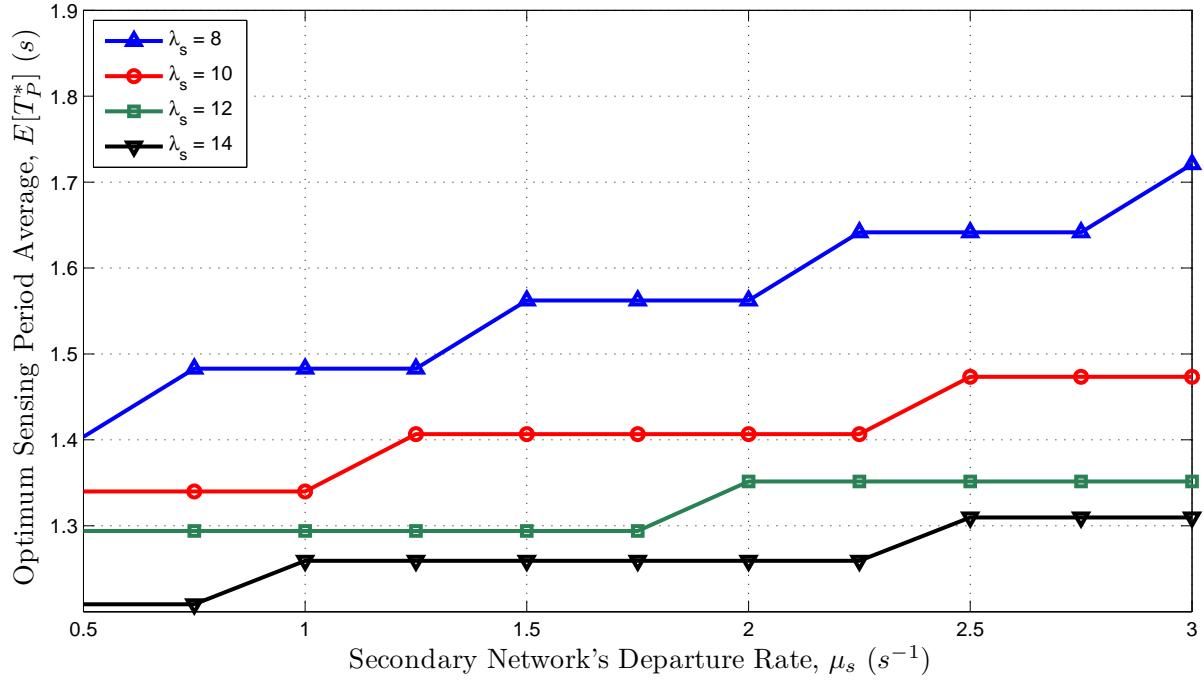
Figure 4.8: The average of the optimum sensing period in Case-II.
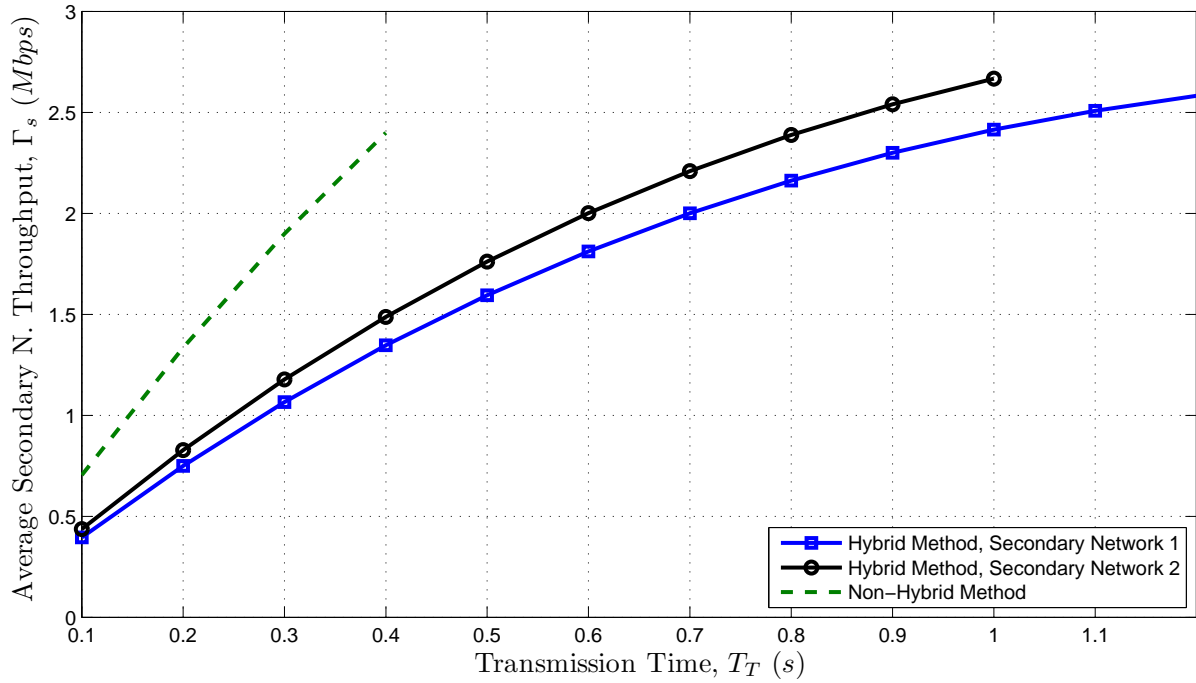
Figure 4.9: The average throughput of the secondary networks (theoretical results).

the non-hybrid approach. As shown, the proposed method manages to reduce the power consumption by as low as 33% of the non-hybrid method for the secondary network 1. Table 4.2 shows the simulation parameters used in this computer experiment.

As noted before, the proposed method aims to maximize the idle time T_I during the idle state. While the maximization of T_I is desirable to reduce the secondary network's power consumption, it is in contrast with the achievable throughput of the secondary network. In other words, larger idle time yields to less spectrum usage by the secondary network. Hence, there is a trade-off between the power consumption minimization and the throughput maximization.

In addition to the numerical analysis, we conduct simulation analysis to compare the performance of the application-specific method with the non-application-specific scheme. As shown in Fig. 4.11 and Fig. 4.12, the simulation results agree with the numerical results presented in this chapter.

Table 4.2: Simulation parameters
for the throughput and power consumption analyses.

Parameter	Value	Parameter	Value
W	200 KHz	G	1
E_{s0}	1 (mJ)	P_{t0}	10 (mW)
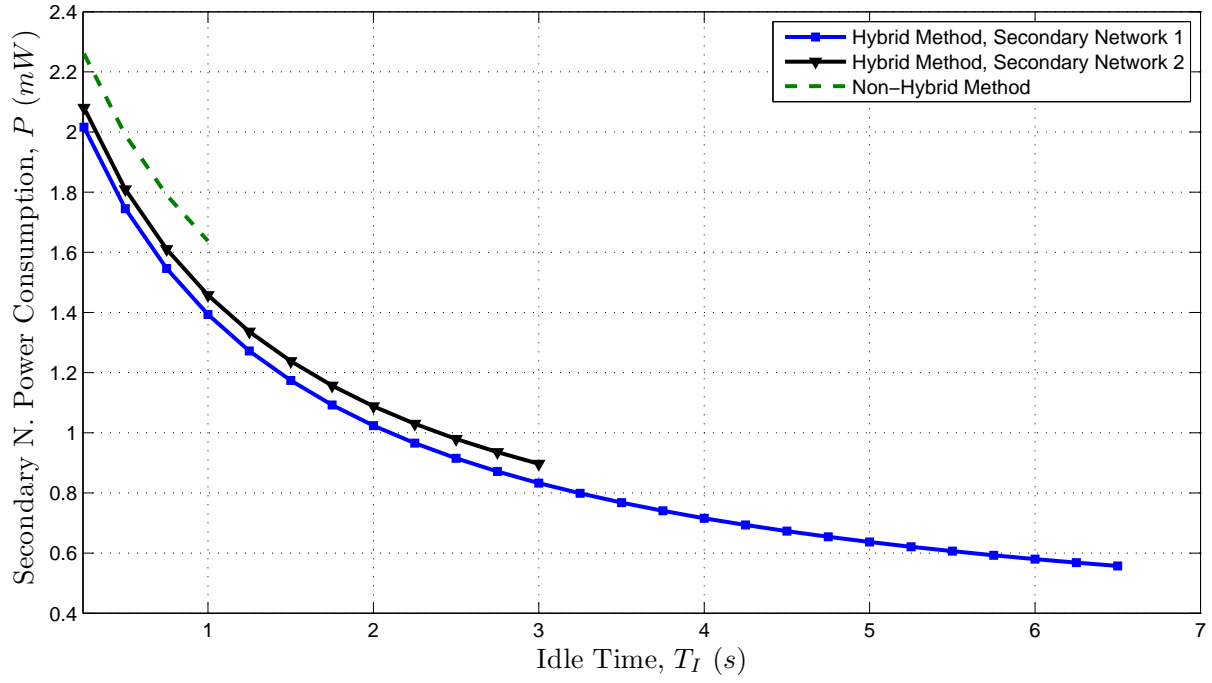
Figure 4.10: Total power consumption of the secondary networks (theoretical results).
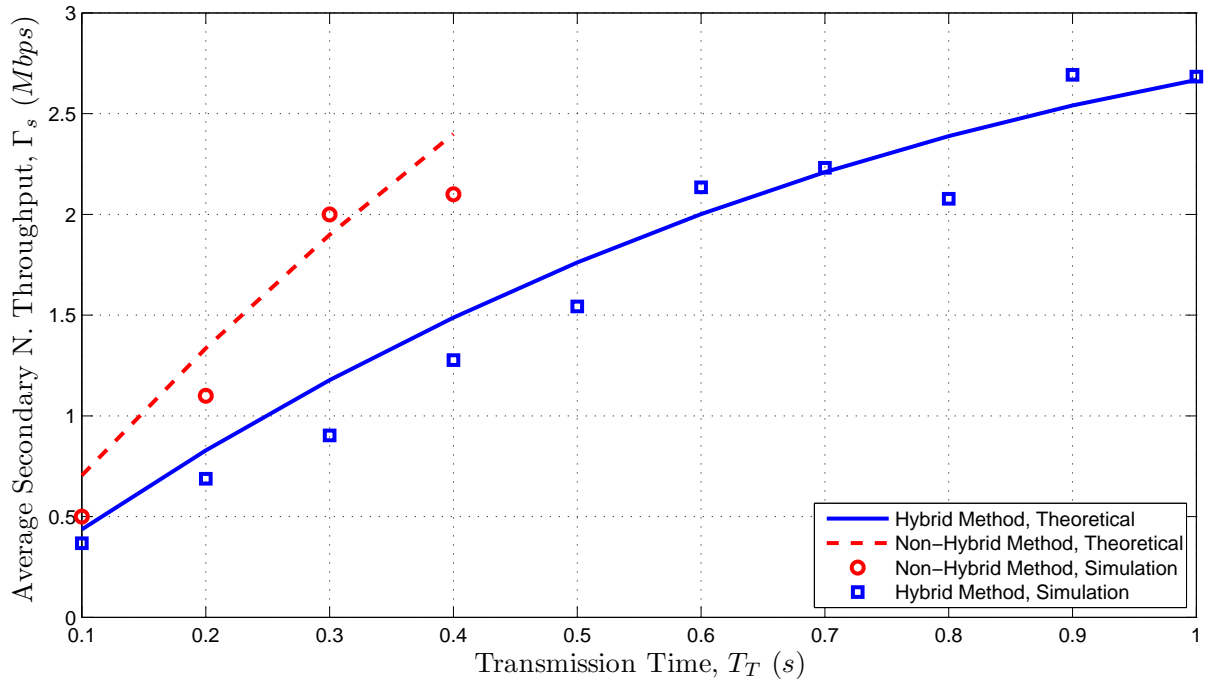
Figure 4.11: The secondary network's average throughput, simulation analysis.
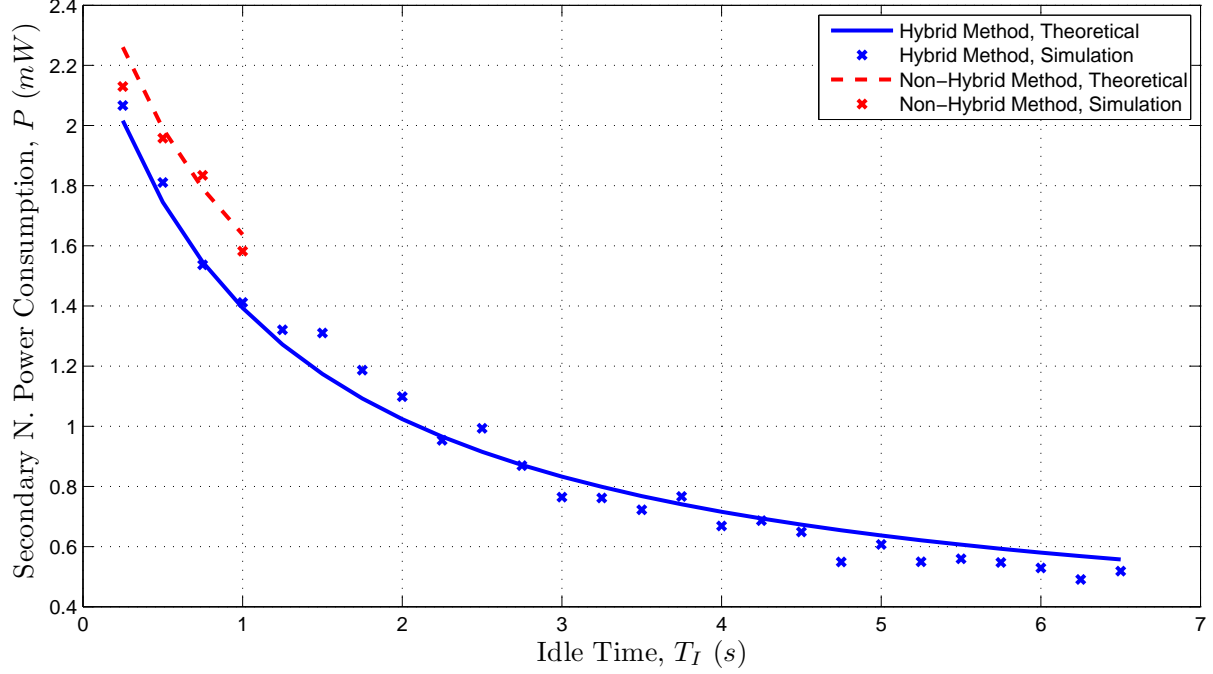
Figure 4.12: The secondary network's power consumption, simulation analysis.

4.6 Summary

In this chapter, we studied the problem of local sensing optimization in a cognitive sensor network. In contrast with the majority of existing work, where the sensing optimization is performed according to the properties of the primary network, we proposed an application-specific method that obtains the sensing period based on the properties of both primary and secondary networks. We then formulated two optimization problems to find the optimum sensing periods based on the secondary network's CTMC state.

In addition, the non-interfered system throughput and the total power consumption of the secondary network were derived by using a probability tree-diagram. We compared

the performance of the proposed method with a non-application-specific scheme. In the following chapter, we will employ cooperative spectrum sensing to further improve the performance of the spectrum sensing.

Chapter 5

Energy-Aware Secondary User

Selection in Cooperative Spectrum

Sensing

5.1 Motivations

Cooperative spectrum sensing is a promising scheme to tackle the hidden terminal problem[1] by exploiting multi-user diversity [24, 25, 70]. The performance of the spectrum sensing is influenced by several factors, including sensing accuracy and energy consumption especially in an energy-constrained CR network, such as a CR-based sensor network.

---

[1]The hidden terminal problem occurs when several users accessing a channel while they cannot see or hear each other.

In the literature, significant research effort has been made to tackle both issues individually. In [70], a partial spectrum sensing algorithm with decision result prediction and decision result modification is developed to reduce the cooperative spectrum sensing energy. A new channel management scheme for the CR sensor networks is proposed in [71], that increases the energy efficiency while not greatly disturbing PUs. According to the outcome of the channel sensing, the algorithm adaptively selects its operating mode among channel sensing, channel switching, and data transmission/reception. In [72], an optimal scheduling of sensor active time in sensor-aided CR networks is proposed to extend the network lifetime. The sensors are divided into a number of non-disjoint subsets such that only one subset of sensors is turned on at any time. Each subset is activated successively while other sensors sleep.

Another major focus of research is on the sensing accuracy – the precision in the task of the PU's signal detection – in a CR network. The sensing accuracy is evaluated by two metrics: the probability of detection P_d and the probability of false alarm P_f. The larger the P_d, the better are PUs protected from SU interference. On the other hand, the smaller the P_f, the more efficiently the licensed channel can be used by SUs. A new cooperative wideband sensing scheme is proposed in [73] which exploits the spatial diversity among multiple SUs to improve the sensing accuracy. In [74], a large scale cognitive radio is considered, and a sequential sensing and fusion approach is presented to minimize the

average sensing time by dividing the users into different sets according to their SNR parameters. Moreover, the sensing accuracy is evaluated in [75] for a cooperative sensing technique through multiuser cooperation.

However, the performance of the cooperate spectrum sensing relies on several uncertainties, such as the probability of error in the spectrum sensing task. A cognitive framework, therefore, should be aware of each SU's sensing accuracy, and give higher weight to more accurate sensing reports. Most of the existing work has overlooked the importance of the selection of the *most eligible* SUs for cooperate sensing.

In this chapter, we combine energy consumption and sensing accuracy in cooperative spectrum sensing and propose a novel method that is both energy-aware and accurate. First, we formulate and analytically solve an optimization problem to find the minimum number of required cooperative users, while satisfying the sensing task requirements. Then, we define a metric for sensing accuracy according to the most recent sensing reports, and employ a probability-based approach to identify the most eligible SUs. We also compare the network's lifetime for several sensing accuracy thresholds, and discuss the trade-off between the sensing accuracy and the network lifetime.

5.2 Cooperative Spectrum Sensing

In the cooperative spectrum sensing, information from multiple SUs are incorporated to decide on the presence of the PU. In this approach, each SU performs local spectrum sensing independently and makes a binary decision on the presence or the absence of the PU. The local decision is then forwarded to a single entity called fusion centre (FC). Finally, the FC gathers all the local sensing results and makes a final conclusion to infer the presence or absence of the primary network. The final decision is then forwarded to all SUs, as shown in Fig. 5.1. We assume that the reporting channel is ideal in this work.

Several fusion rules have been discussed in the literature [76]. Here, we employ the *k-out-of-N* fusion rule, where the spectrum is considered to be occupied by the PU when at least k out of N cooperative users declare that the PU is present. Therefore, the resulting hypothesis at the FC is given by

$$
\begin{aligned}
\sum_{i=1}^{N} D_i(n) \;&<\; k \qquad : H_0 \\
\sum_{i=1}^{N} D_i(n) \;&\geq\; k \qquad : H_1
\end{aligned}
\tag{5.1}
$$

In (5.1), N is the number of cooperative SUs, and $D_i(n) \in \{0,1\}$ denotes the local sensing result of the ith secondary user at the nth sensing process. $D_i(n) = 0$ corresponds to the absence of the PU, and $D_i(n) = 1$ corresponds to the presence of the PU. The
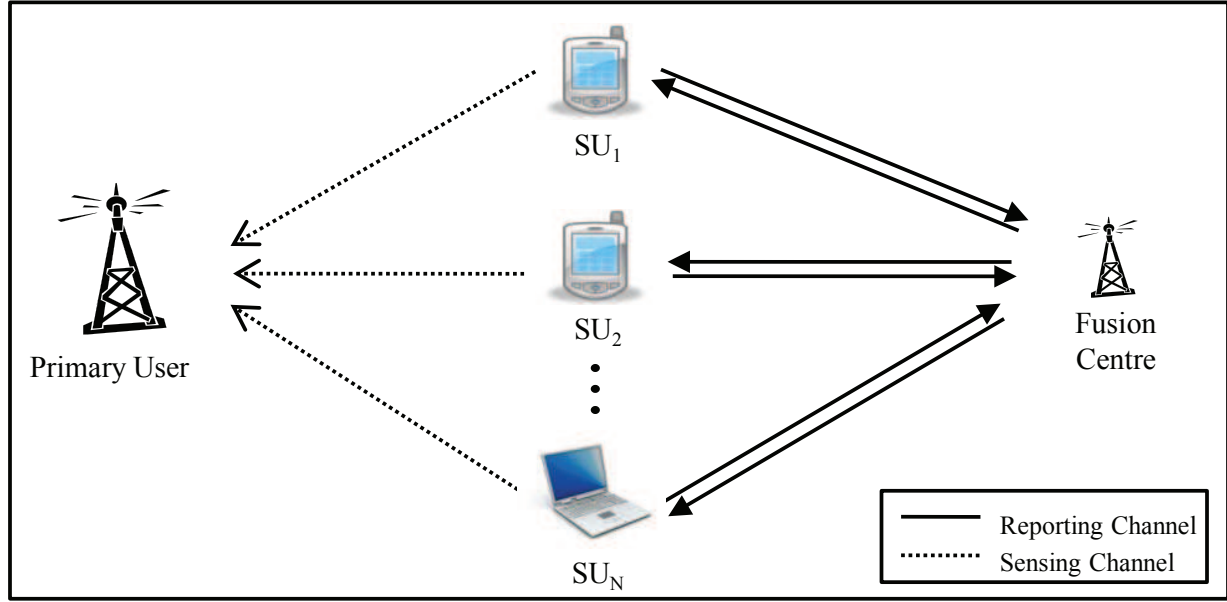
Figure 5.1: Cooperative spectrum sensing in a CSN.

probability of false alarm P_f in (4.4) is considered for the case of no signal transmission (H_0) and as such is identical for all secondary users [77]. In addition, we assume that, compared with the distance from any SU to the primary transmitter, the distance between any two SUs is small, so that the received signal at each SU experiences almost identical path loss. In the case of an AWGN environment, therefore, we can assume σ_s^2 is identical for all the secondary users. Consequently, P_d in (4.5) will be identical for all SUs [78]. Therefore, the probability that at least k secondary users declare that the PU is present

given that the PU is absent, the *global probability of false alarm Q_f*, is given by

$$Q_f = \sum_{i=k}^{N} \binom{N}{i} \left(P_f.P_{act}\right)^i \left(1 - P_f.P_{act}\right)^{N-i} \tag{5.2}$$

where P_{act} is the probability that the secondary network is active. Moreover, the probability that at least k secondary users declare that the spectrum is occupied by the PU, given that the spectrum is occupied by the PU, the *global probability of detection Q_d*, is obtained by

$$Q_d = \sum_{i=k}^{N} \binom{N}{i} \left(P_d.P_{act}\right)^i \left(1 - P_d.P_{act}\right)^{N-i}. \tag{5.3}$$

The AND rule will be an special case of the k-out-of-N rule by letting $k = N$. The global probability of false alarm and the global probability of detection, therefore, are obtained by plugging in $k = N$ in (5.2) and (5.3), as follows:

$$Q_f^{AND} = (P_f.P_{act})^N \tag{5.4}$$

$$Q_d^{AND} = (P_d.P_{act})^N. \tag{5.5}$$

Similarly, the OR rule will be an special case of the k-out-of-N rule by letting $k = 1$

in (5.2) and (5.3) as follows:

$$Q_f^{OR} = 1 - (1 - P_f.P_{act})^N.$$

(5.6)

$$Q_d^{OR} = 1 - (1 - P_d.P_{act})^N.$$

(5.7)

5.3 Energy-Aware Cognitive User Selection

The proposed method aims to improve the performance of the spectrum sensing in two directions. First, it selects a subset of SUs to perform the sensing/reporting task. The minimum number of required secondary users (N^*) in the subset is derived to minimize the network's energy consumption, while satisfying the spectrum sensing requirements. Second, the proposed method identifies the most eligible SUs to perform the sensing/reporting task.

5.3.1 Minimum Number of Required Cognitive Users in the Subset

As noted before, it is expected to minimize the number of cooperative users in the subset, so that the overall energy consumption of the secondary network is reduced. However, the performance of the cooperative sensing will also degrade with fewer SUs (less multi-

user diversity); therefore, there is an optimum size for the subset. We formulate the cooperative sensing problem as follows:

Minimize: N^*

Subject to: $Q_f \leq \gamma_f$, and $Q_d \geq \gamma_d$

where N^* is the minimum number of required cooperative SUs, and γ_f and γ_d are the system thresholds set for the global probability of false alarm and the global probability of detection respectively. In order to solve the above optimization problem, we first derive ϵ from (4.5) as follows:

$$\epsilon = \left(\sigma_s^2 + \sigma_n^2\right)\left(Q^{-1}(P_d)\sqrt{2M} + M\right) \tag{5.8}$$

where $Q^{-1}(\cdot)$ is the inverse Q-function. Next, ϵ is plugged into (4.4) as follows:

$$P_f = Q\left(\frac{Q^{-1}(P_d).(\sigma_s^2 + \sigma_n^2)\sqrt{2M} + M\sigma_s^2}{\sigma_n^2\sqrt{2M}}\right). \tag{5.9}$$

Note that Q_f in (5.2) follows a binomial distribution. Therefore, we can use the

incomplete beta function[2] I to express P_f as a function of Q_f as follows:

$$Q_f = 1 - \Pr(i < k) = 1 - \Pr(i \le k - 1) = 1 - I_{1-P_f \cdot P_{act}}(N - k + 1, k) \qquad (5.10)$$

where $I_z(a, b) = \frac{B(z;a,b)}{B(a,b)}$ is the regularized incomplete beta function, $B(z; a, b) = \int_0^z t^{a-1}(1-t)^{b-1}dt$ is the incomplete beta function, and $B(a, b) = \int_0^1 t^{a-1}(1-t)^{b-1}dt$ is the beta function. Using the inverse of the regularized incomplete beta function, P_f can be written as follows:

$$P_f = \frac{1}{P_{act}}\left(1 - I^{-1}_{1-Q_f}(N - k + 1, k)\right) \qquad (5.11)$$

where $I^{-1}_{1-Q_f}(\cdot)$ is the inverse of the regularized incomplete beta function.

In a similar way, P_d can be derived from Q_d in (5.3) as follows:

$$P_d = \frac{1}{P_{act}}\left(1 - I^{-1}_{1-Q_d}(N - k + 1, k)\right). \qquad (5.12)$$

Note that for a given k and N in the k-out-of-N fusion rule, I and I^{-1} are monotonically increasing functions. Therefore, the optimization problem constraint $Q_f \le \gamma_f$ can be written as

$$P_f = \frac{1}{P_{act}}\left(1 - I^{-1}_{1-Q_f}(N - k + 1, k)\right) \le \varsigma_f \qquad (5.13)$$

---

[2]The incomplete beta function is the cumulative distribution function of a random variable x with a binomial distribution, where the probability of success is p and the sample size is n. Hence, $\Pr[x \le k] = I_{1-p}(n - k, k + 1)$ [79], page 1112.

where $\varsigma_f = \frac{1}{P_{act}}\left(1 - I_{1-\gamma_f}^{-1}(N - k + 1, k)\right)$.

Similarly, $Q_d \geq \gamma_d$ can be written as

$$P_d = \frac{1}{P_{act}}\left(1 - I_{1-Q_d}^{-1}(N - k + 1, k)\right) \geq \varsigma_d \qquad (5.14)$$

where $\varsigma_d = \frac{1}{P_{act}}\left(1 - I_{1-\gamma_d}^{-1}(N - k + 1, k)\right)$.

As shown in (5.14), $P_d \geq \varsigma_d$. Also, $Q^{-1}(\cdot)$ is a monotonically decreasing function, therefore, we get

$$Q^{-1}(P_d) \leq Q^{-1}(\varsigma_d). \qquad (5.15)$$

In addition, $Q(\cdot)$ is a monotonically decreasing function as well. Hence, (5.9) and (5.14) yield

$$P_f \geq Q\left(\frac{Q^{-1}(\varsigma_d).(\sigma_s^2 + \sigma_n^2)\sqrt{2M} + M\sigma_s^2}{\sigma_n^2\sqrt{2M}}\right). \qquad (5.16)$$

Therefore, based on (5.13) and (5.16), the minimum number of required cooperative users N^* will be the minimum solution of the following inequality,

$$Q\left(\frac{Q^{-1}(\varsigma_d).(\sigma_s^2 + \sigma_n^2)\sqrt{2M} + M\sigma_s^2}{\sigma_n^2\sqrt{2M}}\right) \leq \varsigma_f. \qquad (5.17)$$

Finally, an exhaustive search for N from 1 to the first value that satisfies (5.17) is

employed to find N^*.

5.3.2 Identification of the Most Eligible SUs

In this section, we assume that the cognitive users achieve different sensing accuracy levels. The probability of detection P_d, therefore, would be different for each secondary user. However, P_f is identical for all the SUs because it is calculated for the case of no signal transmission (H_0), as discussed in the previous section. The operation of the proposed method is divided into time units called *epochs*. Each epoch is further divided into several sub-units called *rounds*, where each round lasts for T_P^* seconds (the optimum sensing period). Fig. 5.2 depicts a timeline for the proposed method. As shown, the first W rounds in each epoch are assigned to the *setup phase*, and the remaining L rounds are reserved for the *operational phase*. The secondary network will be active for a fraction of L rounds within the operation phase with the probability of P_{act}.
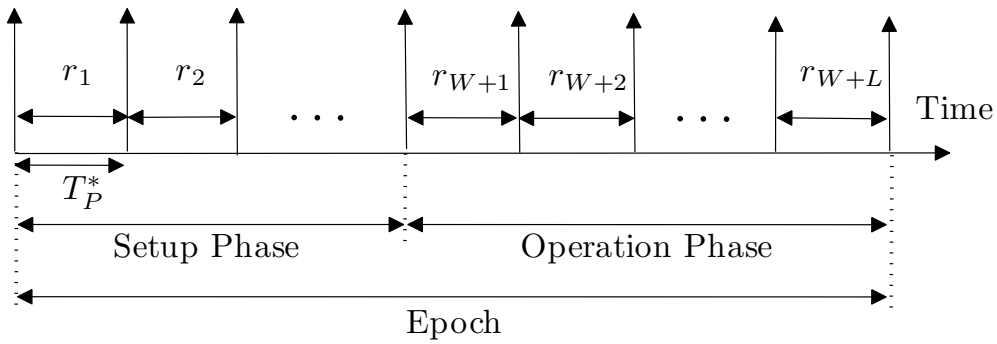
Figure 5.2: The proposed method's timeline.

As mentioned earlier, $D_i(n) \in \{0, 1\}$ denotes the result of local sensing performed by the ith secondary user during the nth sensing task. Also, let $F(n) \in \{0, 1\}$ denote the result of FC's decision that is obtained by fusing all the collected reports at the FC within the nth round. At the end of the setup phase, we define $\Delta_i(n)$ as the total number of differences between the ith secondary user's local sensing and the FC's global decision within the last W rounds as follows:

$$\Delta_i(n) \;=\; \sum_{j=0}^{W-1} |D_i(n-j) - F(n-j)|. \tag{5.18}$$

We assume that the FC does not know the performance of the SUs a priori. Therefore, during the setup phase, all SUs are required to perform the spectrum sensing/reporting task. The most eligible SUs are then selected based on the SUs performance within this phase. The smaller the $\Delta_i(n)$ is, the more accurate the local sensing will be and vice versa. Therefore, a probability-based method is proposed that selects a subset of SUs that has the most accurate sensing results. Let us define η_i as a weighting factor assigned to the ith SU (u_i), where the probability to select u_i is proportional to η_i. Since the proposed method aims to reduce the amount of inaccurate sensing results, the probability that a user u_x with low $\Delta_x(n)$ is selected must be higher than the probability that a user u_y

with a high $\Delta_y(n)$ is selected. Hence, we define $\eta_i(n)$ as

$$\eta_i(n) = \frac{1}{1 + r\Delta_i(n)} \tag{5.19}$$

where r is a positive real number such that $r > 1$. The probability to select u_i within the nth sensing task, therefore, is defined as the weighting factor assigned to u_i over the summation of all weighting factors, as follows:

$$P_i(n) = \frac{\eta_i(n)}{\sum_{j=1}^{N} \eta_j(n)}. \tag{5.20}$$

We note that the energy consumption is one of the biggest concerns in a CR-based sensor network. Therefore, it is not prudent to choose the active users without considering the remaining energy of each SU. In particular, there might be circumstances where a particular SU has a high sensing accuracy due to its location (for instance, being close to the PU). In such cases, if the energy level is not considered, the same SU would be repeatedly selected, and its energy will be drained quickly. As a result, in addition to the sensing accuracy, we consider the ratio of each SU's energy to the initial secondary network's energy within each round, and revise the $\eta_i(n)$ function defined in (5.19) as follows:

$$\eta_i(n) = \frac{1}{1 + r\Delta_i(n) + g\frac{e_0}{e_i(n)}} \tag{5.21}$$

where g is a positive real number such that $g > 1$, e_0 is the initial energy of the cognitive users, and $e_i(n)$ is the remaining energy of u_i at the nth sensing process. We assume that each time a SU is selected, its energy level will be drained by e_u, where e_u is the energy consumed to perform a single sensing/reporting task. Note that (5.21) reduces to (5.19) for $g = 0$. Fig. 5.3 depicts the proposed method's flowchart, where r denotes the current round, c_setup and c_op are the current number of rounds in the setup and operation phases respectively, and $epoch$ is the number of rounds in an epoch. As shown, when $mod(r - 1, epoch) \leq W - 1$, the algorithm goes into the setup phase. Otherwise, it transits to the operation phase. The Check-Dead function is invoked at the beginning of both phases to check if (1) any SU is dead, and (2) the secondary network is dead. We consider an SU to be *dead* when its energy level is less than e_u. Moreover, the CNS is pronounced *dead* if the number of alive SUs is less than N^*. Fig. 5.4 presents a subroutine to check the number of dead SUs, called the Check-Dead function.

Let x denote the ratio of the accuracy multiplier to the energy level multiplier, i.e., $x = \frac{r}{g}$. Therefore, (5.21) is re-written as,

$$\eta_i^x(n) = \frac{1}{1 + g(x\Delta_i(n) + \frac{e_0}{e_i(n)})}. \tag{5.22}$$

We consider (5.22) and study two cases highlighting the emphasis on the accuracy or
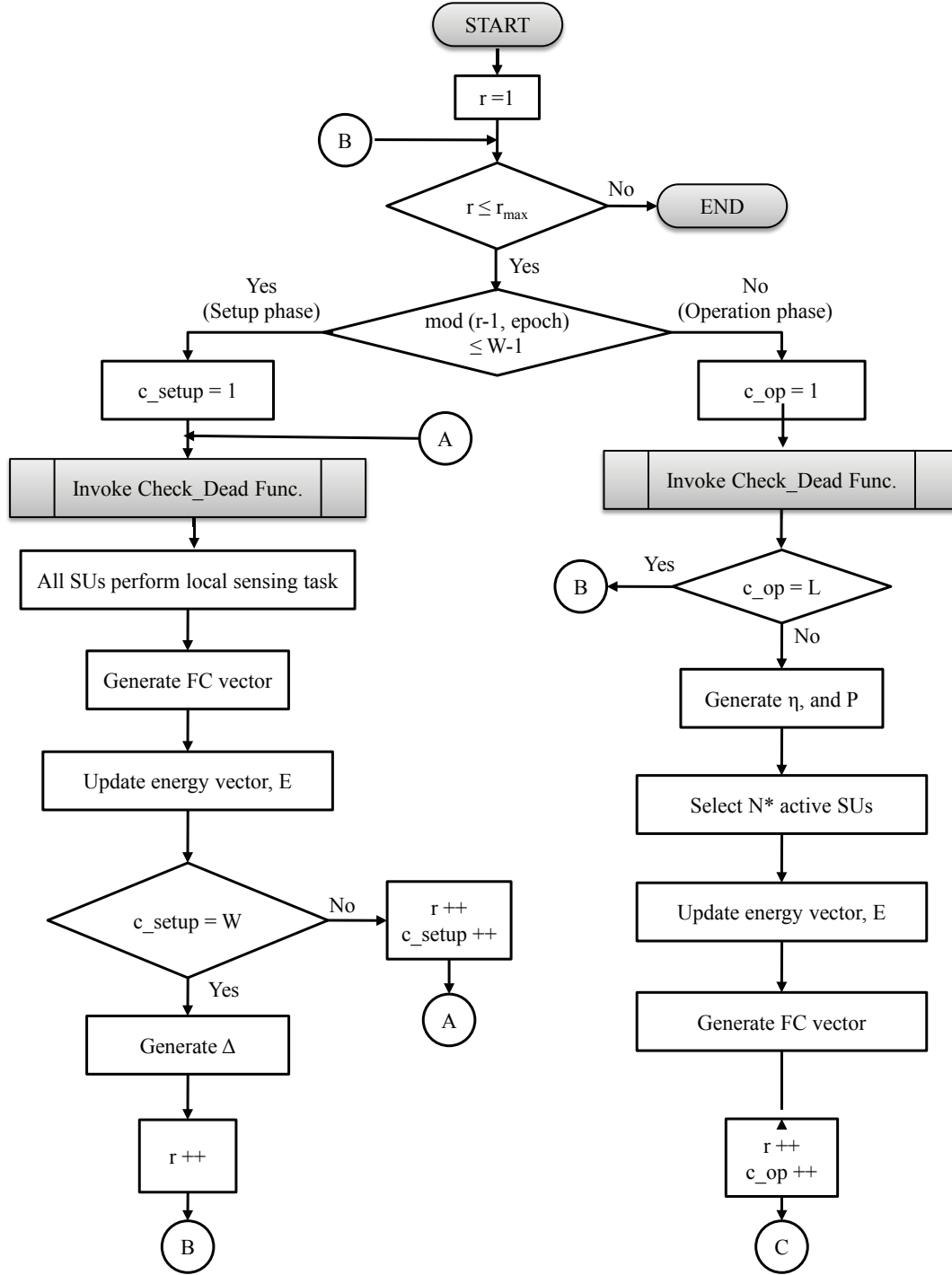
93

Figure 5.3: The proposed method's flowchart; r denotes the current round, *c_setup* and *c_op* are the current number of rounds in the setup and operation phases respectively, and *epoch* is the number of rounds in an epoch.
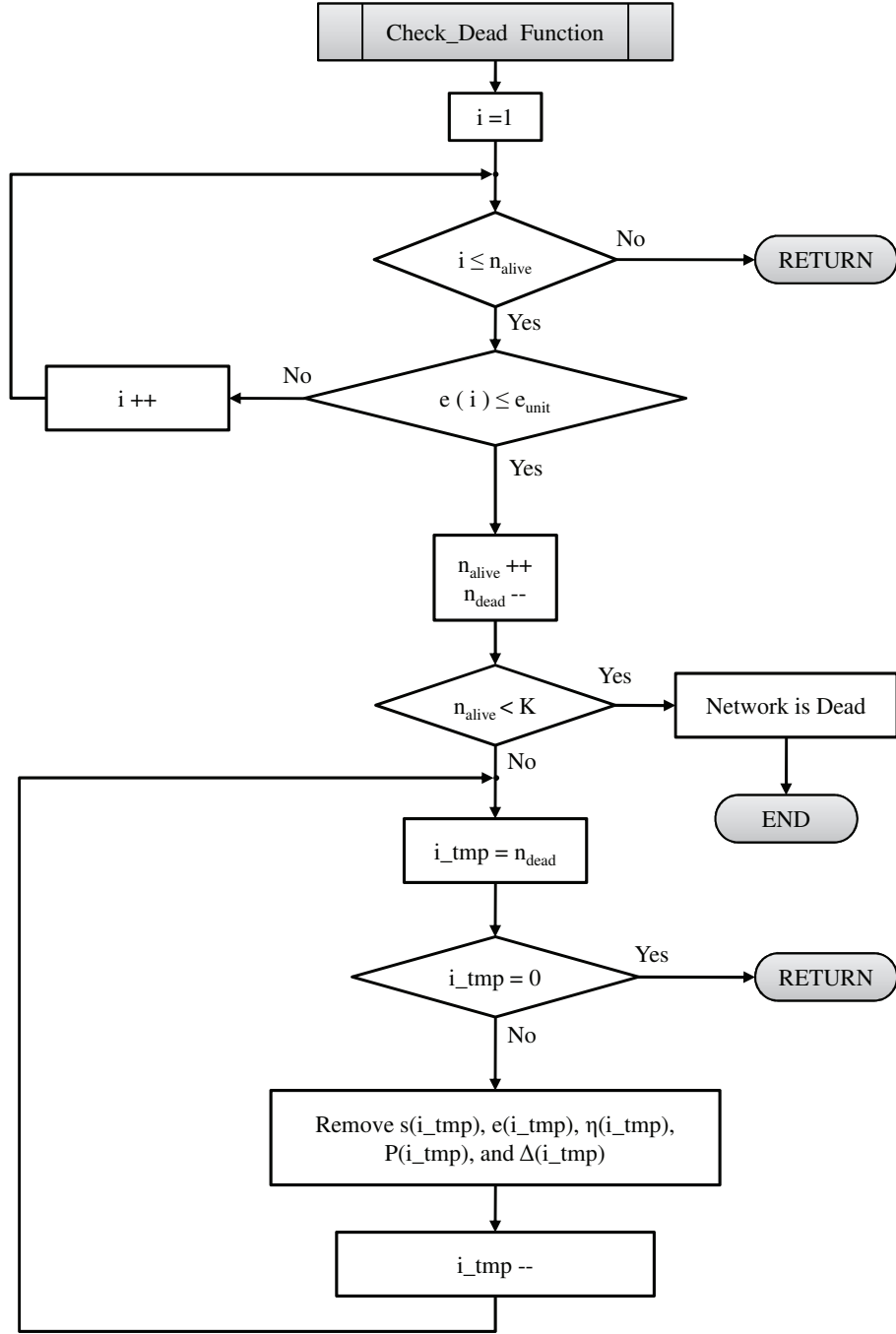
Figure 5.4: Check-Dead: a subroutine to check the number of dead SUs. n_{dead} and n_{alive} are the number of dead and alive SUs respectively.

on the energy level of the secondary network, as follows:

- Case-I ($x > 1$): in this case, the sensing accuracy is emphasized by making the accuracy multiplier (r) greater than the energy multiplier (g).

- Case-II ($x \leq 1$): in this case, the emphasis is on the energy level by making the accuracy multiplier (r) smaller than the energy multiplier (g).

During the operation phase, based on $P_i(n)$, the most N^* secondary users will be selected at each round to perform the sensing/reporting tasks. The rest of the SUs, however, will be inactive to save the secondary network's energy consumption.

The probability to select the ith secondary user within the nth sensing task defined in (5.20) can be revised to identify the most eligible secondary users with a reasonable accuracy level, as follows:

$$P'_i(n) = \begin{cases} \frac{\eta_i(n)}{\sum_{j=1}^{N} \eta_j(n)} & \text{, if } \Delta_i(n) \leq \Delta_{th} \\ 0 & \text{, if } \Delta_i(n) > \Delta_{th} \end{cases} \tag{5.23}$$

where Δ_{th} is a predefined system threshold set for the sensing accuracy. Hence, the secondary users that have a Δ function greater than Δ_{th} in each round are not eligible to be selected, i.e., the probability to select those secondary users is zero.

96

5.3.3 Evaluation Benchmarks

In the following, we set two benchmarks for the performance evaluation of the proposed method:

- *Sensing accuracy benchmark (P_0)* is defined as the probability to select an SU that has $\Delta_i(n) = 0$, averaged over the simulation time as follows:

$$P_0 = E\{ \sum_{i=1}^{N} \Pr[\Delta_i(n) = 0] \} \tag{5.24}$$

  where $E\{.\}$ is the average function. Note that the greater the P_0 is, the more accurate the cooperative sensing will be.

- *Energy benchmark (P_{le})* is defined as the probability to select an SU which has the lowest level of energy at each round (averaged over the simulation time). Hence, it would be desirable to have the lowest value for the P_{le}.

5.4 Numerical and Simulation Results

In this section, we conduct several computer experiments to evaluate the performance of the proposed method and to study the effects of adjustable parameters on the proposed method. In the first place, the effect of system thresholds ς_f and ς_d on the minimum

number of required cooperative users (N^*) is studied. Fig. 5.5 depicts N^* as ς_f varies; as depicted, N^* is reduced when the system requirement on P_f is more relaxed. Moreover, as shown in Fig. 5.5, the minimum number of required cooperative users is increased when the SNR is decreased ($SNR = 10 \log \frac{\sigma_s^2}{\sigma_n^2}$).

In the second place, Fig. 5.6 shows the minimum number of required cooperative users as a function of ς_d. As depicted, N^* is increased when the system requirement on the probability of detection is more tight, i.e., when ς_d is larger. Moreover, as expected, a larger number of cooperative users (N^*) are needed to perform the cooperative sensing task when the system has a smaller SNR.

Here, we study the effect of the number of rounds within the setup phase (W) on the sensing accuracy. As shown in Fig. 5.7, P_0 is greater for greater values of W. In other words, the sensing accuracy will be improved by larger values of W.

In addition, the weighting function $\eta_i^x(n)$ defined in (5.22) is applied to investigate the effect of emphasizing the accuracy versus emphasizing the remaining level of energy. We use an arbitrary $x > 1$ value to emphasize the accuracy, and an arbitrary $x < 1$ value to emphasize the energy. The simulation is run for $1 \leq g \leq 50$, and the corresponding P_0 and P_{le} values are recorded. Table 5.1 summarizes the results of this simulation. As depicted, the emphasis on the sensing accuracy improves the sensing accuracy benchmark by 22%. Similarly, emphasis on the energy improves the energy benchmark by as much
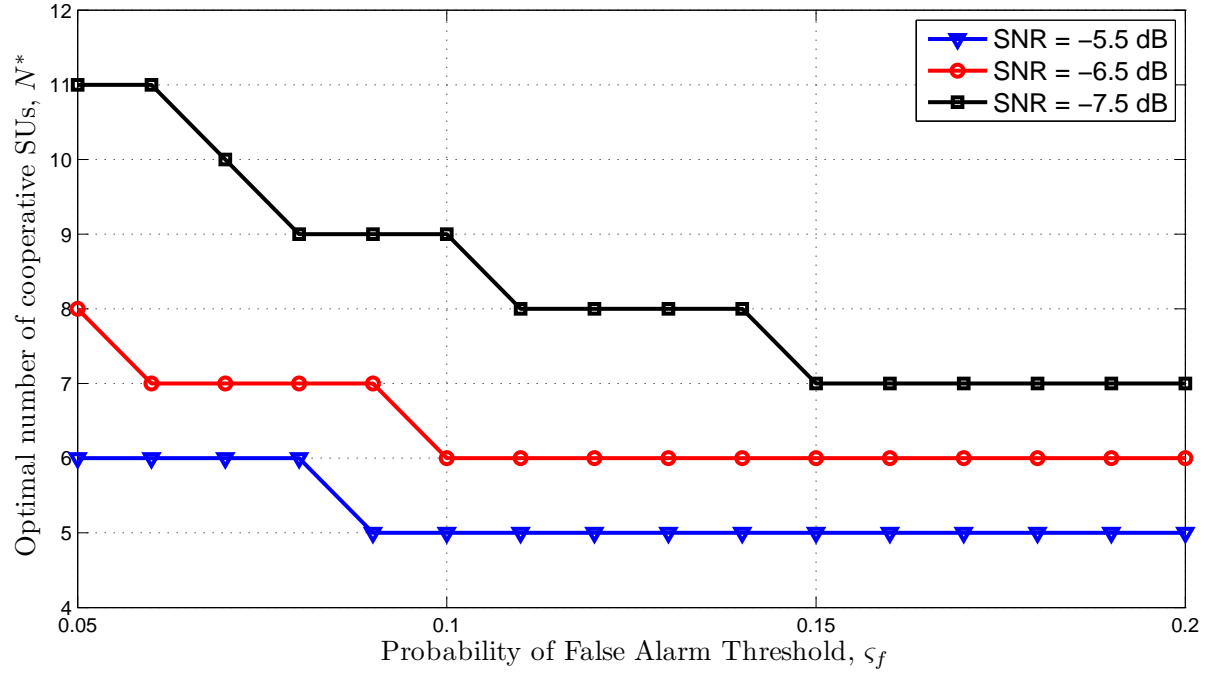
Figure 5.5: Minimum number of required cooperative users as a function of ς_f, ($\varsigma_d = 0.85$).
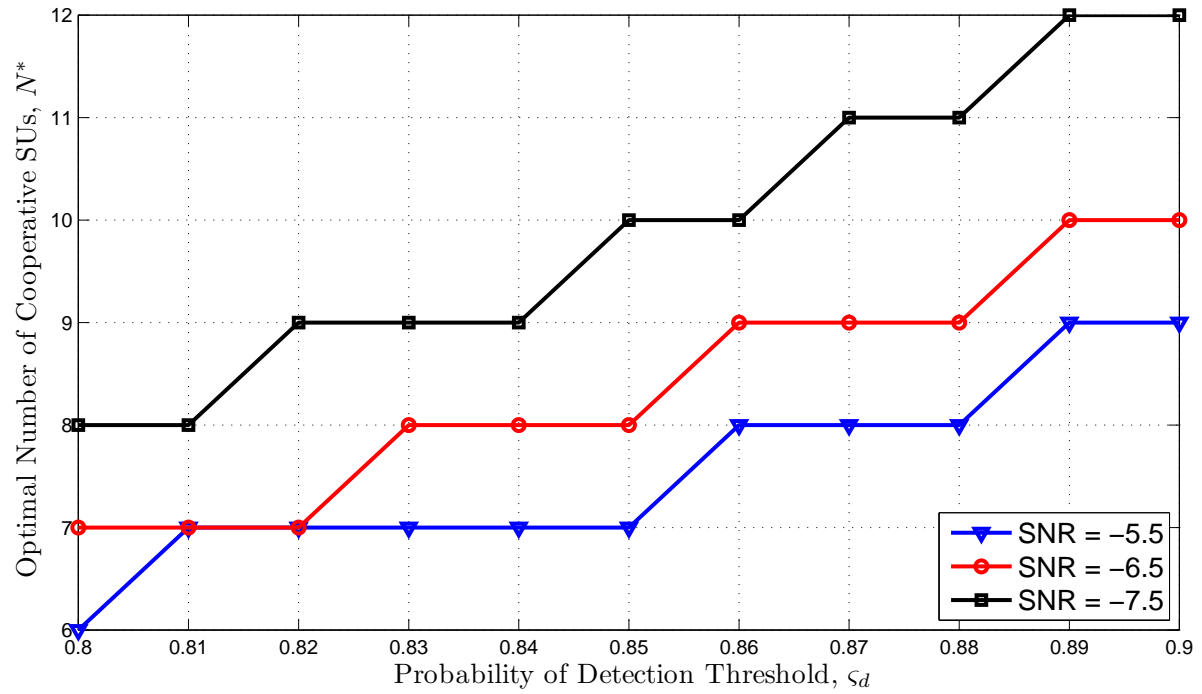
Figure 5.6: Minimum number of required cooperative users as a function of ς_d, ($\varsigma_f = 0.2$).
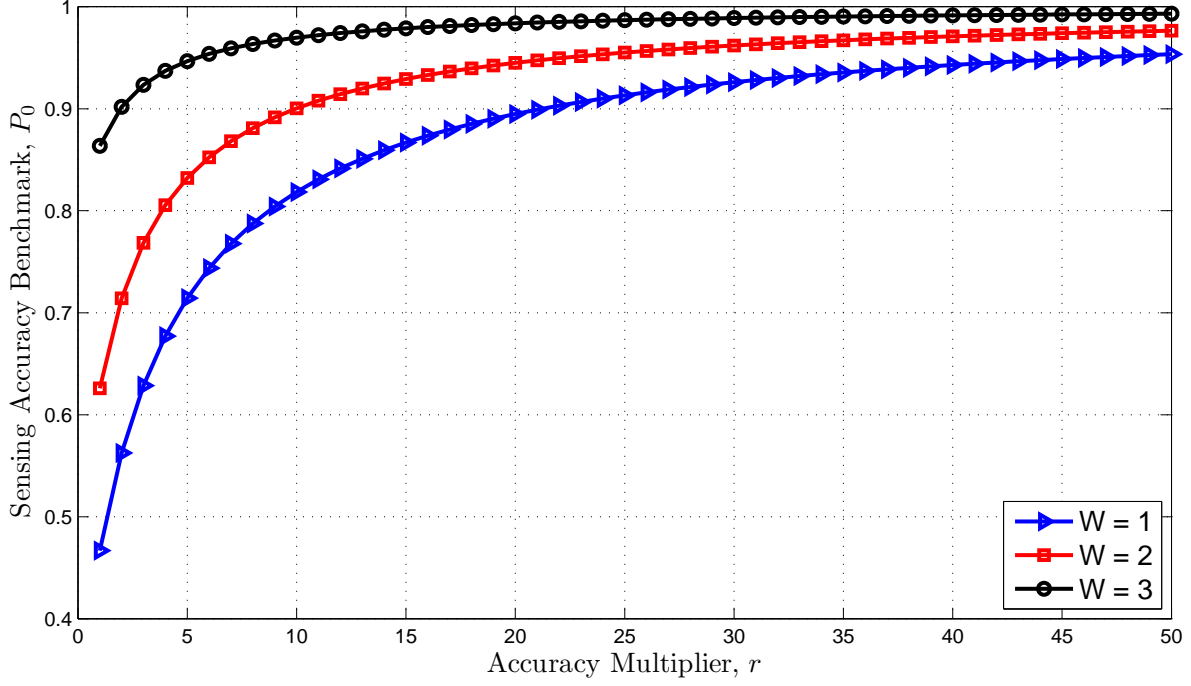
Figure 5.7: The effect of the number of rounds within the setup phase (W).

as 20%.

We also examine the following extreme cases: in Case-A, the remaining level of energy is not considered in the selection of the SUs, i.e., $g = 0$ in (5.21). Similarly, in Case-B, the accuracy of the spectrum sensing is not considered, i.e., $r = 0$ in (5.21). Fig. 5.8 depicts

Table 5.1: Emphasizing the sensing accuracy vs. the secondary network's energy.

	Max. of the sensing accuracy benchmark, $\max\{P_0\}$	Min. of the energy benchmark, $\min\{P_{le}\}$
Emphasis on the accuracy, ($x = 5$)	0.93	0.29
Emphasis on the energy, ($x = 0.2$)	0.76	0.24
Comparison	Emphasis on the sensing accuracy increases P_0 by 22%	Emphasis on the network's energy reduces P_{le} by 20%

P_0 and P_{le} benchmarks for the Case-A and the Case-B. As shown, the sensing accuracy is improved when the accuracy multiplier (r) increases. However, the performance of the proposed method in regard to P_{le} deteriorates. In addition, the performance of the proposed method with respect to P_{le} is improved by increasing the energy multiplier (g) in Case-B, while the accuracy (P_0) does not vary with the change in the energy multiplier.

Therefore, among the Case-A and the Case-B, it is concluded that the algorithm provides a better performance with respect to the sensing accuracy in Case-A, and it has a better performance in regard to P_{le} in Case-B. As shown in Fig. 5.8, the accuracy benchmark P_0 is increased by as much as 39% in Case-A. Additionally, the energy benchmark P_{le} is reduced by as low as 76% in Case-B.

5.4.1 The Secondary Network's Lifetime

In another study, we consider a CSN with $N = 9$ secondary users. The minimum number of required SUs to perform the sensing/reporting task is assumed to be $N^* = 5$. We use the $P_i'(n)$ definition in (5.23), and apply the k-out-of-N rule for $k = 3$. The number of rounds in the setup and operational phases are set to be $W = 10$ and $L = 90$ respectively. Furthermore, the initial energy of each SU is assumed to be $e_0 = 75$ (J), and the energy consumed to perform each sensing/reporting task is set to be $e_u = 0.1$ (J). Table 5.2 summarizes the above parameters. Based on the sensing accuracy, SUs are also grouped
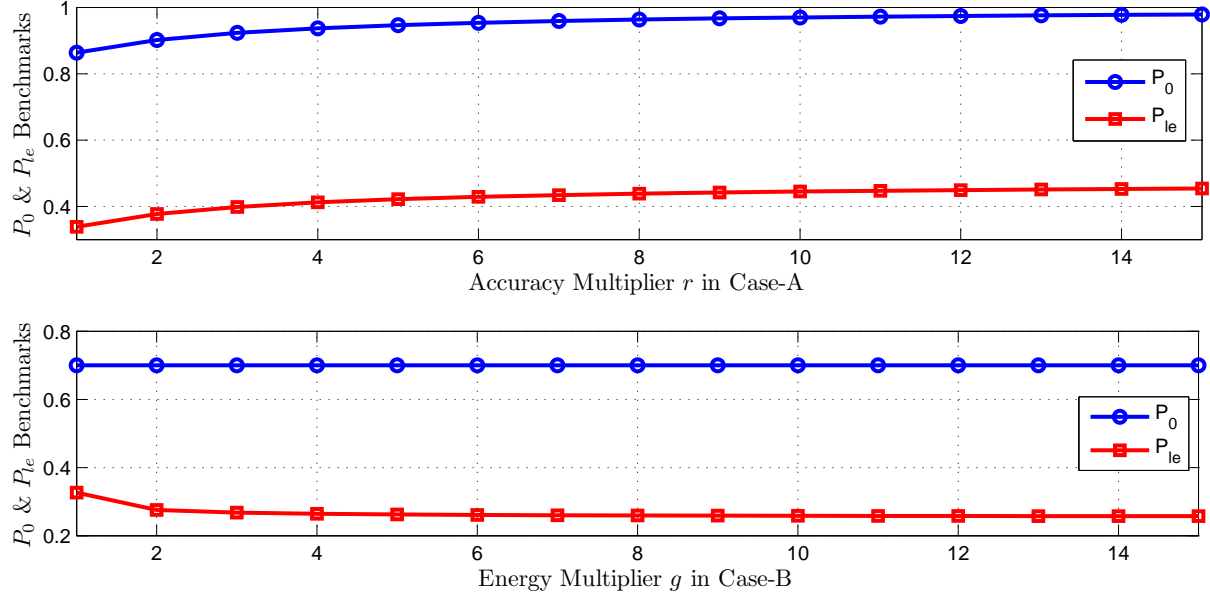
Figure 5.8: The accuracy and energy benchmarks in Case-A and Case-B.

into three categories, as depicted in Table 5.3.

The secondary network's lifetime is compared at different sensing accuracy thresholds. The simulation is run and the number of SUs is recorded until the number of alive SUs is greater than N^*; then we consider the network to be dead. As depicted in Fig. 5.9, the secondary network's lifetime is shortened by enforcing a better sensing accuracy (an smaller accuracy threshold, Δ_{th}). In other words, there is a trade-off between the secondary network's lifetime and the sensing accuracy.

Table 5.2: Simulation parameters.

Parameter	Value	Parameter	Value
N	9	N^*	5
W	10	L	90
e_0	75 (J)	e_u	0.1 (J)

Table 5.3: Classification of the secondary users into three categories.

	$SU_1 - SU_3$	$SU_4 - SU_6$	$SU_7 - SU_9$
P_d	0.9	0.85	0.8
Sensing Accuracy	Good	Average	Poor

Note that by setting a smaller value for the sensing accuracy threshold, SUs that have better sensing accuracy would be selected more often; therefore, the energy of such users will be deployed sooner. This is also depicted in Fig. 5.10. As shown, in the case of $\Delta_{th} = 0$, SUs that have higher sensing accuracy are selected with higher frequency compared to those that have lower sensing accuracy. For instance, SU_1, SU_2, and SU_3 which have the highest sensing accuracies (see table 5.3) are selected more often, as depicted in Fig. 5.10. However, in case of $\Delta_{th} = 4$, SUs are selected with almost the same frequency.

5.4.2   The Fusion Rule's Effect

In this section, several computer simulations are conducted to examine the effects of different fusion rules on the proposed method's performance. First, the average P_d of the secondary users is varied, and the simulation is run for 10,000 rounds. Fig. 5.11 depicts the probability of interference (P_I) for the OR Rule, the AND Rule, and the Majority Rule. As shown, the OR rule provides the smallest probability of interference among the mentioned fusion rules. In the OR rule, even if one SU reports a local sensing decision
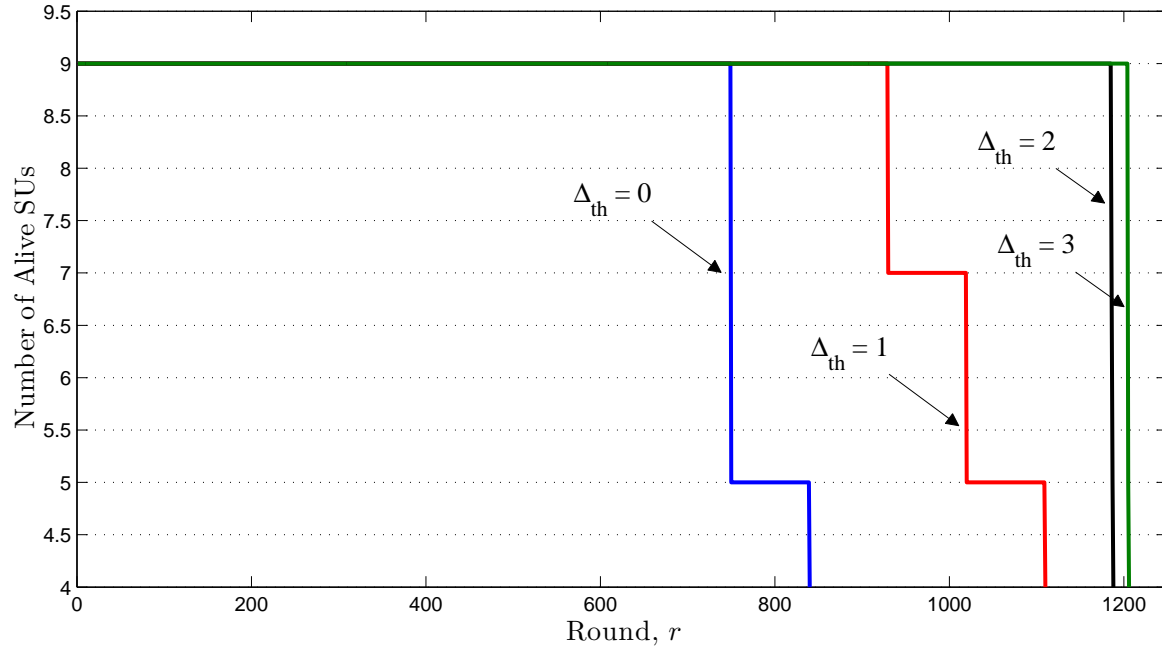
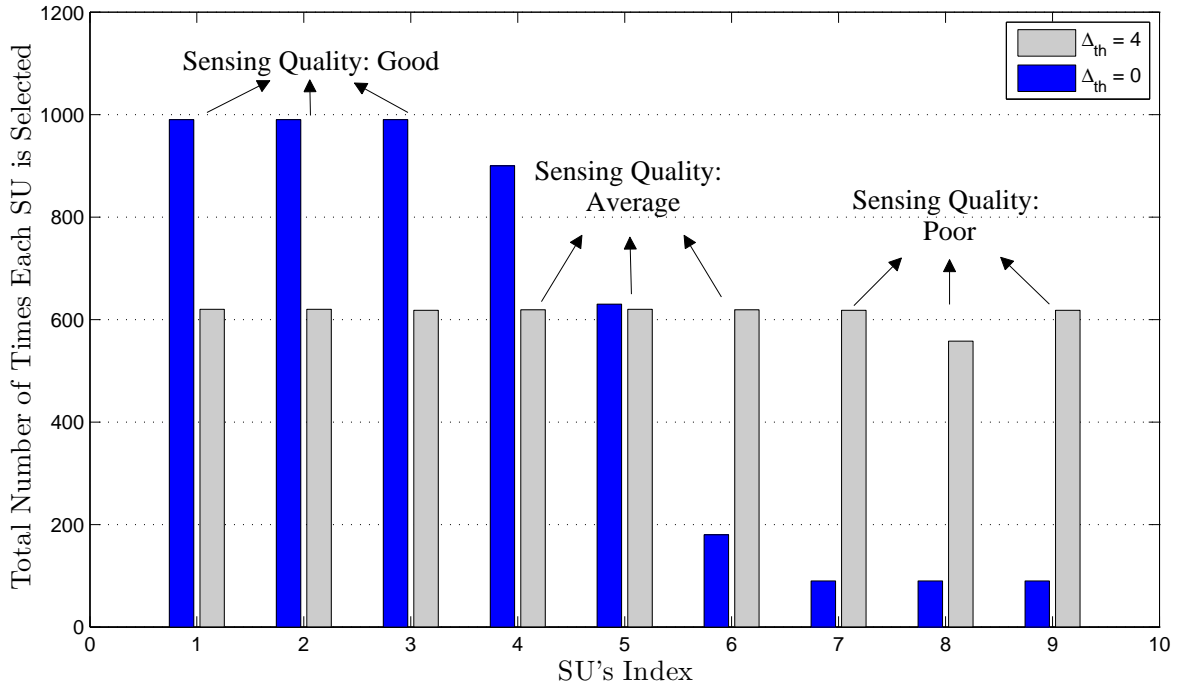Figure 5.9: The secondary network's lifetime at different values of Δ_{th}.

Figure 5.10: Total number of times each secondary user is selected at $\Delta_{th} = 0$ and $\Delta_{th} = 4$.

of "1", the FC will conclude that the PU is operating in the spectrum. Hence, the PU is fully protected from the SUs interference unless all the cooperative SUs report a "0". On the other hand, in the AND rule, even if one SU sends a local decision of "0", the FC will conclude that the PU is not operating in the spectrum. Therefore, the AND rule has the largest probability of interference. The probability of false alarm P_f is set to be 0.05. The acceptable range of P_d (the operation region) is set to $P_d \geq 0.8$.

We also vary the average P_f of the cognitive users and run the simulation for 10,000 rounds. The probability of missed opportunities (P_m) is then examined among the mentioned rules. As shown in Fig. 5.12, the OR rule has the worst performance with the largest probability of missed opportunities. In the OR rule, even one local sensing of "1" makes the FC conclude that the PU is present. Therefore, if the sensing report is not correct, a missed opportunity will occur. On the other hand, the AND rule has the best performance with the smallest P_m. This is due to the fact that unless all SUs report a "1", the AND rule will conclude that the PU is not present. Hence, the number of missed opportunities is minimal. For this computer simulation, the probability of detection P_d is set to be 0.8, and the acceptable range of P_f (the operation region) is set to $P_f \leq 0.2$.

As depicted in Fig. 5.11 and Fig. 5.12, the OR rule has the best performance with respect to the probability of interference. However, it has the worst performance from the missed opportunities point of view. On the other hand, the AND rule has the best
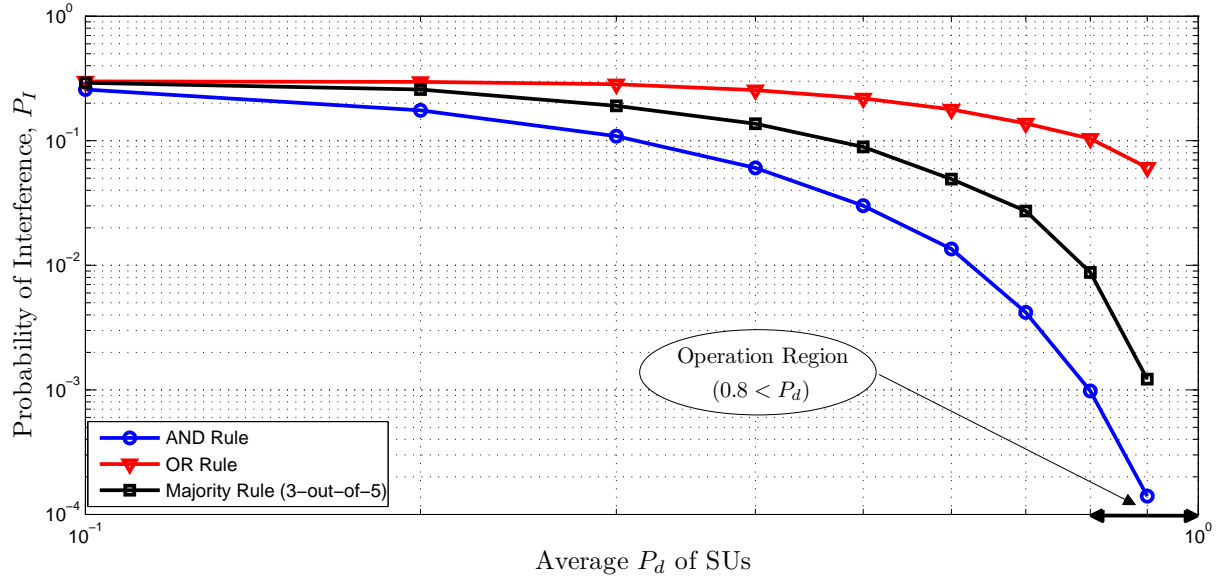
105

Figure 5.11: The probability of interference P_I for different fusion rules.
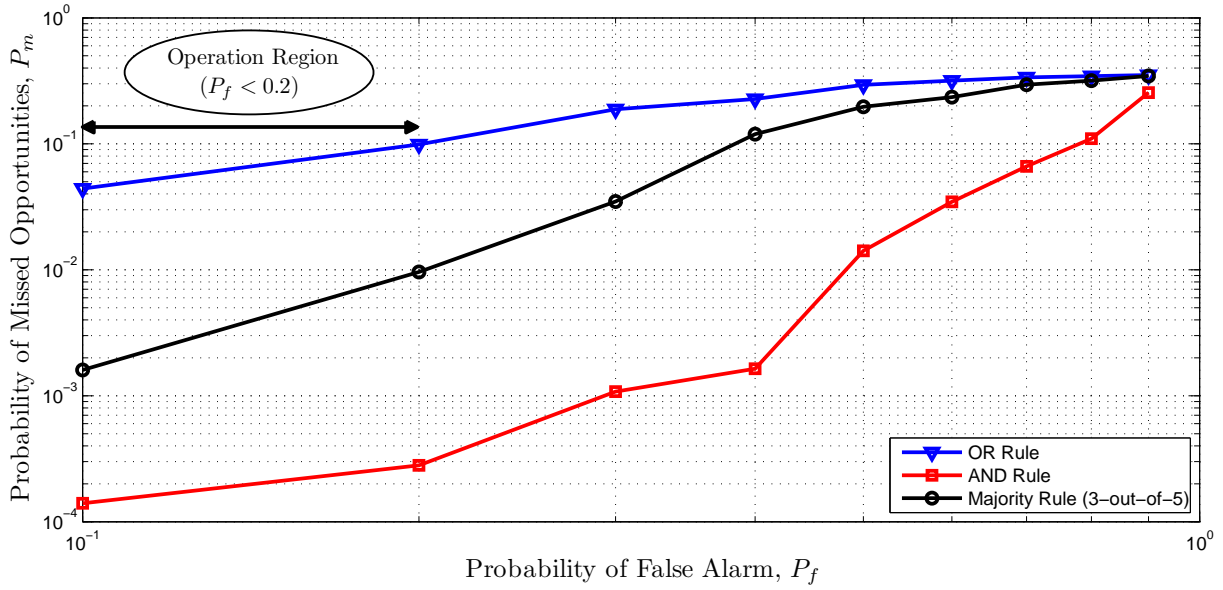

Figure 5.12: The probability of missed opportunities P_m for different fusion rules.

performance with respect to the missed opportunities, but it has the worst performance with respect to interference. However, as shown in Fig. 5.11 and Fig. 5.12, the Majority rule provides a close result to the best options (that is the OR rule in the interference study, and the AND rule in the missed opportunities study). Therefore, we conclude that the Majority rule has the best overall performance among the examined rules. This can be also verified by studying the probability of error (P_e), as performed in Fig. 5.13. As shown, the Majority rule has the smallest probability of error. Similarly, the probability of false alarm P_f is set to be 0.05, and the operation region is set to $P_d \geq 0.8$.

In another computer simulation, we consider a CSN with $N = 20$ secondary users, and assume that the minimum required number of cooperative users is $N^* = 10$. We run the simulation for 10,000 rounds and record the probability of error for different values of k in the k-out-of-N rule to examine the effect of other fusion rules. As depicted in Fig. 5.14, the Majority rule has the best performance with the minimum P_e. The OR rule and the AND rule, however, have the worst performances as discussed before.

In addition, we perform numerical analysis for rounds $1 \leq r \leq 10$ to further enlighten the proposed method's approach for spectrum sensing. We consider a CSN with five SUs ($N = 5$), where the minimum number of required SUs is assumed to be $N^* = 2$. Moreover, the initial energy of each SU is set to $e_0 = 1$ (J), and the energy consumed to perform each sensing/reporting task is $e_u = 0.1$ (J). The duration of the setup phase is
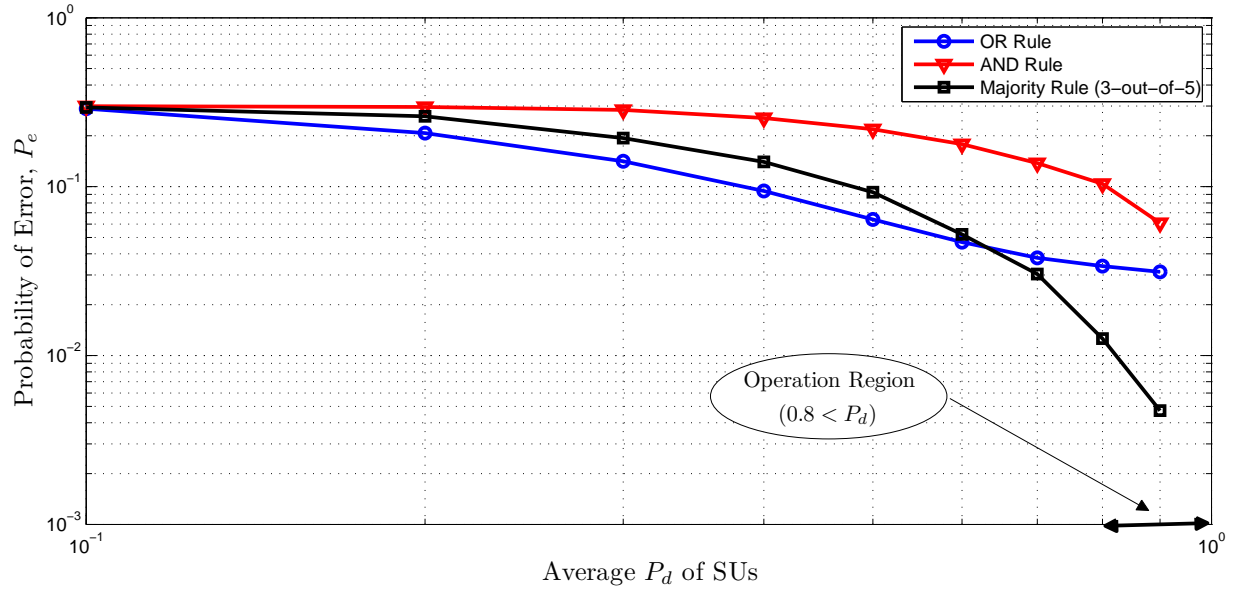
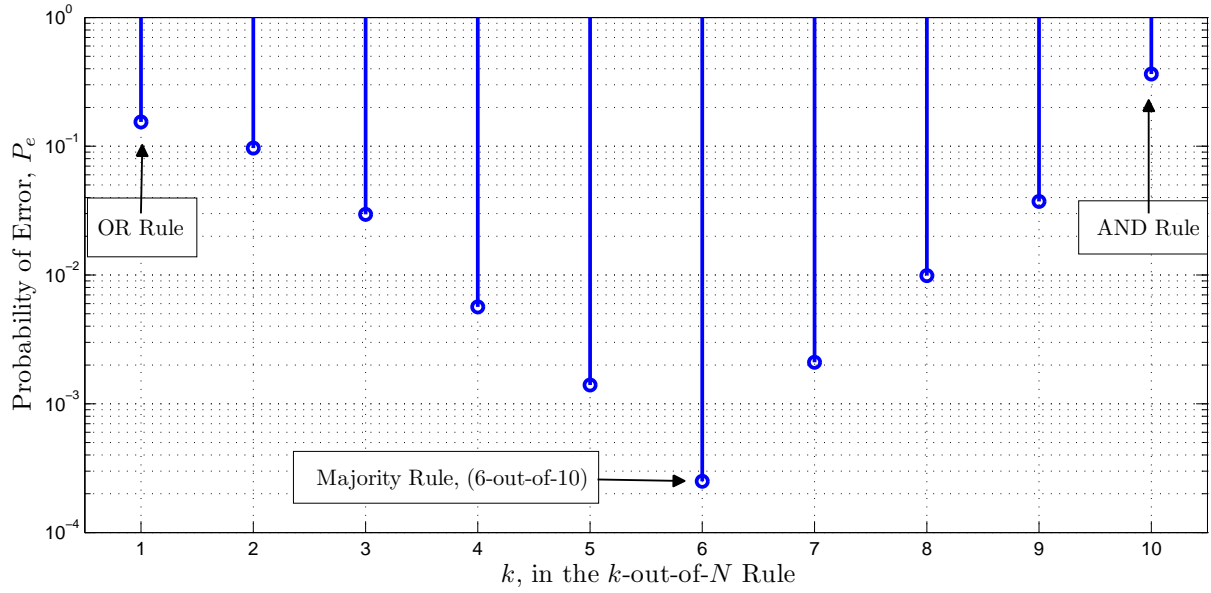Figure 5.13: The probability of error P_e for different fusion rules.

Figure 5.14: The probability of error P_e for different values of k in the k-out-of-N rule ($1 \leq k \leq 10$). The minimum required number of cooperative users is considered to be $N^* = 10$.

set to be $W = 2$ rounds, and the number of rounds within the operation phase is $L = 4$ rounds. As shown in Fig. 5.15, rounds $\{r_1, r_2, r_7, r_8\}$ are assigned to the setup phase, and rounds $\{r_3, r_4, r_5, r_6, r_9, r_{10}\}$ are assigned to the operation phase. The PU's ON-OFF pattern is also depicted in Fig. 5.15 as $[1\ 1\ 0\ 0\ 0\ 1\ 1\ 0\ 1\ 1]$. As discussed, at the end of the setup phase, the Δ vector is generated. The Δ vector, therefore, is generated as $\Delta(2) = [0\ 1\ 2\ 1\ 2]^T$ and $\Delta(8) = [0\ 0\ 0\ 1\ 1]^T$ at round r_2 and r_8 respectively.

Similar to the previous simulation, we assume that each SU can accomplish a sensing accuracy that might be different from other SUs. Let $n_e(i)$ denote the total number of errors between the ith SU's sensing result and PU's ON-OFF state[3]. Without loss of generality, we assume that $n_e = [0, 1, 3, 4, 6]$. Secondary users are then classified based on their sensing accuracy into three groups: good (SU_1 and SU_2), average (SU_3 and SU_4), and poor (SU_5).

In the operation phase, first the weighting function and P matrices are calculated. We use η_i^x defined in (5.22), and emphasize the sensing accuracy ($x = 5, g = 20$). Second, $N^* = 2$ secondary users that have the greatest P values are selected to perform the sensing/reporting tasks. Fig. 5.16 depicts the above matrices, where $N^* = 2$ secondary users that are selected are indicated by an "*" sign. For instance, (SU_1 and SU_2) are selected in round r_3, and (SU_1 and SU_4) are selected in round r_4. The selected SUs then

---

[3]Although the secondary network is not aware of the primary user's state, we use this information for the evaluation purpose.

	Setup Phase		Operation Phase				Setup Phase		Operation Phase	
ROUND	r_1	r_2	r_3	r_4	r_5	r_6	r_7	r_8	r_9	r_{10}
PU	1	1	0	0	0	1	1	0	1	1
FC (OR-Rule)	1	1	0	0	1	1	1	0	1	1
SU 1	1	1	0	0	0	1	1	0	X	X
SU 2	0	1	0	X	0	X	1	0	1	1
SU 3	0	0	X	X	X	X	1	0	1	1
SU 4	1	0	X	0	X	0	0	0	X	X
SU 5	0	0	X	X	X	X	0	0	X	X

Figure 5.15: The operation of the proposed method is divided into the setup phase and the operational phase. An "X" indicates that the corresponding SU does not perform senseing/reporting, a "1" means the PU is detected, and a "0" means the PU is not detected.

report their local sensing results to the FC. Third, the final decision is made by the FC according to the received sensing reports. Fig. 5.15 shows the sensing results obtained by the selected SUs, where an "X" indicates that non-selected SUs do not perform the sensing/reporting tasks.

In addition, each time an SU is selected, its energy level will be reduced by e_u. Fig. 5.16 depicts the energy level of each SU in the e matrix. As shown, during the early rounds, the difference in η^x values is mostly due to the sensing accuracy, because all SUs start with the same level of energy (e_0). However, after a few rounds, when the energy level of SUs is not balanced any more (SUs that have better sensing accuracy have been selected more often), the selection of SUs is performed due to both sensing accuracy $\Delta_i(n)$ and $e_i(n)$, as discussed in (5.22).

	Setup Phase		Operation Phase				Setup Phase		Operation Phase		
	r_1	r_2	r_3	r_4	r_5	r_6	r_7	r_8	r_9	r_{10}	
$\eta =$	0	0	0.0385	0.0338	0.0291	0.0244	0	0	0.0099	0.0099	← SU_1
	0	0	0.0079	0.0077	0.0077	0.0074	0	0	0.0196	0.0148	← SU_2
	0	0	0.0044	0.0044	0.0044	0.0044	0	0	0.0291	0.0244	← SU_3
	0	0	0.0079	0.0079	0.0077	0.0077	0	0	0.0066	0.0066	← SU_4
	0	0	0.0044	0.0044	0.0044	0.0044	0	0	0.0074	0.0074	← SU_5
$P =$	0	0	0.6087*	0.5798*	0.5453*	0.5039*	0	0	0.1362	0.1568	← SU_1
	0	0	0.1256*	0.1323	0.1445*	0.1538	0	0	0.2697*	0.2341*	← SU_2
	0	0	0.07	0.0759	0.0828	0.0914	0	0	0.4006*	0.3863*	← SU_3
	0	0	0.1256	0.1361*	0.1445	0.1595*	0	0	0.0911	0.1049	← SU_4
	0	0	0.07	0.0759	0.0828	0.0914	0	0	0.1024	0.1179	← SU_5
$e =$	0.9	0.8	0.7	0.6	0.5	0.4	0.3	0.2	0.2	0.2	← SU_1
	0.9	0.8	0.7	0.7	0.6	0.6	0.5	0.4	0.3	0.2	← SU_2
	0.9	0.8	0.8	0.8	0.8	0.8	0.7	0.6	0.5	0.4	← SU_3
	0.9	0.8	0.8	0.7	0.7	0.6	0.5	0.4	0.4	0.4	← SU_4
	0.9	0.8	0.8	0.8	0.8	0.8	0.7	0.6	0.6	0.6	← SU_5

Figure 5.16: Illustration of the weighting factor η, the probability matrix P, and the energy consumption matrix e for rounds $1 \leq r \leq 10$. An "*" in P matrix indicates the active SUs at each round.

As shown in Fig. 5.16, during rounds $r_3 - r_6$ and $r_9 - r_{10}$, SU_1, SU_2, SU_3, SU_4, and SU_5 are selected 4, 4, 2, 2, and 0 times respectively. In other words, the selection process took place 6 times, with 2 SUs selected each time (12 times in total). Out of the 12 selections, 8 times selected SUs belonged to the good sensing accuracy (66%), 4 times selected SUs belonged to the average sensing accuracy (33%), and 0 times selected SUs belonged to the poor sensing accuracy (0%).

5.5   Summary

In this chapter, we reviewed cooperative sensing in cognitive sensor networks. An optimization problem was formulated and analytically solved to find the minimum number of required cooperative users. We then defined a metric for spectrum sensing accuracy and proposed a novel energy-aware user selection method that identifies the most eligible cooperative users through a probability-based approach that employs weighting functions.

In addition, two benchmarks were defined for the purpose of the proposed method's evaluation. We also compared the network lifetime for several sensing accuracy thresholds, and discussed the trade-off between the sensing accuracy and the network lifetime. Moreover, the effect of different fusion rules were discussed and it was concluded that the Majority rule has the best overall performance among the examined rules. The chapter

ends with a numerical analysis to further enlighten the proposed method's approach to

the cooperative spectrum sensing.

Chapter 6

Conclusions and Future Work

6.1 Concluding Remarks

In this dissertation, we studied spectrum sensing in cognitive radio networks. We high-lighted the importance of spectrum occupation modeling and described the spectrum usage in cognitive radio by a continuous-time Markov chain model. The model was mathematically defined by deriving the transition rate matrix and the probability state vector. Through numerical analyses, we validated the model for several cases including an extreme case with a very large number of secondary users. The model was also ex-amined for a special case with no active secondary user and compared with an existing model in the literature; it was discussed that the model agrees with the existing work in this case. The Markov chain served as a base model for our analysis through this

114

dissertation.

We elaborated the significance of sensing period optimization on the secondary network power consumption and throughput. We also discussed the current drawback in the most existing methods where the sensing period is obtained based on the primary network's properties only. This drawback is highlighted by knowing that there exist numerous cognitive radio applications with various sets of design requirements. On the other hand, a cognitive radio network should be aware of its surroundings, and the traffic characteristics of the secondary network are important, especially when it has exceptionally low or high probability of presence. We, therefore, proposed an application-specific spectrum sensing method that finds the local sensing period according to the properties of both primary and secondary networks. We defined and analytically derived the interference ratio and the undetected opportunity ratio parameters. Then, two optimization problems were formulated based on the secondary network's state in the Markov chain, and the optimum sensing period in each state was analytically derived.

In addition, we examined the secondary network's power consumption and its throughput in the application-specific and the non-application-specific sensing approaches. It was elaborated that while the non-application-specific method provides an identical solution for different types of secondary networks, the application-specific approach provides a customized solution for each network. The performance of these schemes were compared

through various numerical and simulation analyses. It was concluded that, as compared with the non-application-specific approach, the proposed method managed to increase the average throughput of the secondary networks by up to 11%. Also, the proposed method significantly decreased the secondary network's power consumption by as low as 33% of the non-hybrid approach. We also discussed the trade-off between the throughput maximization and the power consumption minimization.

We also investigated the cooperative spectrum sensing in cognitive radio and discussed the main advantages of cooperative techniques in spectrum sensing. We then addressed and analytically solved two important problems in the cooperative spectrum sensing: the minimum number of cooperative users and the most eligible cooperative users. We also defined a metric for the sensing accuracy and proposed a novel method that identifies the most eligible secondary users through a probability-based approach that uses a weighting function.

Two benchmarks were defined to examine the effects of emphasizing on the sensing accuracy and the remaining energy level of the secondary users. In particular, we studied two extreme cases where only one of the parameters was considered in each case. By numerical analysis, it was concluded that the accuracy benchmark was increased by as much as 39% by only considering the sensing accuracy and ignoring the remaining energy level. Additionally, the energy benchmark was reduced by as as low as 76% by

only considering the remaining level of energy and ignoring the sensing accuracy. We also compared the network's lifetime at several sensing accuracy thresholds and discussed the trade-off between the sensing accuracy and the network's lifetime. Moreover, the effects of several fusion rules were studied, including the OR-Rule, the AND-Rule and the Majority rule. Through several simulations, it was concluded that the Majority rule had the best overall performance among the fusion rules. Finally, a numerical analysis was performed to further enlighten the proposed method's approach to the spectrum sensing.

6.2 Future Directions

The proposed sensing methods through this dissertation are based on a continuous-time Markov chain model that is developed as part of this work. The proposed sensing methods can be further enriched by assuming more sophisticated spectrum occupation models.

In addition, the current work assumes a fixed network structure where the location of the primary and secondary users does not vary by time. However, in reality, there exist a number of applications where the location of the users is not fixed. Therefore, it is essential to address the spectrum sensing optimization in cognitive radio networks with mobile users. Adding mobility to SUs can provide sensing diversity as a single SU might obtain the channel usage information from different geographical locations. The probability of detection, therefore, is expected to be improved. A possible direction to

117

reduce the complexity of sensing period optimization in a mobile cognitive radio network

would be to estimate the channel usage information based on the previous sensing results.

References

[1] H. Kim and K. Shin, "Efficient discovery of spectrum opportunities with MAC-layer sensing in cognitive radio networks," *IEEE Trans. Mobile Computing*, vol. 7, pp. 533–545, May 2008.

[2] X. Zhu, L. Shen, and T.-S. Yum, "Analysis of cognitive radio spectrum access with optimal channel reservation," *Communications Letters, IEEE*, vol. 11, pp. 304 –306, Apr. 2007.

[3] S. M. M. D. Cabric and R. Brodersen, "Implementation issues in spectrum sensing for cognitive radios," in *Proc. Asilomar Conf. Signals, Systems and Computers*, pp. 772–776, Nov. 2004.

[4] FCC, "Spectrum policy task force," in *ET Docket No. 02- 135*, Nov. 2002.

[5] I. Mitola, J. and J. Maguire, G.Q., "Cognitive radio: Making software radios more personal," *Personal Communications, IEEE*, vol. 6, pp. 13 –18, Aug. 1999.

[6] J. Mitola, *Cognitive Radio: An Integrated Agent Architecture for Software Defined Radio.* PhD thesis, Royal Inst. Technology, Stockholm, Sweden, 2000.

[7] S. Haykin, "Cognitive radio: Brain-empowered wireless communications," *Selected Areas in Communications, IEEE Journal on*, vol. 23, pp. 201– 220, Feb. 2005.

[8] M. C. V. I. F. Akyildiz, W. Lee and S. Mohanty, "A survey on spectrum management in cognitive radio networks," *Communications Magazine, IEEE*, vol. 46, pp. 40–48, Apr. 2008.

[9] R. V. Prasad and H. S. B. P. Pawczak, James A. Hoffmeyer, "Cognitive functionality in next generation wireless networks: Standardization efforts," *Communications Magazine, IEEE*, vol. 46, pp. 72–78, Apr. 2008.

[10] W. Heinzelman, A. Chandrakasan, and H. Balakrishnan, "An application-specific protocol architecture for wireless microsensor networks," *IEEE Trans. Wireless Communications*, vol. 1, pp. 660 – 670, Oct. 2002.

[11] A. Zahmati, S. Hussain, X. Fernando, and A. Grami, "Cognitive wireless sensor networks: Emerging topics and recent challenges," in *Proc. IEEE TIC-STH*, pp. 593 –596, Sept. 2009.

[12] N. Shankar, C. Cordeiro, and K. Challapali, "Spectrum agile radios: Utilization and sensing architectures," in *Proc. IEEE DySPAN*, pp. 160 –169, Nov. 2005.

[13] J. W. D. Cavalcanti, S. Das and K. Challapali, "Cognitive radio based wireless sensor networks," in *Proc. IEEE ICCCN*, pp. 1–6, Ieee, 2008.

[14] S. Gao, L. Qian, and D. Vaman, "Distributed energy efficient spectrum access in wireless cognitive radio sensor networks," in *Proc. WCNC*, pp. 1442 – 1447, Mar. 2008.

[15] S. Gao, L. Qian, D. Vaman, and Q. Qu, "Energy efficient adaptive modulation in wireless cognitive radio sensor networks," in *Proc. IEEE ICC*, pp. 3980 –3986, June 2007.

[16] S. Maleki, A. Pandharipande, and G. Leus, "Energy-efficient distributed spectrum sensing for cognitive sensor networks," *Sensors Journal, IEEE*, vol. 11, pp. 565 –573, Mar. 2011.

[17] I. F. Akyildiz, W. Lee, M. C. Vuran, and S. Mohanty, "Next generation/dynamic spectrum access/cognitive radio wireless networks: A survey," *Computer Networks, Elsevier*, vol. 50, pp. 2127–2159, Sept. 2006.

[18] F. K. Jondral, "Software-defined radio - basic and evolution to cognitive radio," *Wireless Commun. and Networking, EURASIP*, 2005.

[19] A. Ghasemi and E. Sousa, "Spectrum sensing in cognitive radio networks: Requirements, challenges and design trade-offs," *Communications Magazine, IEEE*, vol. 46, pp. 32 –39, Apr. 2008.

[20] N. H. A. Sahai and R. Tandra, "Some fundamental limits on cognitive radio," in *Proc. Allerton Conference on Communication, Control, and Computing*, pp. 1662–1671, 2004.

[21] A. Ghasemi and E. Sousa, "Collaborative spectrum sensing for opportunistic access in fading environments," in *Proc. IEEE DySPAN*, pp. 131 –136, Nov. 2005.

[22] H. Tang, "Some physical layer issues of wide-band cognitive radio systems," in *Proc. IEEE DySPAN*, pp. 151 –159, Nov. 2005.

[23] A. Fehske, J. Gaeddert, and J. Reed, "A new approach to signal classification using spectral correlation and neural networks," in *Proc. IEEE DySPAN*, pp. 144 –150, Nov. 2005.

[24] J. Zhao, H. Zheng, and G.-H. Yang, "Distributed coordination in dynamic spectrum allocation networks," in *Proc. IEEE DySPAN*, pp. 259 –268, Nov. 2005.

[25] H. Zheng and L. Cao, "Device-centric spectrum management," in *Proc. IEEE DySPAN*, pp. 56 –65, Nov. 2005.

[26] IEEE, "IEEE 802.22 WG on wireless regional area networks," *http://www.ieee802.org/22*.

[27] W. Yu-chun, W. Haiguang, and P. Zhang, "Protection of wireless microphones in IEEE 802.22 cognitive radio network," in *Proc. IEEE ICC Workshops*, pp. 1 –5, June 2009.

[28] FCC, "Unlicensed operations in the tv broadcast bands, second memorandum opinion and order, document number: 2010-30184," Dec. 2010.

[29] O. Akan, O. Karli, and O. Ergul, "Cognitive radio sensor networks," *Network, IEEE*, vol. 23, pp. 34 –40, Jul.-Aug. 2009.

[30] K. Shenai and S. Mukhopadhyay, "Cognitive sensor networks," in *Proc. International Conference on Microelectronics*, pp. 315 –320, May 2008.

[31] P. Boonma and J. Suzuki, "Exploring self-star properties in cognitive sensor networking," in *Proc. International Symposium on Performance Evaluation of Computer and Telecommunication Systems*, pp. 36 –43, June 2008.

[32] S. Gao, L. Qian, D. Vaman, and Q. Qu, "Energy efficient adaptive modulation in wireless cognitive radio sensor networks," in *Proc. IEEE ICC*, pp. 3980 –3986, June 2007.

[33] ECMA, "Ecma 392: MAC and PHY for operation in TV white space," *Tech. report, 2nd ed.*, June 2012.

[34] M. Mueck, A. Piipponen, K. Kallioja andrvi, G. Dimitrakopoulos, K. Tsagkaris, P. Demestichas, F. Casadevall, J. Pe andrez Romero, O. Sallent, G. Baldini, S. Filin, H. Harada, M. Debbah, T. Haustein, J. Gebert, B. Deschamps, P. Bender, M. Street, S. Kandeepan, J. Lota, and A. Hayar, "Etsi reconfigurable radio systems: Status and future directions on software defined radio and cognitive radio standards," *Communications Magazine, IEEE*, vol. 48, pp. 78 –86, Sept. 2010.

[35] M. McHenry, "NSF spectrum occupancy measurements project summary," *Shared spectrum company report*, 2005.

[36] "IEEE standard for information technology–telecommunications and information exchange between systems wireless regional area networks (WRAN)–specific requirements part 22: Cognitive wireless RAN medium access control (MAC) and physical

layer (PHY) specifications: Policies and procedures for operation in the tv bands," *IEEE Std 802.22-2011*, pp. 1 –680, Jan. 2011.

[37] C. Cordeiro, K. Challapali, D. Birru, and N. Sai Shankar, "IEEE 802.22: The first worldwide wireless standard based on cognitive radios," in *Proc. DySPAN*, pp. 328–337, Nov. 2005.

[38] E. S. C. R. Stevenson, C. Cordeiro and G. Chouinard, "Functional requirements for the 802.22 WRAN standard," *IEEE 802.22-05/0007r46*, Sept. 2005.

[39] J. Wang, M. S. Song, S. Santhiveeran, K. Lim, G. Ko, K. Kim, S. H. Hwang, M. Ghosh, V. Gaddam, and K. Challapali, "First cognitive radio networking standard for personal/portable devices in tv white spaces," in *Proc. IEEE DySPAN*, pp. 1 –12, Apr. 2010.

[40] C. Ghosh, C. Cordeiro, D. Agrawal, and M. Rao, "Markov chain existence and hidden markov models in spectrum sensing," in *Proc. IEEE PerCom*, pp. 1 –6, Mar. 2009.

[41] L. Luo and S. Roy, "A two-stage sensing technique for dynamic spectrum access," in *Proc. IEEE ICC*, pp. 4181 –4185, May 2008.

[42] T. Rondeau, C. Rieser, T. Gallagher, and C. Bostian, "Online modeling of wireless channels with hidden markov models and channel impulse responses for cognitive radios," in *Proc. IEEE MTT-S*, vol. 2, pp. 739 – 742 Vol.2, June 2004.

[43] S.-M. L. C-H. Park, S-W. Kim and M.-S. Song, "HMM based channel status predictor for cognitive radio," in *Proc. IEEE Asia-Pacific Microwave Conference*, pp. 1–4, Dec. 2007.

[44] I. Akbar and W. Tranter, "Dynamic spectrum allocation in cognitive radio using hidden markov models: Poisson distributed case," in *Proc. IEEE SoutheastCon*, pp. 196 –201, Mar. 2007.

[45] H. Kim and K. G. Shin, "Adaptive mac-layer sensing of spectrum availability in cognitive radio networks," *Tech. Report, Real-Time Computing Laboratory, University of Michigan*, 2006.

[46] H. Kim and K. Shin, "Fast discovery of spectrum opportunities in cognitive radio networks," in *Proc. IEEE DySPAN*, pp. 1 –12, Oct. 2008.

[47] L. T. S. Geirhofer and B. M. Sadler, "Dynamic spectrum access in the time domain: Modeling and exploiting white space," *Communications Magazine, IEEE*, vol. 45, pp. 66–72, May 2007.

[48] S. Geirhofer, L. Tong, and B. Sadler, "Cognitive medium access: Constraining interference based on experimental models," *Selected Areas in Communications, IEEE Journal on*, vol. 26, pp. 95 –105, Jan. 2008.

[49] L. T. S. Geirhofer and B. M. Sadler, "A measurement-based model for dynamic spectrum access," in *Proc. IEEE MILCOM*, vol. 26, 2006.

[50] A. Min, K.-H. Kim, J. Singh, and K. Shin, "Opportunistic spectrum access for mobile cognitive radios," in *Proc. IEEE INFOCOM*, pp. 2993 –3001, April 2011.

[51] B. Wang, Z. Ji, K. Liu, and T. Clancy, "Primary-prioritized markov approach for dynamic spectrum allocation," *IEEE Trans. Wireless Communications*, vol. 8, pp. 1854 –1865, Apr. 2009.

[52] Y. Xing, R. Chandramouli, S. Mangold, and S. N, "Dynamic spectrum access in open spectrum wireless networks," *Selected Areas in Communications, IEEE Journal on*, vol. 24, pp. 626 – 637, Mar. 2006.

[53] C. G. Cassandras and S. Lafortune, *Introduction to discrete event systems*, vol. 11. Kluwer academic publishers, 1999.

[54] J. N. Daigle, *Queueing theory with applications to packet telecommunication.* Springer, 2005.

[55] V. G. Kulkarni, *Modeling and analysis of stochastic systems.* CRC Press, 1995.

[56] H. d. M. G. Bolch, S. Greiner and K. S. Trivedi, *Queueing networks and Markov chains: Modeling and performance evaluation with computer science applications.* John Wiley and Sons, 2006.

[57] J. Wang, M. Ghosh, and K. Challapali, "Emerging cognitive radio applications: A survey," *Communications Magazine, IEEE*, vol. 49, pp. 74 –81, Mar. 2011.

[58] Z. Liang, S. Feng, D. Zhao, and X. Shen, "Delay performance analysis for supporting real-time traffic in a cognitive radio sensor network," *IEEE Trans. Wireless Communications*, vol. 10, pp. 325 –335, Jan. 2011.

[59] Y. Chen, W. L. Woo, and C.-X. Wang, "Channel modeling of information transmission over cognitive interrogator-sensor networks," *IEEE Trans. Vehicular Technology*, vol. 60, pp. 2 –15, Jan. 2011.

[60] O. Elgezabal and C. Salazar, "Technological foundation for future intra-aircraft wireless applications: Technology assessment," in *Proc. IEEE FBW*, pp. 1 –19, June 2011.

[61] E. Peh, Y.-C. Liang, Y. L. Guan, and Y. Zeng, "Optimization of cooperative sensing in cognitive radio networks: A sensing-throughput tradeoff view," *IEEE Trans. Vehicular Technology*, vol. 58, pp. 5294 – 5299, Nov. 2009.

[62] S. S. Jeong, W. S. Jeon, and D. G. Jeong, "Collaborative spectrum sensing for multiuser cognitive radio systems," *IEEE Trans. Vehicular Technology*, vol. 58, pp. 2564 –2569, Jun. 2009.

[63] J. Salt and H. Nguyen, "Performance prediction for energy detection of unknown signals," *IEEE Trans. Vehicular Technology*, vol. 57, pp. 3900 – 3904, Nov. 2008.

[64] Y. C. Liang, Y. Zeng, E. Peh, and A. T. Hoang, "Sensing-throughput tradeoff for cognitive radio networks," *IEEE Trans. Wireless Communications*, vol. 7, pp. 1326 –1337, Apr. 2008.

[65] G. Ganesan and Y. Li, "Agility improvement through cooperative diversity in cognitive radio," in *Proc. IEEE GLOBECOM*, vol. 5, pp. 2505 –2509, Dec. 2005.

[66] T. Yucek and H. Arslan, "A survey of spectrum sensing algorithms for cognitive radio applications," *Communications Surveys Tutorials, IEEE*, vol. 11, pp. 116 –130, Quarter 2009.

[67] F. Digham, M.-S. Alouini, and M. Simon, "On the energy detection of unknown signals over fading channels," in *Proc. IEEE ICC*, vol. 5, pp. 3575 – 3579, May 2003.

[68] H. Tang, "Some physical layer issues of wide-band cognitive radio systems," in *Proc. IEEE DySPAN*, pp. 151 –159, Nov. 2005.

[69] T. M. Cover and J. A. Thomas, *Elements of Information Theory*. New York: Wiley-Interscience, 1990.

[70] W. B. Chien, C. K. Yang, and Y. H. Huang, "Energy-saving cooperative spectrum sensing processor for cognitive radio system," *IEEE Trans. Circuits and Systems I: Regular Papers*, vol. 58, pp. 711 –723, Apr. 2011.

[71] J. A. Han, W. S. Jeon, and D. G. Jeong, "Energy-efficient channel management scheme for cognitive radio sensor networks," *IEEE Trans. Vehicular Technology*, vol. 60, pp. 1905 –1910, May 2011.

[72] R. Deng, J. Chen, C. Yuen, P. Cheng, and Y. Sun, "Energy-efficient cooperative spectrum sensing by optimal scheduling in sensor-aided cognitive radio networks," *IEEE Trans. Vehicular Technology*, vol. 61, pp. 716 –725, Feb. 2012.

[73] Z. Quan, S. Cui, A. Sayed, and H. Poor, "Optimal multiband joint detection for spectrum sensing in cognitive radio networks," *IEEE Trans. Signal Processing*, vol. 57, pp. 1128 –1140, Mar. 2009.

[74] Y. Rao, W. Chen, and Z. Cao, "A sequential sensing data transmission and fusion approach for large scale cognitive radios," in *Proc. IEEE ICCE*, pp. 1 –5, May 2010.

[75] W.-Y. Lee and I. Akyildiz, "Optimal spectrum sensing framework for cognitive radio networks," *IEEE Trans. Wireless Communications*, vol. 7, pp. 3845 –3857, Oct. 2008.

[76] R. Viswanathan and P. Varshney, "Distributed detection with multiple sensors I. fundamentals," *Proceedings of the IEEE*, vol. 85, pp. 54 –63, Jan. 1997.

[77] F. Digham, M.-S. Alouini, and M. Simon, "On the energy detection of unknown signals over fading channels," in *Proc. IEEE ICC*, vol. 5, pp. 3575 – 3579 vol.5, May 2003.

[78] W. Zhang, R. Mallik, and K. Letaief, "Optimization of cooperative spectrum sensing with energy detection in cognitive radio networks," *IEEE Trans. Wireless Communications*, vol. 8, pp. 5761 –5766, Dec. 2009.

[79] N. M. Temme, "Uniform asymptotic expansions of the incomplete gamma functions and the incomplete beta function," *Mathematics of Computation*, vol. 29, pp. 1109–1114, Oct. 1975.